RADIOLOGY AND ONCOLOGY

vol.45 no.3

september 2011

AROMASIN®
eksemestan

ENDOKRINO ZDRAVLJENJE BOLNIC Z RAKOM DOJK PO MENOPAVZI

BISTVENE INFORMACIJE IZ POVZETKA GLAVNIH ZNAČILNOSTI ZDRAVILA

AROMASIN 25 mg obložene tablete
Sestava in oblika zdravila: obložena tableta vsebuje 25 mg eksemestana. **Indikacije:** Adjuvantno zdravljenje žensk po menopavzi, ki imajo invazivnega zgodnjega raka dojke s pozitivnimi estrogenskimi receptorji in so se uvodoma vsaj 2 do 3 leta zdravile s tamoksifenom. Zdravljenje napredovalega raka dojke pri ženskah z naravno ali umetno povzročeno menopavzo, pri katerih je bolezen napredovala po antiestrogenskem zdravljenju. Učinkovitost še ni bila dokazana pri bolnicah, pri katerih tumorske celice nimajo estrogenskih receptorjev. **Odmerjanje in način uporabe:** 25 mg enkrat na dan, najbolje po jedi. Pri bolnicah z zgodnjim rakom dojke je treba zdravljenje nadaljevati do dopolnjenega petega leta adjuvantnega hormonskega zdravljenja oz. do recidiva tumorja. Pri bolnicah z napredovalim rakom dojke je treba zdravljenje nadaljevati, dokler ni razvidno napredovanje tumorja. **Kontraindikacije:** znana preobčutljivost na učinkovino zdravila ali na katero od pomožnih snovi, ženske pred menopavzo, nosečnice in doječe matere. **Posebna opozorila in previdnostni ukrepi:** predmenopavzni endokrini status, jetrna ali ledvična okvara, bolniki z redko dedno intoleranco za fruktozo, malabsorpcijo glukoze/galaktoze ali pomanjkanjem saharoza-izomaltaze. Lahko povzroči alergijske reakcije ali zmanjšanje mineralne gostote kosti ter večjo pogostnost zlomov. Ženskam z osteoporozo ali tveganjem zanjo je treba na začetku zdravljenja izmeriti mineralno kostno gostoto s kostno denzitometrijo. Čeprav še ni dovolj podatkov, kako učinkujejo zdravila za zdravljenje zmanjšane mineralne kostne gostote, ki jo povzroča Aromasin, je treba pri bolnicah s tveganjem uvesti zdravljenje ali profilakso osteoporoze ter bolnice natančno spremljati. **Medsebojno delovanje z drugimi zdravili:** Sočasna uporaba zdravil – npr. rifampicina, antiepileptikov (npr. fenitoina ali karbamazepina) ali zdravil rastlinskega izvora s šentjaževko – ki inducirajo CYP 3A4, lahko zmanjša učinkovitost Aromasina. Uporabljati ga je treba previdno z zdravili, ki se presnavljajo s pomočjo CYP 3A4 in ki imajo ozek terapevtski interval. Kliničnih izkušenj s sočasno uporabo zdravila Aromasin in drugih zdravil proti raku ni. Ne sme se jemati sočasno z zdravili, ki vsebujejo estrogen, saj bi ta izničila njegovo farmakološko delovanje. **Vpliv na sposobnost vožnje in upravljanja s stroji:** Po uporabi zdravila je lahko psihofizična sposobnost za upravljanje s stroji ali vožnjo avtomobila zmanjšana. **Neželeni učinki:** neželeni učinki so bili v študijah, v katerih so uporabljali standardni odmerek 25 mg, ponavadi blagi do zmerni. Zelo pogosti (> 10 %): vročinski oblivi, bolečine v sklepih, mišicah in kosteh, utrujenost, navzea, nespečnost, glavobol, močnejše znojenje, ginekološke motnje. **Način in režim izdajanja:** zdravilo se izdaja le na recept, uporablja pa se po navodilu in pod posebnim nadzorom zdravnika specialista ali od njega pooblaščenega zdravnika. **Imetnik dovoljenja za promet:** Pfizer Luksembourg SARL, 51, Avenue J. F. Kennedy, L-1855, Luksemburg. **Datum zadnje revizije besedila:** 11.12.2009
Pred predpisovanjem se seznanite s celotnim povzetkom glavnih značilnosti zdravila.

"SAMO ZA STROKOVNO JAVNOST"

ARO-01-11

Pfizer

Pfizer Luxembourg SARL, Grand Duchy of Luxembourg, 51, Avenue J.F. Kennedy, L-1855,
PFIZER, Podružnica za svetovanje s področja farmacevtske dejavnosti, Ljubljana, Letališka 3c, 1000 Ljubljana, SLOVENIJA

RADIOLOGY AND ONCOLOGY

September 2011
Vol. 45 No. 3
Pages 159-226
ISSN 1318-2099
UDC 616-006
CODEN: RONCEM

Publisher
Association of Radiology and Oncology

Affiliated with
Slovenian Medical Association – Slovenian Association of Radiology, Nuclear Medicine Society,
Slovenian Society for Radiotherapy and Oncology, and Slovenian Cancer Society
Croatian Medical Association – Croatian Society of Radiology
Societas Radiologorum Hungarorum
Friuli-Venezia Giulia regional groups of S.I.R.M.
Italian Society of Medical Radiology

Aims and scope
Radiology and Oncology is a journal devoted to publication of original contributions in diagnostic and interventional radiology, computerized tomography, ultrasound, magnetic resonance, nuclear medicine, radiotherapy, clinical and experimental oncology, radiobiology, radiophysics and radiation protection.

Editorial office

Radiology and Oncology
Zaloška cesta 2
P. O. Box 2217
SI-1000 Ljubljana
Slovenia
Phone: +386 1 5879 369
Phone/Fax: +386 1 5879 434
E-mail: gsersa@onko-i.si

Reader for English
Vida Kološa

Secretary
Mira Klemenčič
Zvezdana Vukmirović

Design
Monika Fink-Serša, Samo Rovan, Ivana Ljubanović

Layout
Matjaž Lužar

Printed by
Tiskarna Ozimek, Slovenia

Published quarterly in 600 copies

Beneficiary name: DRUŠTVO RADIOLOGIJE IN ONKOLOGIJE
Zaloška cesta 2
1000 Ljubljana
Slovenia

Beneficiary bank account number: SI56 02010-0090006751
IBAN: SI56 0201 0009 0006 751
Our bank name: Nova Ljubljanska banka, d.d.,
Ljubljana, Trg republike 2,
1520 Ljubljana; Slovenia

SWIFT: LJBASI2X

Subscription fee for institutions EUR 100, individuals EUR 50

The publication of this journal is subsidized by the Slovenian Book Agency.

Indexed and abstracted by:
Science Citation Index Expanded (SciSearch®)
Journal Citation Reports/Science Edition
Scopus
EMBASE/Excerpta Medica
DOAJ
Open J-gate
Chemical Abstracts
Biomedicina Slovenica

This journal is printed on acid- free paper

On the web: ISSN 1581-3207
http://versitaopen.com/ro
http://versita.com/science/medicine/ro/
http://www.onko-i.si/radioloncol/

contents

experimental oncology

clinical oncology

radiophysics

I *slovenian abstracts*

RADIOLOGY AND ONCOLOGY is covered in Science Citation Index Expanded (SciSearch®),Journal Citation Reports/Science Edition, Scopus, DOAJ, EMBASE/Excerpta Medica, Open J-gate, Chemical Abstracts, Biomedicina Slovenica

review

New developments in surgery of malignant gliomas

Andrej Vranic

Department of Neurosurgery, UMC Ljubljana, Slovenia

Received 4 April 2011
Accepted 12 May 2011

Correspondence to: Andrej Vranič, MD, MSc, Clinical Department of Neurosurgery, UMC Ljubljana, Zaloska 7, SI - 1525 Ljubljana, Slovenia. Phone: +386 1 522 5112; E-mail: andrej.vranic@kclj.si

Disclosure: No potential conflicts of interest were disclosed.

Background. Malignant gliomas account for a high proportion of brain tumours. With new advances in neurooncology, the recurrence-free survival of patients with malignant gliomas has been substantially prolonged. It, however, remains dependent on the thoroughness of the surgical resection. The maximal tumour resection without additional postoperative deficit is the goal of surgery on patients with malignant gliomas. In order to minimize postoperative deficit, several pre- and intraoperative techniques have been developed.

Conclusions. Several techniques used in malignant glioma surgery have been developed, including microsurgery, neuroendoscopy, stereotactic biopsy and brachytherapy. Imaging and functional techniques allowing for safer tumour resection have a special value. Imaging techniques allow for better preoperative visualization and choice of the approach, while functional techniques help us locate eloquent regions of the brain.

Key words: malignant gliomas; surgery; neuronavigation; image-guided surgery; transcranial magnetic stimulation; fluorescence-guided resection

Introduction

Recent advances in various disciplines have delineated the molecular basis of brain tumours and introduced new technologies in oncology and immunology. New chemotherapeutic agents with few systemic adverse effects have become available, offering hope of better treatment options for patients with malignant gliomas.[1,2] These agents work by inhibiting tumour growth, angiogenesis, proliferation, invasion and spread of the tumour. Monoclonal antibodies, either alone or carrying a cytotoxic payload, promise to control the tumour growth. Gene therapy is maturing, with several clinical trials under way in which improved vectors and new therapeutic genes are being used to target tumour cells. Additional therapeutic approaches include the use of radiation sensitizers, optimization of current radiation modalities, electrophysiological interference with cell proliferation and stem cell-based approaches.[2]

In spite of all these advances, the survival of patients with malignant gliomas is still closely correlated with the more extensive tumour resection.[3,4] Even when the radical removal of a brain tumour is not possible, surgery provides the diagnosis and prevents symptoms of mass effect. Tissue obtained during surgery is critical to allow for the individualized approach in designing treatments with newer therapies that are becoming available.

In recent years, several new techniques facilitating malignant brain tumour surgery have become available. Technical advances help us to minimize the injury to the surrounding healthy brain tissue and the consequent postoperative neurological deficit. This is especially important in case of tumours, growing in or bordering to the *eloquent regions* of the brain. In narrow terms, eloquent regions are regions enabling the fluent speech (*lat. eloquens* = fluent). In broader meaning, eloquent regions are all cortical regions essential for human integrity – speech, motor, visual and sensory areas. While removing brain tumours or obtaining brain tumours tissue for diagnosis, damage of eloquent regions during brain surgery should be avoided by any cost.

TABLE 1: Different techniques facilitating malignant glioma surgery

	preoperative	intraoperative
imaging	• CT • MRI • angiography • 3D planning • PET CT	• neuronavigation • intraoperative ultrasound • fluorescence–guided resection • intraoperative MRI
functional	• fiber tracking • functional MRI • transcranial magnetic stimulation	• direct cortical stimulation • awake surgery

Microsurgery

The microsurgical resection remains the basic technique in neurosurgery and the most important therapeutic modality in the management of malignant gliomas. There has never been a controlled, randomized study to determine whether simple debulking of tumours is as effective as maximal cytoreduction. However, evidence suggests that the more extensive surgical resection is associated with longer life expectancy for patients with high-grade gliomas.[3,4] Next to the operating microscope, basic microsurgical tools are the bipolar forceps, micro aspirator and other micro instruments. *CUSA (Cavitron Ultra Sonic Aspirator)* can be useful when removing tumours that are less vascularized. Precise knowing of brain anatomy structures is of paramount importance and no technique can replace surgeon's microanatomical knowledge. However, anatomic and functional variability of cortical gyri and sulci can make surgery in the cerebral hemispheres difficult. The exact spatial location of a deep-seated intracranial lesion is often difficult to define on the basis of two-dimensional CT and MR images.[5]

Several pre- and intraoperative techniques are available to make the microsurgical resection of brain tumours more feasible. Most of the techniques are imaging techniques helping us to visualize the tumour before or during surgery. Others are functional techniques enabling us to determine where the eloquent brain areas are located (Table1).

Three-dimensional (3D) planning

The problem of the exact spatial localization of the tumour on the basis of two-dimensional MR images has always posed a problem for neurosurgeons. It has been partially overcome by the introduction of computer programs for 3D visualization of medical images. Preoperative 3D visualization of medical images allows a neurosurgeon to perform interactive preoperative 3D planning. The virtual reality environment in which the surgeon reaches with both hands into a computer-generated stereoscopic 3D space can be created.[6] Surgical targets can be defined and the most suitable surgical approach to the lesion can be selected. In addition, 3D visualization can be employed intraoperatively to locate planned targets by visually matching the computer generated 3D surfaces with the intraoperative view.[5] 3D visualization proves to be adequate and accurate for locating superficial brain tumours in cases where transfer of planned surgical targets to the surgical field is possible.[5]

Neuronavigation

At the end of the 20th century, neurosurgery has entered in the era of image guided surgery or neuronavigation.[7] Frameless, image-guided neuronavigation system is based on MRI scans taken preoperatively and is thus not considered a real-time intraoperative imaging procedure. However, it can provide the surgeon with interactive, dynamic feedback during surgery. The technology uses anatomical points on the patient's face or adhesive markers attached to the patient's head as reference points. The working station fuses the position of reference points with preoperative MR scans. The position of the hend-held pointer relatively to the lesion is shown on the screen. With the help of neuronavigation, borders of brain lesions can be easily determined at the beginning of the surgery. Craniotomy and dural incision can be sized accordingly. Craniotomy can be made smaller and more precise owing to the accuracy afforded by image guidance.[7] Brain shift after craniotomy can disrupt the accuracy and must be accounted for. Neuronavigation is especially suitable for detecting small intraparenchymal lesions where cortex of the brain is expected to be normal. It enables the exact spatial location of small deep-seated lesions

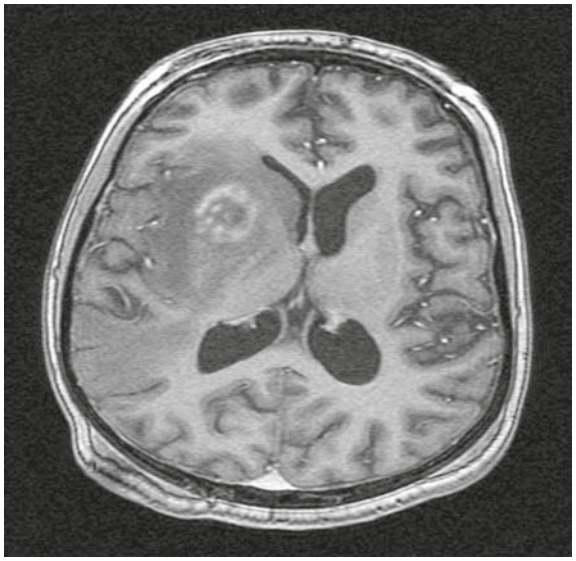

FIGURE 1. Thalamic glioma eligible for neuronavigation-guided needle biopsy.

before and during the surgical procedure, with about 2 mm accuracy. Biopsy of lesions as small as 0.5 cm in diameter can be safely and successfully performed with the help of neuronavigation-guided biopsy needle (Figure 1).

Intraoperative ultrasound (iUS)

Improved orientation and visualization of the tumour, adjacent ventricles and peritumoural vasculature is one of the main advantages of the ultrasonography-assisted microsurgery. Its usefulness is most obvious in subcortical cystic gliomas surgery.[8] Intra-operative ultrasound can be successfully integrated into the neuronavigation system thus offering helpful real-time images of brain tumours.[8]

Fluorescence-guided resection of malignant gliomas

The use of fluorescent tumour marker for intraoperative detection brain tumours has been shown to enhance the macroscopic total resection of malignant gliomas.[9] The technique involves oral administration of the nonfluorescent prodrug, 5-aminolevulinic acid (ALA). In tumour tissue, 5-ALA is metabolized to fluorescent protoporphyrin IX (PpIX) through the heme biosynthesis pathway. PpIX is accumulated in WHO grade III and IV malignant gliomas. Explanations for the higher 5-ALA uptake into the tumour tissue include disrupted BBB, increased neovascularization, and overexpression of membrane transporters in glioma tissue.[10] The altered pattern of expression of enzymes involved in haemoglobin biosynthesis in tumour cells may also be involved. PpIX levels in normal brain tissue are very low, creating a high tumour-to-normal tissue contrast. The use of a specially adapted operating microscope omitting blue light with wavelength of 400 nm allows the surgeon to visualize brain tissue as "blue" and the tumour as "red" in colour (Figure 2). The intraoperative tumour resection is thereby optimized. A phase 3 study reported a longer recurrence-free survival of patients with malignant gliomas who underwent the fluorescence-guided tumour resection.[9] Minimal side effects have been reported, including skin photo-

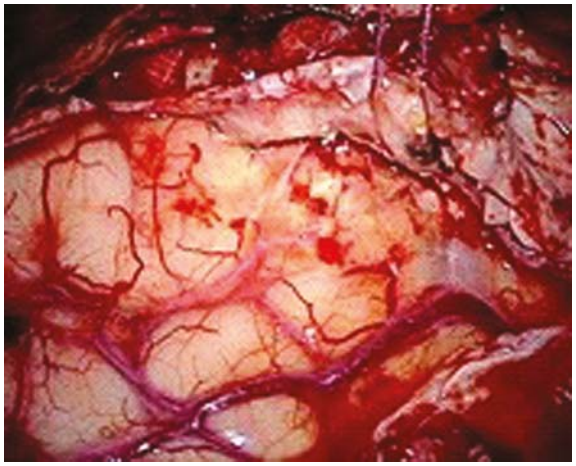

FIGURE 2A. Resection of a malignant glioma - an intraoperative microscopic view of the tumour resection cavity (white light).

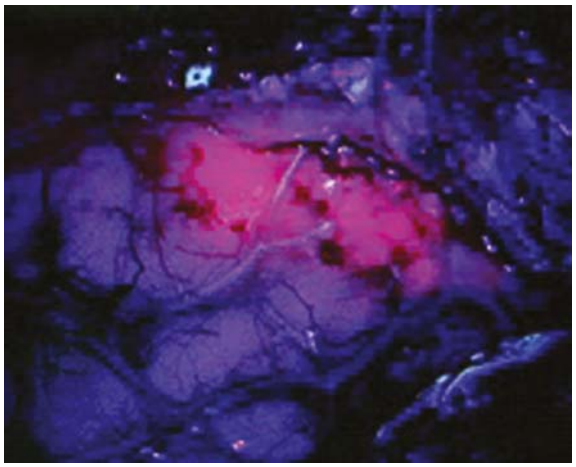

FIGURE 2B. Resection of a malignant glioma using intraoperative fluorescence - an intraoperative microscopic view (blue light).

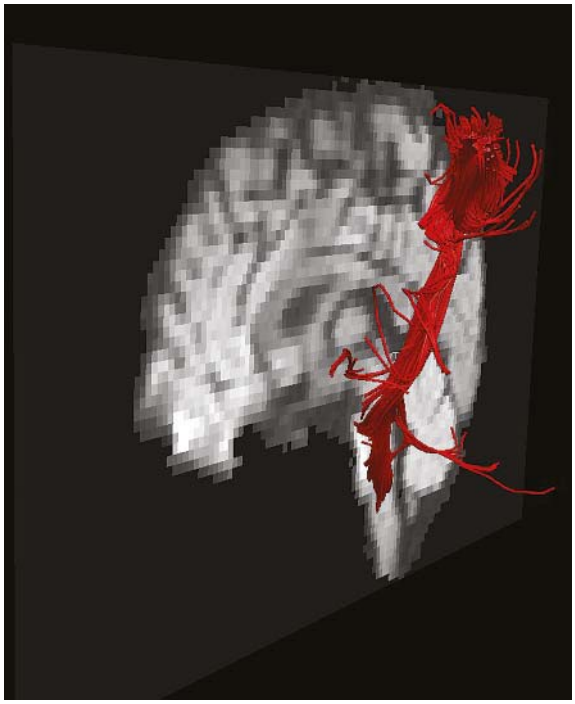

FIGURE 3. DTI of the corticospinal tract. Kindly provided by Dr. Blaž Koritnik, Institute of Neurophysiology, UMC Ljubljana.

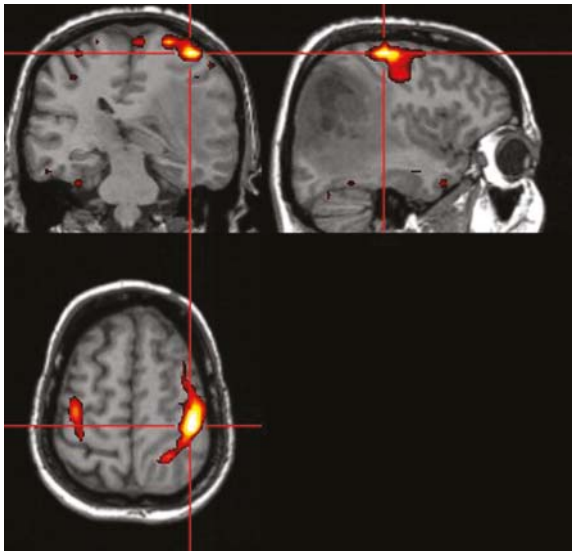

FIGURE 4. fMRI scan showing primary motor cortex on the right side, anteriorly to a malignant glioma. Kindly provided by Dr. Blaž Koritnik, Institute of Neurophysiology, UMC Ljubljana.

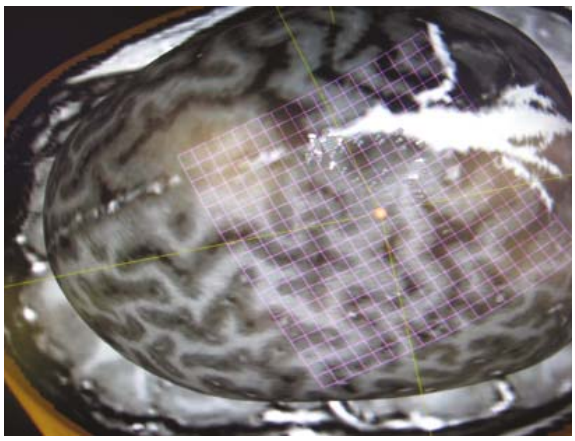

FIGURE 5. TMS of brain cortex around a glioma of the primary motor cortex.

sensitivity after the oral administration. Currently, ALA is not yet approved by the FDA in the United States for the surgical resection of brain tumours.[10] Efforts are underway to perform a controlled, randomized, multicentric trial using fluorescence-guided surgery to determine an effect on the extent of resection.

Intraoperative MRI (iMRI)

Next to the iUS and fluorescence-guided surgery, iMRI is the only real-time intraoperative technique for visualizing malignant gliomas. It allows surgeons to take MR scans during surgery, while the patient is still in the operating room. Surgery can be temporarily stopped, MRI is performed and MR scans are analysed to determine if the tumour has been removed completely, or if the surgery should continue. Decisions based on current information can be made within minutes. A specially equipped operation theatre is needed, with no ferromagnetic material built into the operation table, surgery tools or the anesthetic equipment. The biggest advantage of the use of the iMRI is that it can help the surgeon to identify the normal tissue in eloquent areas. Although this costly procedure has been on market for more than a decade, only few centres in the world have been able to afford it. Presently around 100 centres worldwide have been equipped with this state-of-art technology.

Fiber tracking

Diffusion tensor imaging (DTI) provides information about eloquent white matter structures. Long tracts, especially the corticospinal tract, can be visualized by means of a technique called *DTI fiber tracking* (Figure 3). Fiber tracking can be integrated into neurosurgical planning software and be used for navigated surgery. During surgery, the corticospinal tract should be avoided.

Functional MRI (fMRI)

With the help of the fMRI, active parts of the brain are visualized. Higher blood flow through the active regions of the brain is registered while the patient is talking or moving his limbs. MRI scan shows active areas of the brain in different colour (Figure 4). The drawback of this imaging technique is its insufficient accuracy. However, gross impression of the lesion can be obtained by studying fMRI scans preoperatively. Accordingly, eloquent regions can be avoided during surgery.

Transcranial magnetic stimulation (TMS)

TMS is a noninvasive method for analysing the cortical function. Its main use is in preoperative functional mapping of the primary motor cortex in parietal tumour surgery. With the help of TMS, the location of primary motor cortex can be determined before surgery, with the patient awake. The manually guided brain stimulator is moved around the patient's head and small strength magnetic impulses are generated, stimulating brain areas. When primary motor cortex is stimulated, a response on patient's limbs is recorded by means of electromyography (EMG). *Navigated TMS* fuses the principles of TMS, EMG and neuronavigation.[11] It allows us to see on the MRI scans exactly where in the cortex the TMS stimulus is given. Exact points of the stimulation are recorded on MR scans in the computer program. With the help of neuronavigation, these images can be used pre- or intraoperatively to enhance the safe microsurgical resection of motor cortex tumours (Figure 5).

Direct cortical stimulation

Alternatively to TMS, the location of primary motor areas can be determined intraoperatively, with the help of the direct cortical stimulation. Bi- or unipolar electrode is used manually, touching the surface of the brain. Stimulation parameters must be adjusted according to the stimulated area. Motor responses are recorded on the limbs as motor evoked potentials, while the patient is only mildly relaxed. *Brain mapping* is performed as the areas leading to a motor response in the limbs are marked with sterile paper markers and avoided during the tumour removal.

FIGURE 6. Awake craniotomy on a patient with malignant glioma.

Awake surgery

In all cases where real-time monitoring of higher neurological functions is wishful, awake craniotomy has found its place. Awake surgery is a variant of the direct cortical stimulation. It is used mainly to determine speech areas of the brain, however motor and sensory areas can also be localized. It remains a challenge for the anaesthesiologist to guide the patient in a stable and comfortable way through the procedure while keeping him awake for the sufficient interaction. Local anaesthetics play an important role in the awake surgery. During craniotomy and dural incision, a mild sedation without intubation is usually used. During the tumour removal, both the neurosurgeon and the neurophysiologist communicate with the patient to detect any speech disturbances while the speech area is stimulated by means of the direct cortical stimulation (Figures 6,7).

FIGURE 7. Surgery for a malignant glioma on awake patient.

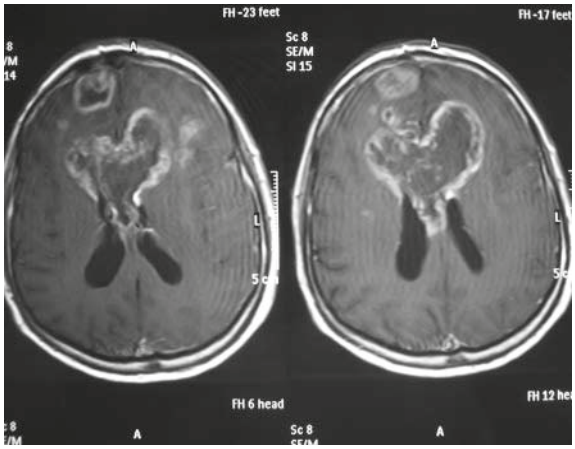

FIGURE 8. Nonresectable glioblastoma of the corpus callosum.

Neuroendoscopy

Neuroendoscopy can provide a minimally invasive approach for biopsy or resection of the tumour, as well as the management of concurrent obstructive hydrocephalus.[10,12] Neuroendoscopic approaches use the natural CSF-filled ventricular cavities in the brain as a conduit for accessing tumours. Illumination from the tip of the neuroendoscope allows the neurosurgeon to navigate within the ventricular system and optimally visualize the tumour. The neuroendoscope can be used to perform resections of intraventricular and paraventricular tumours involving deep midline portions of the brain. The direct visualization of tumours can allow for more accurate tissue sampling and improved haemostasis. In addition, the ability to simultaneously manage tumour-related hydrocephalus through a third ventriculostomy can prevent the placement of ventriculo-peritoneal shunts.

The approach to the ventricular system is usually through the right frontal lobe. Because the diameter of the neuroendoscope is less than 1 cm, the exposure and trajectory to the CNS lesion is achieved in a minimally invasive fashion. Most skin incisions measure approximately 2-3 cm in length, and the opening in the skull is about 1-2 cm. No significant brain retraction is needed. Neuronavigation technology allows the surgeon to properly correlate the location of the endoscope with MRI of the brain.

Stereotactic needle biopsy

A needle biopsy should be offered to all patients with nonresectable gliomas (Figure 8) to allow for the histology-guided adjuvant therapy.[13] Even with resectable tumours, prior needle biopsy is sometimes preferred to the immediate tumour resection in order to allow for the more individualized approach. While frameless neuronavigation–guided needle biopsy is more comfortable for the patient and easier to perform, several centres opt for more accurate stereotactic needle biopsy. *Stereotactic frame* is based on an imaginary 3D Cartesian coordinate system and is also used in stereotactic radiosurgery and deep brain stimulation.

Brachytherapy

BCNU wafers or iodine-125 seed implants are indicated as an adjunct to surgery in patients with newly-diagnosed or recurrent high-grade gliomas after the microsurgical resection.[14,15] Increasing body of data suggests that the combination of BCNU implants within the multimodal treatment strategy

may provide a prolonged survival in patients with glioblastoma.[14.16] Known surgical complications include convulsions, intracranial infections, abnormal wound healing and brain oedema.[16] The communication between the surgical resection cavity and the ventricular system should be avoided to prevent implants from migrating.

Nanotecnology

Although not yet used in neurosurgical practice, it is expected that within the next 10 years, nanotechnology will furtherly advance the surgical management of malignant gliomas.[10] The multifunctional clinical nature of nanotechnology will provide for the targeting, imaging, and therapy of infiltrating brain tumour cells that escape the surgical treatment. Therapeutic nanoparticles coated with various drugs and conjugated to brain tumour-specific antibodies will be delivered systemically or locally to brain tumours. The ability to image nanoparticles by conventional methods, such as MRI, will provide precise information regarding therapeutic agent delivery and therapeutic follow-up. The local hyperthermia treatment of malignant gliomas might also be possible with nanoparticles using alternating magnetic fields that are safe for non-cancerous cells.[10] However, the surgical resection will still be required to debulk malignant brain tumours and alleviate the mass effect on the surrounding brain.

Conclusions

Although the recent prolongation of the survival of patients with malignant brain tumours is primarily attributed to chemo- and radiotherapy, the surgical intervention remains crucial. The use of several new techniques in brain surgery can facilitate the extensive resection of these tumours and make it safer for the patient.

References

1. Baur M, Preusser M, Piribauer M, Elandt K, Hassler M, Hudec M, et al. Frequent MGMT (06-methylguanine-DNA methyltransferase) hypermethylation in long-term survivors of glioblastoma: a single institution experience. *Radiol Oncol* 2010; **44:** 113-20.
2. Velnar T, Smrdel U, Popovic M, Bunc G. Genetic markers in oligodendroglial tumours. *Radiol Oncol* 2010; **44:** 13-8.
3. Sanai N, Berger MS. Glioma extent of resection and its impact on patient outcome. *Neurosurgery* 2008; **62:** 753-64.
4. Vuorinen V, Hinkka S, Färkkilä M, Jääskeläinen J. Debulking or biopsy of malignant glioma in elderly people - a randomised study. *Acta Neurochir (Wien)* 2003; **145:** 5-10.
5. Žele T, Matos B, Knific J, Bajrović FF, Prestor B. Use of 3D visualisation of medical images for planning and intraoperative localisation of superficial brain tumours: our experience. *Br J Neurosurg* 2010; **24:** 555-60.
6. Kockro RA, Serra L, Tseng-Tsai Y, Chan C, Yih-Yian S, Gim-Guan C, et al. Planning and simulation of neurosurgery in a virtual reality environment. *Neurosurgery* 2000; **46:** 118-35.
7. Wadley J, Dorward N, Kitchen N, Thomas D. Pre-operative planning and intra-operative guidance in modern neurosurgery: a review of 300 cases. *Ann R Coll Surg Engl* 1999; **81:** 217-25.
8. Enchev Y, Bozinov O, Miller D, Tirakotai W, Heinze S, Benes L, et al. Image-guided ultrasonography for recurrent cystic gliomas. *Acta Neurochir (Wien)* 2006; **148:** 1053-63.
9. Stummer W, Pichlmeier U, Meinel T, Wiestler OD, Zanella F, Reulen HJ. Fluorescence-guided surgery with 5-aminolevulinic acid for resection of malignant glioma: a randomised controlled multicentre phase III trial. *Lancet Oncol* 2006; **7:** 392-401.
10. Van Meir EG, Hadjipanayis CG, Norden AD, Shu H, Wen PY, Olson JJ. Exciting new advances in neuro-oncology: The avenue to a cure for malignant glioma. *CA Cancer J Clin* 2010; **60:** 166-93.
11. Picht T, Mularski S, Kuehn B, Vajkoczy P, Kombos T, Suess O. Navigated transcranial magnetic stimulation for preoperative functional diagnostics in brain tumor surgery. *Neurosurgery* 2009; **65(6 Suppl):** 93-8.
12. Cappabianca P, Cinalli G, Gangemi M, Brunori A, Cavallo LM, de Divitiis E, et al. Application of neuroendoscopy to intraventricular lesions. *Neurosurgery* 2008; **62(Suppl 2):** 575-97.
13. Simon M, Schramm J. Surgical management of intracranial gliomas. *Recent Results Cancer Res* 2009; **171:** 105-24.
14. Bock HC, Puchner MJ, Lohmann F, Schütze M, Koll S, Ketter R, et al. First-line treatment of malignant glioma with carmustine implants followed by concomitant radiochemotherapy: a multicenter experience. *Neurosurg Rev* 2010; **33:** 441-9.
15. Darakchiev BJ, Albright RE, Breneman JC, Warnick RE. Safety and efficacy of permanent iodine-125 seed implants and carmustine wafers in patients with recurrent glioblastoma multiforme. *J Neurosurg* 2008; **108:** 236-42.
16. La Rocca RV, Mehdorn HM. Localized BCNU chemotherapy and the multimodal management of malignant glioma. *Curr Med Res Opin* 2009; **25:** 149-60.

research article

Polydimethylsiloxane: a new contrast material for localization of occult breast lesions

Geraldo Sérgio Farinazzo Vitral[1], Nádia Rezende Barbosa Raposo[1,2]

[1] Research Center for Innovative Health Sciences (NUPICS), Federal University of Juiz de Fora, School of Pharmacy, Juiz de Fora, Brasil

[2] Neuroscience Laboratory (LIM 27), Department and Institute of Psychiatry at the University of São Paulo, School of Medicine, São Paulo, Brasil

Received 6 February 2011
Accepted 12 February 2011

Correspondence to: Geraldo Sérgio Farinazzo Vitral, Avenida Barão do Rio Branco, 2288/1301, Juiz de Fora, Minas Gerais, Brasil, CEP 36016-310 . Tel/Fax: +55 32 32170435; E-mail: geraldovitral@yahoo.com.br

Disclosure: No potential conflicts of interest were disclosed.

Background. The radioguided localization of occult breast lesions (ROLL) technique often utilizes iodinated radiographic contrast to assure that the local injection of ^{99m}Tc-MAA corresponds to the location of the lesion under investigation. However, for this application, this contrast has several shortcomings. The objective of this study was to evaluate the safety, effectiveness and technical feasibility of the use of polydimethylsiloxane (PDMS) as radiological contrast and tissue marker in ROLL.

Materials and methods. The safety assessment was performed by the acute toxicity study in Wistar rats (n = 50). The radiological analysis of breast tissue (n = 32) from patients undergoing reductive mammoplasty was used to verify the effectiveness of PDMS as contrast media. The technical feasibility was evaluated through the scintigraphic and histologic analysis.

Results. We found no toxic effects of PDMS for this use during the observational period. It has been demonstrated in human breast tissue that the average diameter of the tissue marked by PDMS was lower than when marked by the contrast medium ($p < 0.001$). PDMS did not interfere with the scintigraphic uptake ($p = 0.528$) and there was no injury in histological processing of samples.

Conclusions. This study demonstrated not only the superiority of PDMS as radiological contrast in relation to the iodinated contrast, but also the technical feasibility for the same applicability in the ROLL.

Key words: breast cancer; surgery; radiological contrast; ROLL technique

Introduction

Developed in the late 90's, the Radioguided Occult Lesion Localization (ROLL) technique came to fill a gap in the preoperative marking of nonpalpable breast lesions. Since its conception at the European Institute of Oncology, the verification of the correct positioning of the technetium pertechnetate associated with human albumin (^{99m}Tc-MAA) in breast tissue has been identified as a limiting factor of this technique. To correct this problem, it was recommended that a small volume (usually the same as ^{99m}Tc-MAA - 0.2 ml) of radiographic iodinated contrast media be injected with the needle positioned in stereotactic breast tissue together or shortly after ^{99m}Tc-MAA. The mammography control being performed immediately after the injection (about five minutes at most), confirms whether or not the marked area matches the suspected area.[1-3]

Some operational deficiencies may be identified during the performance of the radioguided procedure that uses iodinated contrast media. Often, there is a radiological image without any precise borders and tissue absorption spreading in a short period of time.[4] The risks of adverse reactions in patients are also extremely important, such as skin and subcutaneous tissue necrosis and, especially, allergic and anaphylactic reactions with a risk of death. So, there are some situations of failure with a technique considered the gold standard, with variable levels of efficacy (69-95%) in the complete removal of the impalpable lesions.[5]

To correct this ROLL specific stage, the use of other substances that would both provide an appropriate level of radiological contrast (radiopacity) and act as a tissue marker are required. A product that does not migrate after being positioned in the breast and that remains in the same position for a long period of time is understood as a tissue marker, in order to identify or provide the location coordinates of the area to be studied.

There is evidence that shows features of the radiological opacity of polydimethylsiloxane (PDMS) and its ease of identification by different imaging methods such as X-ray and ultrasound[6], which enables its use as a substitute for the iodinated contrast in the ROLL.

Other studies, primarily in the dermatology area, defined criteria for injection volumes, directions of use, viscosities and other guiding parameters for techniques by which the complications of intra-tissue injection of PDMS occur quite rarely.[7,8]

In this paper, the safety, efficacy and feasibility of the use of high viscosity PDMS in the radioguided location of occult breast lesions (ROLL), replacing the iodinate contrast media, were assessed for the first time.

Material and methods

Animals

This animal study was approval by UFJF Animals Ethical Committee (protocol nº 006/2007) and was conducted according to the EU Directive and Colégio Brasileiro de Experimentação Animal (COBEA).

The experimental animals used in this study were adult female *Wistar* rats (*Rattus norvegicus*, 140-180 g, 70 days old) maintained under a 12h/12h light/dark cycle at an ambient temperature of 24 ± 2 °C with a free access to standard commercial food and tap water *ad libitum*. After completing one week of acclimation, the rats were divided into five groups of ten animals and used in the experiments described below.

Acute toxicity

A synthetic polymer (polydimethylsiloxane, 12.500 centistokes of viscosity, medical grade and sterile) (*Saldanha Rodrigues Ltda*, Brazil) in the volume of 0.2 ml was introduced subcutaneously (sc) in the back of healthy *Wistar* rats anesthetized by inhalation of diethyl ether (single dose). After a period of 1, 7 and 14 days treatment they all were sacrificed to collect samples of blood and tissue. Untreated animals (absolute control group) were sacrificed on the same day at the beginning of the experiments and had neither prior management of the animal nor administration of polymer. Those subjected to the puncture in the same area of application of the polymer, but without the injection of the polymer (relative control group), were sacrificed in the same way, 24 h after the puncture.

Rats were observed thoroughly during the first 24 h for the onset of any immediate toxic signs and daily during the 13 day observation period to record any delayed acute effects. The animals were macroscopically examined, aiming at identifying eventual morphological alterations. Some vital organs (heart, liver and kidney) were forwarded for the histological study. At the end of each experiment, all animals were sacrificed by means of inhalation of diethyl ether according to the Ethical Principles of Animal Experimentation (COBEA) and blood samples were collected (fasting for 12 h before sacrifice).

Body weight

The weight of each rat was recorded on day zero (0) and on the day of the sacrifice of the animals, in their respective groups. In the group "treated 7 days", the animals were also weighed on day 3. In the group "treated 14 days", weighing was also conducted on days 3, 7 and 10. The average weight in each group was calculated.

Haematological profile

Blood samples were collected under 10% EDTA/saline pH 7.2 and examined for hemoglobin concentration, packed cell volume, total erythrocyte count, and total and differential leukocytes counts.

Biochemical analysis of serum

Blood samples were collected and centrifuged (3000 rpm, 15 minutes, room temperature) and clean sera was separated and collected for the following investigations: serum glucose (glucose-oxidase/peroxidase); urea (UV kinetic); creatinine (Jaffe's kinetic reaction); uric acid (end-point colorimetric enzymatic); albumin (colorimetric); aspartate aminotransferase (AST) and alanine aminotransferase (ALT) (optimized ultraviolet kinetic); alkaline phosphatase (colorimetric enzymatic); total cholesterol and triglyceride (colorimetric enzymatic).

Histopathological studies

Slices of heart, liver and kidney were fixed in 10% buffered (pH = 7.0) formaldehyde, embedded in paraffin wax, sectioned at 5 μm and stained with haematoxylin and eosin (HE). A detailed microscopic examination was carried out in those organs of both control and treatment groups. These analyses were performed at the Laboratório de Anatomia Patológica do Hospital Universitário from the Universidade Federal de Juiz de Fora.

Human breast tissue

In this study, 32 samples of human potentially healthy breast tissue (n = 16/group) from patients undergoing reduction mammoplasty performed at the Hospital Universitário (HU) from UFJF were used. All patients gave a written informed consent to participate in this study, which was approved by the Human Ethical Committee of the Universidade Federal de Juiz de Fora (protocol nº 0043.0.180.000-07). Samples were sectioned at 3 cm of diameter, simulating an average size of the surgical specimens obtained with the ROLL, and they were cataloged. A small volume (0.1 ml) of high-viscosity polydimethylsiloxane (12,500 cs) was tested as radiological contrast and tissue marker for ROLL.

Efficacy and technical feasibility of PDMS in human breast tissue

Radiological and scintigraphic analysis

Samples (n=32) were divided into 2 groups: control (iodinated contrast) and experimental (PDMS contrast). In the radiology department, the parts were radiographed (Contour Plus, BENNETT-Hologic USA); 0.1 ml of ^{99m}Tc-MAA (IPEN – CNEN - Brasil) was injected, which corresponds to the doses of 5 μCi and 0.1 ml of test substances: Omnipaque 300® (Ioexol, Farmasa, Amersham Health Limited, U.K.) or PDMS (Saldana Rodriguez Ltda, Brazil), through a needle positioned in the center of the tissue part (same point of ^{99m}Tc- MAA injection). In the PDMS group, 0.01 ml of India ink was also injected right after the polymer, so that it was possible to identify the site of injection in the histological processing. Another mammography was performed after one minute of injection, with the same degree of magnification of images.

The specimens were submitted to radioactive counting (scintigraphic) in a gamma camera (ELSCINT model Apex SP6, Israel) for 30 seconds, using a high-resolution collimator at 17 cm distance between the collimator and the parts. The reading area (ROIs) was of 570 pixels. After the scintigraphic phase the pieces were immediately immersed in 10% buffered (pH = 7.0) formaldehyde for 24 hours, for subsequent histological processing.

A comparative evaluation of the contrast quality between the groups (iodinated and polymer contrast) was performed by measuring the largest diameter of contrast area produced in their mammograms, with the aid of a digital caliper. By the quantitative comparison of scintigraphic uptake levels between the groups, the possibility of interference with the nuclear medicine techniques employed in the ROLL was verified.

Histopathological studies

The appropriate identification of the tissue and cellular structures adjacent to the polymer (region marked with India ink) was considered indicative of deleterious non-interference in the techniques of preparation and histological analysis.

Statistical analysis

The statistical analysis was performed using Statistical Package for the Social Sciences (SPSS) 13.0 for Windows. All values are presented as mean ± standard deviation (SD). For the comparisons of continuous variables among the groups a one-way analysis of variance (ANOVA) was employed with individual differences assessed using Bonferroni correction for the multiple comparisons if the ANOVA was statistically significant. The independent *t* test was also used. Two-tailed p values < 0.05 were considered to be statistically significant.

Results

Animal study

Acute toxicity

Rats administered PDMS did not develop any clinical signs of toxicity either immediately or during the post-treatment period. No mortality occurred in both groups (control and treated animals) either immediately or during the 14-days observation period.

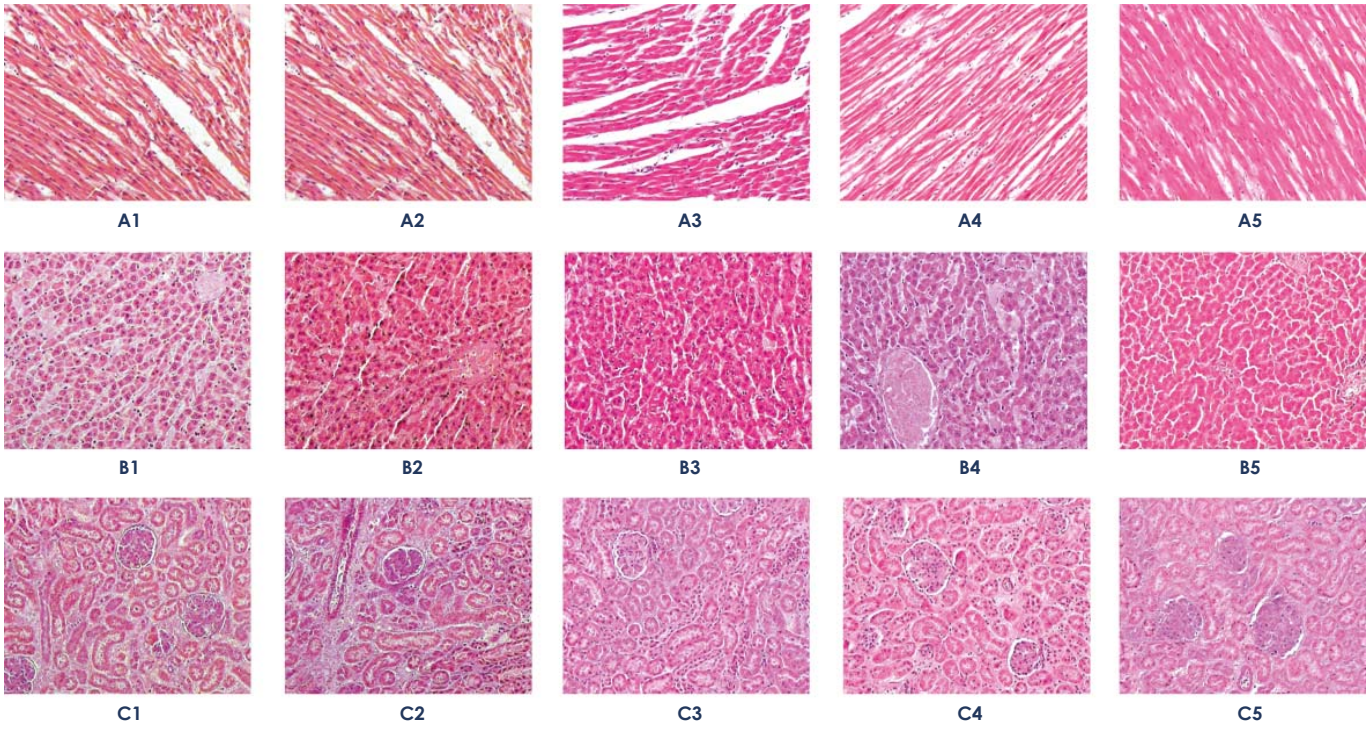

FIGURE 1. Representative images of heart (A), liver (B) and kidney (C) tissues from animals of all groups stained by hematoxylin-eosin. Sections of these tissues were fixed and stained with hematoxylin-eosin (HE) and examined by light microscopy (magnification: 100x). Numbers represent experimental groups (controls: 1 – absolute and 2 – relative; PDMS-treated animals: 3 - Day 1, 4 - day 7 and, 5 - day 14).

Body weight

Body weight, gained during the observation period, was comparable to control groups (p=0.879) (data no shown).

Haematological profile

Data on the various hematological parameters measured in rats PDMS-treated are presented in Table 1.

PDMS caused no significant alterations in HB, RBC and WBC count, except for the percentage of eosinophils (3.00 ± 1.70 % of total leucocytes, $p<0.05$). With respect to this cell type, statistically significant difference was found between the absolute control group and the "treated 14 days" group (ANOVA, Bonferroni test), which indicates the beginning of tissue reaction in this group exposed to a long period of contact with the polymer.

Biochemical analysis

Data on various biochemical parameters measured in the serum of controls and PDMS-treated rats is presented in Table 2.

There were no marked alterations in any of the specific activities of enzymes, AST, ALT and alka-

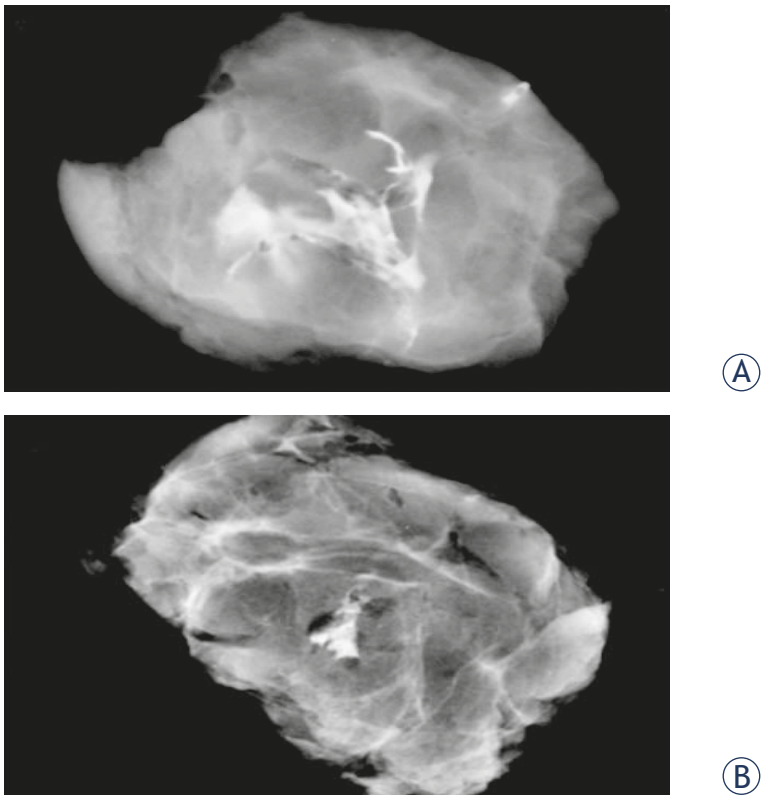

FIGURE 2. Radiological imaging of a specimen of human breast tissue marked with (A) iodinated contrast and (B) polydimethylsiloxane. Samples were sectioned at 3 cm of diameter and presented at the same degree of magnification.

TABLE 1. Haematological data of the control and experimental groups

Haematological profile	Control groups		Experimental groups		
	absolute	relative	Day 1	Day 7	Day 14
Total leucocytes (10^3/mm^3)	9.65 ± 2.79	10.61 ± 2.44	8.92 ± 1.48	10.61 ± 2.65	9.27 ± 1.58
Neutrophils (%)	25.60 ± 9.02	20.70 ± 8.06	19.60 ± 6.33	22.60 ± 5.46	20.00 ± 6.80
Lymphocytes (%)	72.00 ± 8.10	75.70 ± 7.13	77.10 ± 6.31	74.70 ± 5.74	75.20 ± 6.39
Monocytes (%)	1.10 ± 0.88	1.90 ± 1.45	1.80 ± 1.23	1.60 ± 1.35	1.10 ± 0.57
Eosinophils (%)	1.20 ± 1.13	1.80 ± 1.23	1.50 ± 1.35	1.30 ± 1.16	3.00 ± 1.70[a]
Platelets (10^3/mm^3)	577.20 ± 58.60	612.10 ± 75.74	557.00 ± 93.90	617.80 ± 74.26	529.40 ± 87.40
Red blood cels (10^6/mm^3)	6.70 ± 1.32	6.84 ± 0.91	6.44 ± 1.19	7.27 ± 1.14	6.02 ± 1.13
Haemoglobin (g dl^{-1})	13.45 ± 2.40	13.54 ± 1.28	12.78 ± 1.95	14.34 ± 2.22	12.47 ± 1.06
Hematocrit (%)	38.43 ± 6.52	39.04 ± 3.90	36.73 ± 5.32	41.04 ± 6.35	37.85 ± 2.78

All values are expressed as mean ± SD.
[a] p<0.05 (ANOVA followed by *post hoc* Bonferroni).

TABLE 2. Biochemical profile of the control and experimental groups

Biochemical parameters	Control groups		Treated groups		
	absolute	relative	Day 1	Day 7	Day 14
Glucose (mg dl-1)	125.0 ± 11.4	119.0 ± 19.5	122.0 ± 20.9	121.0 ± 18.0	118.0 ± 18.0
Urea (mg dl-1)	29.6 ± 3.5	30.8 ± 4.2	29.2 ± 1.8	30.7 ± 4.1	32.3 ± 3.6
Creatinine (mg dl-1)	0.33 ± 0.06	0.38 ± 0.15	0.38 ± 0.06	0.35 ± 0.13	0.39 ± 0.05
Triglyceride (mg dl-1)	76.0 ± 6.2	74.0 ± 5.8	73.0 ± 5.7	74.0 ± 5.6	74.0 ± 5.9
Total cholesterol (mg dl-1)	60.8 ± 6.3	57.2 ± 8.2	56.9 ± 5.6	57.9 ± 8.1	56.5 ± 6.5
Uric acid (mg dl-1)	0.53 ± 0.10	0.53 ± 0.08	0.49 ± 0.10	0.53 ± 0.10	0.52 ± 0.07
Albumin (g dl-1)	2.8 ± 0.3	2.7 ± 0.4	2.6 ± 0.3	2.9 ± 0.3	2.8 ± 0.3
Alkaline phosphatase (Units)	50.6 ± 8.3	51.9 ± 8.0	52.8 ± 8.6	49.5 ± 7.6	47.4 ± 7.5
ALT (Units)	130 ± 10.3	122 ± 9.6	123 ± 8.7	128 ± 8.9	123 ± 6.1
AST (Units)	74 ± 6.0	73 ± 5.9	76 ± 6.8	73 ± 5.9	75 ± 6.9

Results are expressed as mean ± standard deviation (n=10/group). No differences between groups (ANOVA).

line phosphatase in PDMS-treated rats. A similar trend of results was observed with regard to the levels of serum constituents, glucose, urea, creatinine, uric acid, albumin, total cholesterol and triglyceride during the experimental period.

Histopathology

Sections of liver, kidneys and heart tissues of PDMS-animals showed no pathological alterations under light microscopy (Figure 1).

Efficacy in human breast tissue

Radiological and scintigraphic analysis

In human breast tissue, the mean diameter of PDMS-marked tissue was smaller than that obtained with the iodinated contrast group (8.64 ± 2.14 mm *vs.* 17.26 ± 4.91 mm, p<0.001) (Table 3).

Figure 2 shows that the PDMS also produced a more regular markup compared to the iodinated contrast.

PDMS did not interfere with scintigraphic uptake (p=0.528) (Table 3).

Histopathological analysis

PDMS did not interfere with the histological processing of the breast tissue specimens. Scanty amounts of glandular breast tissue were sometimes observed in both groups, along with abundant adipose tissue, because of the origin of these tissues. In this type of plastic surgery, the emphasis is on the removal of fat, not glandular tissue (Figure 3).

TABLE 3. The greater diameter of radiological marking and scintigraphic uptake in human mammary tissue with proposed treatments

Groups	Greater diameter (mm)	Scintigraphic uptake
Iodinated contrast	17.26 ± 4.91	1,842.63 ± 560.70
Polydimethylsiloxane	8.64 ± 2.14[a]	1,693.00 ± 750.14[b]

Results are expressed as mean ± SD (n=16/group).
[a] p< 0.001 and [b] p = 0.528, *Student t test*.

Discussion

In this study, the possibility of using the synthetic polymer polydimethylsiloxane (PDMS), in lieu of iodinated contrast in ROLL was evaluated. It was assessed aspects of acute toxicity in experimental animals, the quality of radiological contrast and the verification of possible interferences with scintigraphic and histological processing of this technique. The results of this study point to a lack of systemic toxic effects in animals, which confirms other studies about the safety of using this substance in humans.[9,10]

Despite the knowledge of the safety in using PDMS in medical procedures, this research is necessary because it is a new use of this product. It is important to highlight that in this new proposed usage, the injected polymer is completely extracted from the body in a short time interval (3-12 h) by the surgery. This extraction of the tissue marker is demonstrated by the use of the gamma portable radiation detector (gamma-probe), intraoperatively. This is because the polymer is injected by the same needle and in the same tissue position, immediately after the injection of ^{99}mTc-MAA. This feature further contributes to increase the safety profile of PDMS in this application because, as previous studies have shown[11-13], the possibility of local reactions such as "foreign body" or granulomatous reactions using the PDMS free in the tissue tends to manifest itself in about a week after its administration.

Another aspect to be analyzed with the results of this research refers to the fact that the volume injected into experimental animals was the same as proposed for the use in humans (0.2 ml), without adjustment for weight. This adjustment was not done because it is already a very small volume, which could derail the trial. If it was adjusted for body weight, which is an average of 150 g, the equivalent volume in a 60 kg person would be 80 ml. That is to say that the volume of PDMS used in animals in this study was 400 times greater than that proposed for humans. It would, therefore, be expected that if there was any toxicity caused by PDMS in use, detectable changes would likely occur in the evaluated parameters.

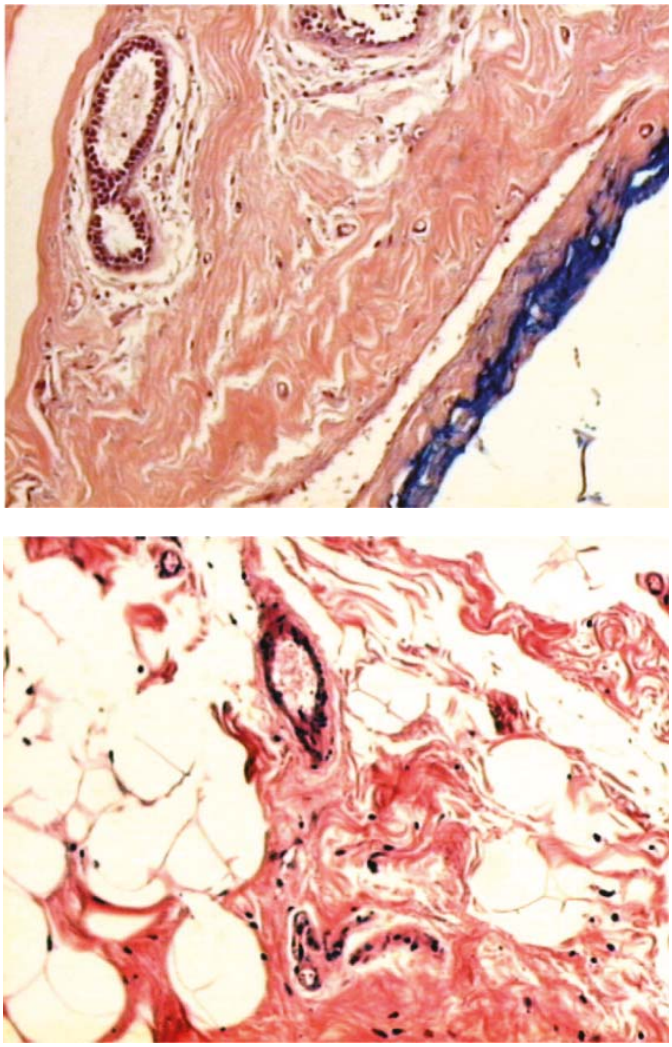

FIGURE 3. Human breast tissue histology of polydimethylsiloxane (A) and iodinated contrast groups (B). Sections of human breast tissue were fixed and stained with hematoxylin-eosin (HE) and examined by light microscopy (magnification: 100x).

Weight reduction observed in the trial within the same group, although not statistically significant ($p<0.05$), is probably due to the fasting imposed to carry out the biochemical analysis. According to the "*Guide to the Care and Use of Experimental Animals*" (1980), the required amount of feed per day for each adult rat, considering the amount ingested and waste, is 25 g. This value is close to that found for the difference between initial and final weight for all groups.

The normal range of biochemical parameters in the serum of PDMS-treated rats clearly suggests

that PDMS causes no disruption of normal physiological and biochemical homeostasis. Regarding the percentage of eosinophils, the statistical difference between the absolute control group and those "treated 14 days" could indicate the beginning of a tissue reaction, because of the long period of exposure of the animal tissue to the polymer.

Data shows a superiority of PDMS contrast quality, compared with the iodinated contrast, in this application (Figure 2). Marking with PDMS was in all cases more regular and punctual, with less scattering areas through the tissue, in addition to remaining identifiable to the later macroscopic histopathology.

PDMS is a polymer that is highly soluble in xylene, a substance used in the histological processing diafanization stage. Thus, at this stage of histological preparation, most, if not all, of the PDMS is extracted from the tissue, so that in the histological slide the area previously occupied by the polymer will be an "empty" area. That's why India ink was used in this experiment, so that the correct evaluation of cellular elements juxtaposed to the polymer could be done, confirming the non-interference with the histological processing.

In ROLL, because it is a diagnostic and sometimes therapeutic procedure[14], the unquestionable need for the histological evaluation of excised tissue is implied. Thus, there would be no sense in using any product or technical step that would undermine the histological processing of surgical specimens. In the present study, no negative interference in routine histological processing was identified. It is noteworthy that the PDMS is insoluble in water, which could result in a waterproofing effect of the tissue, if it is used in inappropriate viscosity (low viscosity). This could affect the process of fixation on the tissue. Thus, it is crucial that the developed technique and the recommended material are used.

The mammary vasculature system and the glandular ductal system itself raise the question of the possibility of embolization of the substances injected during the ROLL. A few cases have been described in which injection and intraductal dissemination of ^{99m}Tc-MAA and iodinated contrast occurred.[15] Such potential exists because of the low viscosity and high solubility of ^{99m}Tc-MAA and the iodinated contrast.

Due to the low caliber of the mammary vasculature[16] and also to the insolubility and high viscosity of PDMS, the risk of embolization would be extremely rare. Possibly, the high viscosity of the polymer could also be a major factor in the relative strengths of the injection pressure and the resistance of the vascular (arterial and venous) walls, much lower than that of a steel needle, which would prevent embolization.

Despite its high viscosity, the PDMS did not interfere with the scintigraphic uptake in the tissues (Table 3). Because it does not reduce the emission scintigraphic tissue marked, it is expected that the use of PDMS does not interfere with the intraoperative detection by gamma-probe, when used in clinical trials.

In conclusion, the analysis of the data suggests that the high viscosity PDMS represents a viable alternative to iodinated contrast in ROLL. The results did not show any toxic effects due to PDMS in animals. Good quality contrast in human breast tissue was obtained, without negative interference detected in the ROLL scintigraphic step and in histological processing of tissues evaluated. Such findings of safety, effectiveness and technical feasibility are essential to carry out assessments in human breast tissue *in vivo*, the objective of future studies.

Acknowledgements

The authors gratefully acknowledge CEDIMAGEM, NUCLEMINAS-NUCLEAR MED CENTER, SALDANHA RODRIGUES LTDA and CIDAP for technical support.

References

1. Galimbert V, Luini A, Paganelli G, Cassano E, et al. Use of Tc-99 labelled colloidal albumin for preoperative and intraoperative localization of non-palpable breast lesions. *Breast* 1997; **6:** 317-8.
2. Barros A, Cardoso MA, Sheng PY, Costa PA, Peizon C. Radioguided localisation of non-palpable breast lesions and simultaneous sentinel lymph node mapping. *Eur J Nucl Med Imaging* 2002; **29:** 1561-5.
3. Paganelli G, Veronesi U. Innovation in early breast cancer surgery: radioguided occult lesion localization and sentinel node biopsy. *Nucl Med Commun* 2002; **23:** 625-7.
4. De Cicco C, Trifirò G, Intra M, Marotta G, Ciprian A, Frasson A, et al. Optimized nuclear medicine method for tumor marking and sentinel node detection in occult primary breast lesions. *Eur J Nucl Med Mol Imaging* 2004; **31:** 349-54.
5. Van der Ploeg IM, Hobbelink M, van den Bosch MA, Mali WP, Borel Hinkes IH, van Hillegersberg R. Radioguided occult lesion localisation (ROLL) for non-palpable breast lesions: A review of the relevant literature. *EJSO* 2008; **34:** 1-5.
6. Scaranelo A M, Maia MFR. Sonographic and mammographic findings of breast liquid silicone injection. *J Clin Ultrasound* 2006; **34:** 273-7.
7. Orentreich DS. Liquid injectable silicone: techniques for soft tissue augmentation. *Clin Plast Surg* 2000; **27:** 595-612.
8. Barnett JG, Barnett CR. Treatment of acne scars with liquid silicone injections: 30-year perspective. *Dermatol Surg* 2005; **31:** 1542-9.

9. Humble G, Mest D. Soft tissue augmentation using silicone: an historical review. *Facial Plast Surg* 2004; **20:** 181-4.

10. Prather C L, Jones DH. Liquid injectable silicone for soft tissue augmentation. *Dermatol Ther* 2006; **19:** 159-68.

11. Autian J. Toxicologic aspects of implants. *J Biomed Mater Res* 1967; **1:** 433-49.

12. Naoum C, Dasiou-Plakida D, Pantelidaki K, Dara C, Chrisanthakis D, Perissios A. A histological and immunohistochemical study of medical-grade fluid silicone. *Dermatol Surg* 1998; **24:** 867-70.

13. Lemperle G, Morhenn V, Charrier U. Human histology and persistence of various injectable filler substances for soft tissue augmentation. *Aesthetic Plast Surg* 2003; **27:** 354-66.

14. Podkrajsek M, Zgajnar J, Hocevar M. What is the most common mammographic appearance of T1a and T1b invasive breast cancer? *Radiol Oncol* 2008; **42:** 173-80.

15. Rampaul RS, Mac Millan RD, Evans JA. Intraductal injection of the breast: a potential pitfall of radioisotope occult lesion localization. *Br J Radiol* 2003; **76:** 425-6.

16. Saint-Cyr M, Chang DW, Robb GL,Chevray PM. Internal mammary perforator recipient vessels for breast reconstruction using free TRAM, DIEP, and SIEA flaps. *Plast Reconstr Surg* 2007; **120:** 1769-73.

research article

Magnetic resonance urography in children - when and why?

Sandra Vegar-Zubovic[1], Spomenka Kristic[1], Lidija Lincender[2]

[1] Clinic of Radiology, Clinical Centre of University of Sarajevo, Sarajevo, Bosnia and Herzegovina
[2] Academy of Sciences and Arts of Bosnia and Herzegovina, Sarajevo, Bosnia and Herzegovina

Received 9 January 2011
Accepted 5 May 2011

Correspondence to: Sandra Vegar-Zubović, MD, PhD, Clinic of Radiology, Clinical Centre of University of Sarajevo, Bolnicka 25, 71000 Sarajevo, Bosnia and Herzegovina. Phone: +387 61 202 880; Fax: +387 33 297 811; E-mail: sandra.vegar@gmail.com

Disclosure: No potential conflicts of interest were disclosed.

Background. The aim of the study was to determine the potential of magnetic resonance urography (MRU) in evaluation of paediatric urinary tract pathologies.

Patients and methods. Twenty-one paediatric urological patients were evaluated with T1, T2 prior and after and 3D gradient echo sequences after the contrast administration. Results were compared with findings obtained with ultrasound which was performed to all of patients, intravenous urography performed to 14 patients with the diagnosis of hydronephrosis and voiding cystouretrography performed to 6 patients where hydronephrosis was suspected to be caused by vesicoureteral reflux (VUR).

Results. MRU not only established the cause of hydronephrosis in all 14 cases (5 ureteropelvic junction (UPJ) stenosis, 1 functional stenosis, 3 residual hydronephrosis, 1 combination of UPJ and vesico-ureteric junction (VUJ) stenosis with hydromegaureter, 2 fetal ureters and 3 insufficient broad ureteral orifices), but gave additional information about existing pathological conditions in all of patients compared to other previously performed examination (1 caliceal lithiasis, 4 UPJ stenosis, 1 VUJ stenosis, 1 neurogenic bladder, 1 hypotonic ureter, 1 urinary infection, 1 duplication of pelvis and ureter, 1 urinary retention and 1 fetal ureter). Other MRU findings were: 3 polycystic kidney disease, 1 caliceal cyst, 2 simple renal cysts, 1 long hypotonic twisted ureters and 1 hypertrophied column of Bertini.

Conclusions. Because of the ability to acquire high contrast and spatial resolution images of the whole urinary tract in any orthogonal plane, MRU enables a precise detection and differentiation of pathological urological conditions. We believe that in the future, because of its advantages, MRU will replace traditional methods in the evaluation of urinary tract pathologies.

Key words: MR urography; urinary tract; paediatrics

Introduction

Diagnostic imaging and therapy protocols of urological disorders in pediatric population are constantly changing because of the introduction and practical application of modern MRI and multislice CT (MSCT) modalities, use of fetal ultrasound, introduction of ultrasound as the obligatory part of the modern urodiagnostic protocol and cognition of the importance of urogenital pathology in children.

During the last seven years we have witnessed a significant development in the introduction of magnetic resonance urography (MRU) in the diagnostic protocol.[1-3] MRU displays the combination of the internal spatial and contrast resolution and it is characterized by the high level of resolution in the imaging of urinary tract anatomy and the fact that it provides a lot of information about kidney functionality.[4]

Modern MRU is performed on the basis of two different imaging strategies. The first technique utilizes unenhanced, heavily T2-weigted pulse sequences to obtain static fluid images of the urinary tract. T2-weighted MR urograms have proved to be excellent in the visualization of the markedly dilated urinary tract, even if the renal excretory function is quiescent. Static-fluid MRU is less suitable for

imaging of disorders that occur in the non-dilated collecting system. The second MRU technique is analogous to the methodology of the conventional intravenous pyelography and is designated as excretory MRU. For this purpose, a gadolinium chelate is intravenously administered and after its renal excretion, the gadolinium-enhanced urine is visualized using fast T1-weighted gradient echo sequences. The combination of gadolinium and low dose furosemid is the key for achieving a uniform distribution of the contrast material inside the entire urinary tract. Gadolinium excretory MRU allows to obtain high quality images of both non-dilated and obstructed urinary tracts in patients with a normal or moderately impaired renal function.[5]

After the application of contrast medium the signal changes. This is correlated with the perfusion, concentration and excretion of contrast. These changes can be analyzed sequentially in the cortex and the medulla. The anatomy and the morphological characteristics of the urinary tract are best analyzed in T2 time and after the application of contrast medium. The information about the urinary tract function comprises of transit time circulation, signal intensity curves compared to a time curve and different estimations of renal functionality.[6]

The introduction of MRU in order to obtain anatomical and functional information gives us the new opportunity to establish the pathophysiology of the urinary tract.[1,7]

Imaging Technique

MRU protocol consists of conventional T1, fast spin echo (FSE) T2-weighted sequences prior and after the administration and 3D gradient echo sequences after the contrast administration.[1,2,8,9]

The important part of the protocol is the forced hydration of all the patients by an intravenous infusion of lactated Ringer's solution (10 ml/kg). All the children younger than seven years of age, require sedation prior to the examination.[1] Once the scout images, which must contain both the kidneys and bladder, are acquired the axial T2-weighted (TR-5,600; TE-160, ETL-23) images through the kidney are obtained.

Furosemide is administered intravenously (1 mg/kg up to maximal dose of 20 mg).[1] In children the furosemide is almost always administered 15 min before contrast. This practice is supported by three reasons: a) the urinary tract is distended, b) the gadolinium concentration is diluted this reduces the susceptibility of artefacts and helps to maintain the signal change which is registered and c) the examination time is shortened which is very important in paediatric population since in spite of sedation the children are not completely calm.[1,9] Then, coronal 2D, T1-weighted (TR=475, TE=17), T2-weighted (TR=5.500, TE=210, ETL=29), T2-weighted 3D (TE=600, ETL=109) sequences are acquired.

2D series are useful for the study of anatomical details, while the heavily T2-weighted 3D scans are used to create the pre-contrast maximum intensity projection (MIP) of the collecting system, ureters and bladder. Ad dynamical acquisition starts approximately 15 minutes after the administration of furosemide which coincides with the administration of contrast in the dose of 0.1 mmol/kg Gd-DTPA with the remark that the contrast injection lasts for 40 seconds. Dynamic series are acquired until both ureters are clearly visualized and for each volume acquisition MIP is automatically generated. After the completion of dynamical series high spatial resolution 3D images are acquired. These 3D images are very useful and valuable in the evaluation of the anatomical malformations including ureteric strictures, ectopic ureteric insertion as well as the postoperative appearance of the urinary tract.[1,9]

In cases where there are no serious obstruction of collecting system total imaging time of MRU is 45 minutes, but in cases of the severe disorder of the excretory function the imaging time can be even 1 hour. The delayed high-resolution anatomic images are particularly valuable in the evaluation of congenital malformations including ureteric strictures, ectopic ureteric insertion as well as the complex postoperative anatomy.[1]

Sedation and preparation for examination

In most cases the sedation is necessary for the children younger than seven years of age. The children younger than two years are sedated by the administration of chloral-hydrate per-rectum, whereas older children before the MRU undergo a pediatric examination and after that the intravenous sedation is administered. For the underage patients parents must consent to their child undergoing the MR examination.

Patients and methods

During the period of one year (January 2010 – December 2010) we included in the study 21 patients on which we performed MRU. All of our patients

were in different phases of the clinical examination: patients with treatment dilemma – conservative or surgical, operated patients, patients with new diagnosed congenital malformations and patients who needed the follow up of therapy effects.

We included in this study the children of different ages: the youngest patient was 2 months old and the oldest patient was 17 years old, the average age of patients was 7.05 years. Of all the patients 43% (n=9) were females and 57% (n=12) were males.

Ultrasound as a screening method was previously performed on all the patients and in some cases other diagnostic procedures (intravenous urography, voiding cystouretrography). All of the patients positively diagnosed with hydronephrosis (n=14) had undergone intravenous urography which was insufficient to establish the cause of the above named condition and were therefore recommended for further investigations via MRU. Where hydronephrosis was suspected (n=6) to have been caused by vesicoureteral reflux (VUR), voiding cystouretrography was also conducted as well as intravenous urography. VUR was positively established as a cause in 3 patients but due to non-typical appearance of hydronephrosis MRU was conducted to eliminate other eventual anomalies which may have remained unidentified via other methodologies. In the case of remaining 3 patients VUR was not established as a cause and due to a diagnostic dilemma patients underwent MRU.

In five patients where single or multiple cysts were identified via ultrasound, MRU was conducted to analyse the form and the shape of the cysts and their potential compressive effect on the collecting system. In the case of a patient with ultrasonographically suspected malign renal tumour with compression on collecting system the second used method was MRU because of its capability to permit the simultaneous morphological and functional analysis, while other methods were avoided in order to reduce the ionizing radiation. With one patient with repeated urinary infection and regular ultrasound finding the clinician requested MRU and the classical examination methodology were avoided.

MRU is the type of examination that requires the preparation because the procedure alone lasts for a quite long period of time. The preparation and the examination together are approximately 1 hour and 45 minutes long. In the case of younger patients the sedation was necessary, all other patients were explained that the examination lasts for a quite long period of time and that during the examination they must remain still and lie calm.

All the examinations were performed on 1.5 T machines (Avanto, Siemens, Erlagen, Germany) and 3.0 T machines (Trio Tim, Siemens, Erlangen, Germany).

Results

All 21 MRU examinations were successfully completed. MR urography images were diagnostically sufficient in all patients. A total of 42 kidneys, 42 collecting systems and 21 bladders in 21 patients were examined. The results of MR urography are presented in Figure 1.

In this study the most common indication for MRU was hydronephrosis of unclear aetiology: 66.7% (n=14) of all our patients were admitted with this diagnosis. In the case of 4 patients where it was challenging to establish the cause of hydronephrosis via classical methods, MRU solved a diagnostic dilemma and established that hydronephrosis was caused by intraluminal ureteropelvic junction (UPJ) stenosis.

MRU was performed on 19% (n=4) of patients with a hydronephrotic collecting system as a part of the postoperative evaluation after pyeloplasty. MRU identified the postoperative presence of functional UPJ stenosis as a cause of hydronephrosis in 1 patient with the additional finding of UPJ stenosis on the contralateral side which wasn't identified with other methods, while in the remaining 3 patients MRU demonstrated that hydronephrosis was the continuation of previously treated stenosis and in one case the additional finding was caliceal lithiasis.

In one case of unclear hydronephrosis the cause was both UPJ and vesico-ureteric junction (VUJ) stenosis with hydromegaureter and the additional finding was UPJ stenosis on the contralateral side.

In two cases of hydronephrosis MRU established not only the cause – fetal ureter, but gave additional findings: UPJ stenosis on the contralateral side in one case and VUJ stenosis on the contralateral side in the second case.

With two patients, where based on previously conducted methodologies (intravenous urography and voiding cystouretrography), hydronephrosis was proved to be connected to VUR, MRU not only identified established insufficient broad ureter orifice but also provided further information. In one case, MRU established the occurrence of neurogenic bladder and hypotonic ureter with further signs of the urinary infection. In the case of the other patient MRU established the condition of urine retention with UPJ stenosis and fetal ureter on the contralateral side.

With one patient where renal hypoplasia and hydronephrosis of the kidney caused by VUR were diagnosed via classical methodology, this diagnosis was corroborated by MRU results which further established the condition of duplication of pelvis and ureter on the contralateral side.

Figure 2 contains the MRU identified pathological conditions that caused hydronephrosis.

MRU identified 6 stenosis at the level of UPJ associated with the hydronephrosis: 5 of this were intraluminal and 1 was functional.

In two patients where cysts were identified *via* ultrasound, MRU not only enabled the diagnosis of cyst type but also the analysis of cyst influence on the collecting system: in one of these two patients a caliceal cyst was identified establishing no repercussion on the collecting system, while in the other patient a simple cortical cyst with a subtle compressive effect on the upper and middle region calices was diagnosed.

MRU conducted on 3 patients, where previously polycystic disease of the kidney - cystic dysplasia was diagnosed via ultrasound, enabled the morphological analysis of cysts, renal parenchyma and collecting system and the analysis of functional capabilities of kidney which were normal in all three cases.

With one patient who previously had normal ultrasound results but had repeated urinary infection MRU revealed long, hypotonic and twisted ureters.

Before performing MRU, 100% (n=21) of our patients were examined with one or more other diagnostic modalities (US, intravenous urography, voiding cystouretrography). MRU findings gave additional information about existing pathological conditions in 100% (n=21) of patients, which have not been identified with other mentioned modalities. In Figure 3 additionally acquired information after performing MR urography is presented.

As a part of MRU examination we evaluated the renal function of 100% (n=21) of our patients. In 19% (n=4) of patients we identified the decreased renal function. We performed MRU due to the suspicion of malign tumour only in 4.8% (n=1) of patients. MRU finding denied the malign diagnosis: we identified the benign condition – hypertrophied column of Bertini (Figures 4–7).

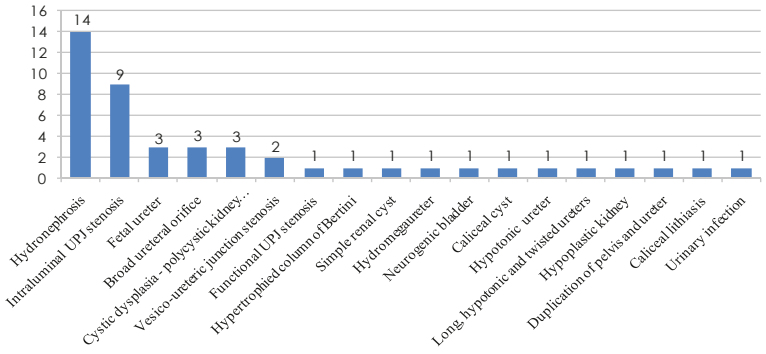

FIGURE 1. MR urography findings.

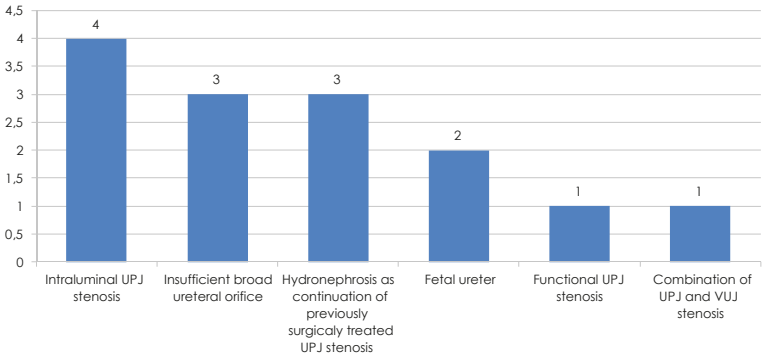

FIGURE 2. Cause of hydronephrosis.

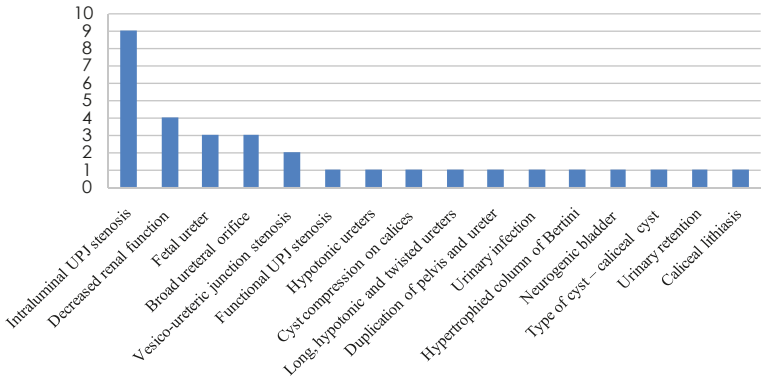

FIGURE 3. Additional MR urography findings.

Discussion

Urinary tract diseases belong to the most frequent paediatric pathology. In the assessment of urinary tract frequently used there are traditional diagnostic procedures such as ultrasound, intravenous urography, voiding cystourethrography, CT and renal scintigraphy. Each of these procedures has some advantages and disadvantages.

Intravenous urography is known to be cost-effective but the reduced image quality by super-positioned bowel gases, prolonged examination time, the use of ionizing radiation which is mutagenic and the use of iodinated contrast media are the disadvantages.[6,7,9,10]

Voiding cystourethrography is considered to be "gold standard" for the diagnosis of VUR but on the

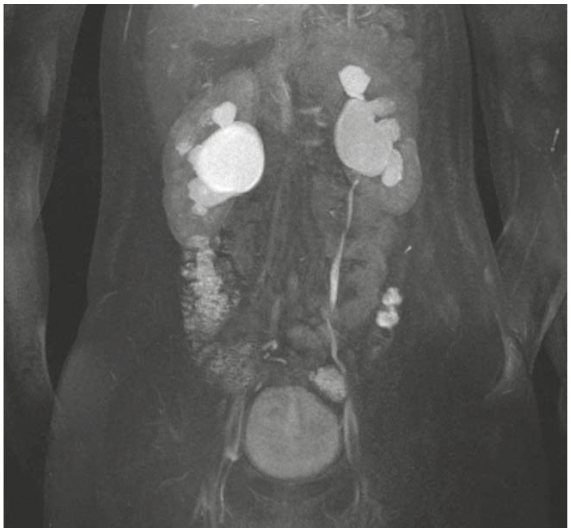

FIGURE 4. Intraluminal UPJ stenosis on the right causing hydronephrosis. Hydronephrosis on the left side is continuation of previously treated stenosis.

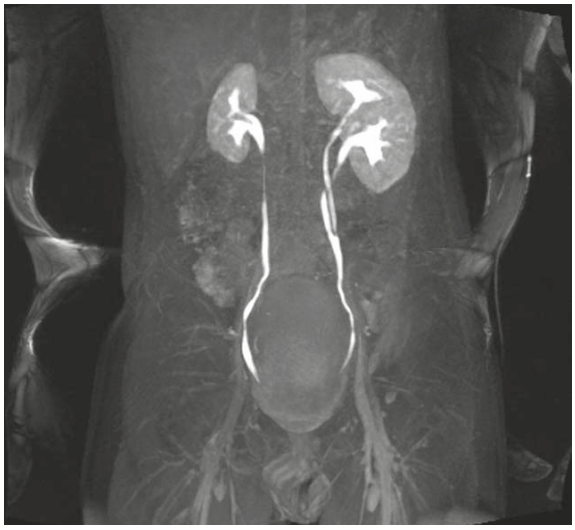

FIGURE 5. Duplication of pelvis and ureter on the left side. Hypoplastic right kidney with vesico-ureteral reflux, grade III.

FIGURE 6. Right kidney is polycystic with fetal ureter. Hydronephrotic left collecting system with vesico-ureteric junction stenosis.

FIGURE 7. Caliceal cyst of left kidney. Vascular impression on the proximal ureter on the right side.

other hand the risk of the urinary infection following the catheterization together with the use of ionizing radiation is relative drawbacks of this method.[11]

Ultrasound is a non invasive non ionizing method but cannot assess the renal function and analyze non-dilated ureters despite the fact that it is an operator dependent method.[11]

Renal scintigraphy uses a low radiation dose and has as a characteristic low spatial resolution and long examination time[7,12]; the main disadvantage of CT is a very high radiation dose and its DNA damage effect is well known.[10,13]

The introduction of MRU was the answer to the problems regarding the assessment of both function and morphology of the urinary tract. The advantages of this diagnostic modality are not only the non-use of ionizing radiation, but the ability to acquire high contrast and spatial resolution images in any orthogonal plane.[1,2]

MRU is very efficient in the assessment of different pathological conditions such as malignant renal tumours, which are very frequent among solid tumours in young children[14], benign solid masses, renal cysts, infections, parenchymal ischemia and

haemorrhage, different types of obstructions and anomalies; in addition it allows the quantification of corticomedullary perfusion and renal excretory function.[6,15,16] The main disadvantages of MRU are: high cost, it requires sedation and hydration.[1-3]

The most common indication for MRU is the evaluation of hydronephrosis.[2-6,15,16] The hydronephrosis in the most cases is the consequence of the obstruction of the urine flow in any point from the kidney to the bladder, and in the minor number of cases of non-obstructive uropathy.[5,17] In the children the obstruction is the most communally at the level of UPJ. The most severe consequence of obstruction is the renal function deterioration. In order to prevent the loss of renal function, in the assessment of hydronephrosis it is very important to establish the type of uropathy (obstructive or non obstructive) and in order of that chose the proper therapy.[17] MRU allows the differentiation between obstructive and non-obstructive uropathies by the calculation of renal transition time (RTT). The arterial phase of the contrast agent in the dynamic study permits the identification of crossing vessels.[18]

Considering the fact that MRU not only enables depiction of whole dilated and non dilated ureters from UPJ to ureteric insertion and their analysis from all angles *via* MIP reconstruction, but it also enables the examination of the internal outlook of ureters and of external structures which may also lead to its compression, hence ureteric anatomy and pathology are well demonstrated with MRU.[19]

The comprehensive morphological and functional analysis of all parts of urinary tract, from kidneys to bladder, gained *via* MRU, offers an opportunity to study congenital malformations of the urinary tract *in vivo* with the increased anatomic resolution.[4-9,11-13,15-19]

Due to enabling depiction of ureteropelvic smooth wall thickening, the renal enlargement and change in the signal intensity of renal parenchyma and perirenal fat, MRU has a significant role in the evaluation of acute pyelonephritis and renal scarring.[6]

Conclusions

Because of the ability to acquire high contrast and spatial resolution images of the whole urinary tract in any orthogonal plane, MRU enables a precise detection and differentiation of pathological urological conditions. In particular MRU is efficient in differentiating causes of hydronephrosis – one of the most common urinary tract pathologies in pediatric population. We believe that in the future, because of its advantages, MRU will replace traditional methods in the evaluation of urinary tract pathologies in children.

References

1. Grattan-Smith JD, Jones RA. MR urography in children. *Pediatr Radiol* 2006; **36:** 1119-32.
2. Jones RA, Easley K, Little SB, Scherz H, Kirsch AJ, Grattan-Smith JD. Dynamic contrast-enhanced MR urography in the evaluation of pediatric hydronephrosis: Part 1, functional assessment. *AJR Am J Roentgenol* 2005; **185:** 1598-607.
3. McDaniel BB, Jones RA, Scherz H, Kirsch AJ, Little SB, Grattan-Smith JD. Dynamic contrast-enhanced MR urography in the evaluation of pediatric hydronephrosis: Part 2, anatomic and functional assessment of ureteropelvic junction obstruction. *AJR Am J Roentgenol* 2005; **185:** 1608-14.
4. Kocaoglu M, Ilica AT, Bulakbasi N, Ergin A, Ustünsöz B, Sanal T, et al. MR urography in pediatric uropathies with dilated urinary tracts. *Diagn Interv Radiol* 2005; **11:** 225-32.
5. Nolte-Ernsting CCA, Adam GB, Gunter RW. MR urography: examination techniques and clinical applications. *Eur Radiol* 2001; **11:** 355-72.
6. Grattan-Smith JD. MR urography: anatomy and physiology. *Pediatr Radiol* 2008; **36(Suppl 2):** S275-80.
7. Borthne A, Pierre-Jerome C, Nordshus T, Reister T. MR urography in children: current status and future development. *Eur Radiol* 2000; **10:** 503-11.
8. Perez-Brayfield MR, Kirsh AJ, Jones RA, Grattan-Smith JD. A prospective study comparing ultrasound, nuclear scintigraphy and dynamic contrast enhanced magnetic resonance imaging in the evaluation of hydronephrosis. *J Urol* 2003; **170:** 1330-4.
9. Grattan-Smith JD, Perez-Brayfield MR, Jones RA, Little S, Broecker B, Smith EA, et al. MR imaging of kidneys: functional evaluation using F-15 perfusion imaging. *Pediatr Radiol* 2003; **33:** 293-304.
10. Miklos M, Gajski G, Garaj-Vrhovac V. Usage of the standard and modified comet assay in assessment of DNA damage in human lymphocytes after exposure to ionizing radiation. *Radiol Oncol* 2009; **43:** 97-107.
11. Choyke PL. The urogram: are rumors of its death premature? *Radiology* 1992; **184:** 33-6.
12. Kuhn JP, Slovis TL, Haler JO. *Caffey's pediatric diagnostic imaging*. 10th edition. Volume 1. Philadelphia: Mosby; 2003.p. 202-36.
13. Lavocat MP, Granjon D, Allard D, Gay C, Freycon MT, Dubois F. Imaging of pyelonephritis. *Pediatr Radiol* 1997; **27:** 159-65.
14. Kachanov DY, Dobrenkov KV, Shamanskaya TV, Abdullaev RT, Inushkina EV, Savkova RF, et al. Solid tumors in young children in Moscow Region of Russian Federation. *Radiol Oncol* 2008; **42:** 39-44.
15. Riccabona M, Avni FE, Dacher JN, Damasio MB, Darge K, Lobo ML, et al. ESPR uroradiology task force and ESUR pediatric working group: imaging and procedural recommendations in pediatric uroradiology, part III. Minutes of the ESPR uroradiology task force minisymposium on intravenous urography, uro-CT and MR-urography in childhood. *Pediatr Radiol* 2010; **40:** 1315-20.
16. Borthne A, Nordshus T, Reiseter T, Geitung JT, Gjesdal KI, Babovic A, et al. MR urography: the future gold standard in pediatric urogenital imaging? *Pediatr Radiol* 1999; **29:** 694-701.
17. Little SB, Jones RA, Grattan-Smith JD. Evaluation of UPJ obstruction before and after pyeloplasty using MR urography. *Pediatr Radiol* 2008; **38(Suppl 1):** S106-24.
18. Jones RA, Perez-Brayfield MR, Kirsh AJ, Grattan-Smith JD. Renal transit time with MR urography in children. *Radiology* 2004; **233:** 41-50.
19. Blandino A, Gaeta M, Minutoli F, Salamone I, Magno C, Scribano E, et al. MR Urography of the ureter. *AJR Am J Roentgenol* 2002; **179:** 1307-14.

case report

With computed tomography confirmed anterolateral left ventricular pseudoaneurysm in patient with dilatative alcoholic cardiomyopathy

Mitja Letonja[1], Marija Santl Letonja[2]

[1] General Hospital Ptuj, Medical Faculty University of Maribor, Maribor, Slovenia
[2] General Hospital Murska Sobota, Murska Sobota, Slovenia

Received 15 January 2011
Accepted 25 March 2011

Correspondence to: Mitja Letonja, MD, General Hospital Ptuj, Potrčeva 23-25, 2250 Ptuj, Medical Faculty University of Maribor: E-mail: mitja.letonja@mf.uni-lj.si

Disclosure: No potential conflicts of interest were disclosed.

Background. Pseudoaneurysms are rare complications of myocardial infarction with propensity for rupture. There is still a challenge with which diagnostic imaging we performed a final diagnosis of pseudoaneurysm and differentiate it from true aneurysm what is clinically important due to the different treatment.

Case report. We presented the unusual case of a 56-year-old man with signs of decompensated heart failure which had worsened a few months before hospitalization. We believed that during worsening of symptoms the patient suffered a silent myocardial infarction complicated by subacute free wall rupture which resulted into left ventricular pseudoaneurysm formation without tamponade. Echocardiography showed dilatative cardiomyopathy which was already present years before and a very rare location of the left ventricular pseudoaneurysm on the anterolateral part of the left ventricle. Pseudoaneurysm was confirmed with CT scan. Due to the severity of contractile dysfunction and no response in treatment for congestive heart failure the directive for the resection was tempered and the patient died due to the progressive heart failure and embolic phenomena.

Conclusions. This report shows the importance of non-invasive imaging diagnostic evaluation of acute decompensated heart failure where echocardiography and chest X-ray are the first diagnostic steps. Based on those findings further imaging diagnostic steps must be performed such as CT scan in our case which finally confirms left ventricular pseudoaneurysm with dilatative cardiomyopathy.

Key words: left ventricular pseudoaneurysm; echocardiography; computed tomography

Introduction

Majority of patients with the acute free wall rupture after the myocardial infarction die suddenly, but only a few of them developed ventricular pseudoaneurysm mostly when the rupture is subacute and confined by epicardium, pericardial adhesions and thrombus formation.[1,2] Pseudoaneurysm can be developed in a few days after a myocardial infarction or even two years later.[3] Pseudoaneurysm of the left ventricle (PSALV) after a silent myocardial infarction is very rare. Most frequently reported clinical symptoms of pseudoaneurysm are a heart failure (reported from 36 to 70%), a chest pain (30%) and a dyspnea (25%).[4,5] Only 10-13% of patients with pseudoaneurysm are asymptomatic. Pseudoaneurysm has propensity for a rupture with a fatal outcome in about half of the cases.[6] Pseudoaneurysms are usually located on the posterolateral or upper lateral site of the left ventricle but usually not in the anterolateral region as in our case.[2,7,8]

Diagnosis of PSALV is mostly confirmed with ventriculography, echocardiography, pulse Doppler, computed tomography (CT), and recently with magnetic resonance imaging (MRI).[9-14] We confirmed the diagnosis of a PSALV with echocardiography and CT scan that are very effective imaging methods for accurate diagnoses of cardiovascular anomalies.[13-16]

Case report

We present a pseudoaneurysm in the anterolateral part of the left ventricle in a patient with dilated alcoholic cardiomyopathy who suffered a heart failure a few months ago after a silent myocardial infarction. Our patient was a 56-year-old man who was an alcoholic and his general practitioner reported a repeated abuse of alcohol despite of the psychiatric treatment. We observed a dilated cardiomyopathy for 5 years before he was admitted to our hospital and it had also been confirmed that he had hepatic cirrhosis Child A 7 years before he was admitted to our hospital. He had been treated for heart failure with the ACE inhibitor and spironolactone but he did not take his medication regularly. We conclude that dilatative cardiomyopathy and hepatic cirrhosis was due the alcohol abuse. Eight months prior the patient's admittance in hospital, the main finding of the echocardiography was a dilated cardiomyopathy with a severely reduced ejection fraction, but without o segmental loss of contractility or aneurysm of the left ventricle. He was also a smoker.

At admission to our hospital the patient complained about progressive dyspnoea, syncope, confusion and 10 kg weight loss during previous 2 months. At physical examination the patient was found to be confused, he had cachexia (56 kg) and jaundice, with blood pressure of 120/95, a regular pulse of 125 beats/min, respiratory rate 27 breaths/min. He had a jugular venous distension to the angle of the jaw at 30 degrees. The chest examination showed dullness on percussion in the basal part of the lungs. The cardiac examination was unremarkable. The liver was enlarged and there was peripheral oedema.

On hospital day 1 we performed haematological tests which were normal except mild makrocytosis (MCV 97 fl). Liver function tests were pathological (total bilirubin 264 μmol/L, direct bilirubin 208 μmol/L, sAST - serum aspartate aminotransferase 1,22 μkat/L, sALT – serum alanin aminotransferase 2,58 μkat/L, γGT - gama glutamiltranspeptidase 0,59 μkat/L, alkaline phosphatase 2,14 μkat/L), he had hyperammoniemia (194 μmol/L) and INR were prolonged (1,68). The levels of cardiac enzymes and troponine were normal. N-terminal pro-B-type natriuretic peptide (NT-proBNP) was highly elevated (24357 ng/L). EKG showed sinus tachycardia 128 beats/min and QS from V1 to V6 with non-specific mild elevation of ST segment. Chest X-ray showed a large soft-tissue mass contiguous with the apical aspect of the heart (Figure 1). We

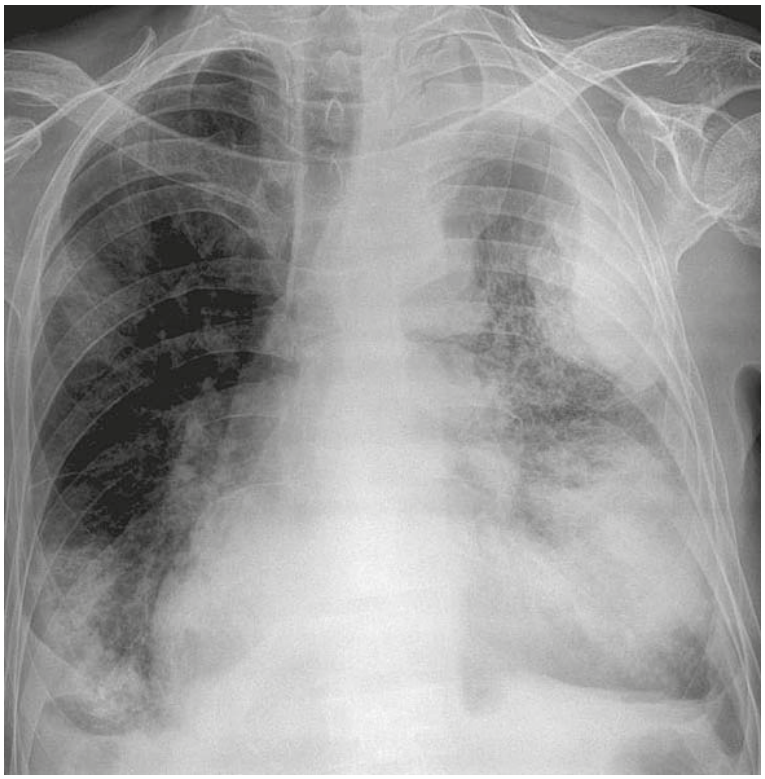

FIGURE 1. Frontal radiograph shows a bulge projected from anterolateral aspect of the ventricle and pleural effusion.

concluded that the patient had the symptoms of hepatic coma and fluid retention due the heart failure. We started treatment with lactulose and furosemid. We also increased the dose of ACE inhibitor and added carvedilol. Hyperammoniemia was resolved with a treatment and the patient became orientated after 3 days. Echocardiography demonstrated an enlarged diastolic volume of the left ventricle (183 ml) with a severely depressed ejection fraction (the left ventricular volume and the ejection fraction were calculated on 10% using bi-plane Simpson's rule). In the apex there was an abrupt interruption of the left ventricular wall, constituting a narrow necked communication between the left ventricular cavity and the pseudoaneurysm, which contains thrombus. We also performed abdominal ultrasound which showed an increase in the echogenicity of the liver and distended hepatic veins consistent with an alcohol-induced liver disease and a heart failure. After 5 days we repeated chest X-ray which showed no difference according to the previous one. CT was performed for further diagnostic step using sagittal and axial cine mode images and showed more precisely a pseudoaneurysm with the site of cardiac rupture. The size of pseudoaneurysm with orifice measured 45 mm

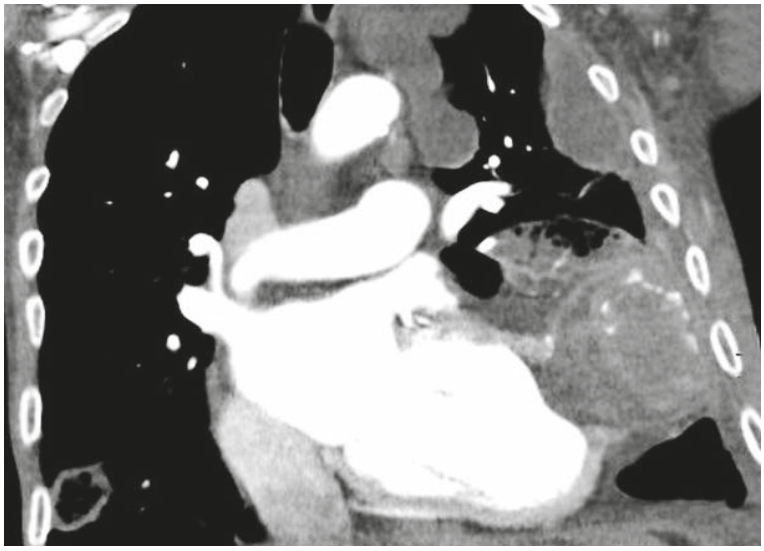

FIGURE 2. CT image shows a neck created by the orifice of the ruptured myocardium and a large thrombus occupying pseudoaneurysmal cavity.

and a cavity of the pseudoaneurysm was larger than orifice and measured 75 mm, including a large thrombus measured 55 mm in length and 70 mm in width (Figure 2). Cardiac Surgery Centre was consulted, but due to the low ejection fraction and no response on heart failure therapy the directive for the resection was tempered. We increased a dose of low molecular heparin and added dobutamine but despite that, progressive heart failure and embolic phenomenon resulted in death.

The pathology report confirmed the presence of marked variations in myocyte size; some myocardial cells were hypertrophied and others were atrophied. There were areas of interstitial and perivascular fibrosis. The report was consistent with the dilated cardiomyopathy. Atherosclerosis was found particularly in the left anterior descending (LAD) coronary artery without thrombosis. Apical aneurysm included only fibrous tissue, pericardium and no myocardial cells consistent with a pseudoaneurysm. There were embolic masses in pulmonary circulation beside congestion of the lung.

Discussion

The PSALV is a rare complication of myocardial infarction in which a ventricular free wall rupture at necrosis site and escape of blood are locally contained by adherent pericardium shaping the aneurysmatic sac. The sac progressively enlarges and its internal surface is covered by thrombus. Less often PSALV has been reported in association with cardiac trauma, myocarditis, infective endocarditis, cardiac surgery, rheumatic fever, syphilis and tuberculosis.[17]

PSALV is usually presented with non-specific symptoms as in our case where the patient complained of dyspnoea, syncope, confusion and weight loss. On admission the patient had clinical manifestation of heart failure and also plasma N-terminal pro-brain natriuretic peptide (NT-proBNP) confirmed the diagnosis of heart failure. We also observed Q waves and ST segment changes which are common although non-specific signs of PSALV. Chest X-ray abnormalities are present with abnormal cardiac contour or cardiomegaly in more than 95% of patients. We also observed a large soft-tissue mass contiguous with the apical aspect of the heart (Figure 1). The enlargement of the aneurysm on sequential radiographs is a characteristic feature of false aneurysm observed in more than 50% of patients.[17] The initial findings of mass on chest X-ray and non-specific electrocadiographic changes require further diagnostic steps and transthoracic echocardiography is usually the first imaging modality used for this purpose.

The most characteristic echocardiographic criteria of PSALV which were also confirmed in our patient include: the saccular space outside the left ventricle, break in the contour of the myocardium, an orifice diameter smaller than the cavity of the pseudoaneurysm and the presence of thrombus in the internal wall of the aneurysmatic sac. The communication between the ventricle and the cavity differentiates the pseudoaneurysm from localized pericardial effusion or haematoma, and a pericardial cyst.[7,10] The major limitation of transthoracic echo is a limited acoustic window so that the pseudoaneurysm orifice could not be accessible to the ultrasound beam.

Although the diagnosis of PSALV is established by transthoracic echocardiography, further imaging with CT or MRI should be performed because pericardial mass can usually not be differentiated with echocardiography as a true or false aneurysm. The difference between true and false aneurysms is clinically important because false aneurysms have propensity for rupture.[1,2,6] With the CT scan a more distinct depiction of the site of the cardiac rupture, the extent of the rupture, the size and location of PSALV are showed (Figure 2). The same information can be obtained with the MRI. As in our case, the histological examination finally confirms the diagnosis of the PSALV where the wall of the false aneurysm has no remnants of myocardial tissue which is the major distinction to true aneurysms.

Most reports considered surgery as the appropriate treatment for PSALV since untreated pseudoaneurysms have an approximately 30% to 45% risk of rupture. Mortality rates are in patients who underwent surgery from 19% to 35% what was significantly lower than in those who were treated medically (48% to 55%). Operative mortality in most reports is related to the severity of the contractile dysfunction in the reminder of the ventricle.[4,5]

In our patient physical findings and laboratory evidence of a liver failure (confusion due hyperamoniemia, abnormal prothrombin time and hypoalbuminemia in addition to elevated aminotransferases) with a documented history of alcohol abuse were consistent with the diagnosis of the alcoholic liver disease. The liver disease was combined with dysfunction of heart due to dilated alcoholic cardiomyopathy and coronary artery disease which was complicated with PSALV.[16] The most possible scenario concerning our patient was that the anterolateral myocardial infarction was complicated by the subacute free wall rupture which resulted into pseudoaneurysm formation without tamponade. Although the time of acute necrosis or the moment of cardiac rupture cannot be precisely determined it must have occurred after the echocardiography, which had been done eight months before the patient was admitted to our hospital, (during the echocardiography we did not observe PSALV) and before the clinical deterioration which was reported two months before hospitalisation. Because of pre-existing dilated cardiomyopathy due to alcohol abuse with a severe reduced ejection fraction PSALV did not rupture for quite a long period of time. Dilated cardiomyopathy also enabled the survival of rare aneurism in the anterolateral surface of the left ventricle which usually leads to haemopericardium and death. Besides the normal value of cardiac necrosis enzymes and the ECG changes did not reveal recent acute transmural necrosis. The existence of large laminated thrombus makes us speculate that acute necrosis and cardiac rupture occurred a long time before the admission. Because of no response in drug therapy for congestive heart failure in our patient the directive for the resection was tempered and the patient died due to the progressive heart failure and embolic phenomena.

Conclusions

This report highlights the importance of basic non-invasive imaging diagnostic evaluation (echocardiography and chest X-ray) of the acute decompensated heart failure and afterwards the decision for further non-invasive imaging modalities or invasive cardiologic imaging. The case shows that we cannot presume the diversity or combination of the clinical picture based on the clinical ground. CT scan finally differentiates left ventricular pseudoaneurysm from true aneurysm as the complication of a silent myocardial infarction in our patient with alcoholic dilatative cardiomyopathy.

References

1. Dachman AH, Spindola-Franco H, Solomon N. Left ventricular pseudoaneurysm. Its recognition and significance. *JAMA* 1981; **246:** 1951-3.
2. Martin RH, Almond CH, Saab S, Watnon LE. True and false aneurysms of the left ventricle following myocardial infarction. *Am J Med* 1997; **62:** 418-24.
3. Davidson KH, Paris A, Harrington J, Barsamian E, Fischbein M. Pseudoaneurysm of the left ventricle: an unusual echocardiographic presentation. Review of the literature. *An Intern Med* 1977; **86:** 430-3.
4. Frances C, Romero A, Grady D. Left ventricular pseudoaneurysm. *J Am Coll Cardiol* 1998; **32:** 557-61.
5. Eren E, Bozbuga N, Toker EM, Keles C, Rabus MB, Yildirim O, et al. Surgical treatment of post-infarction left ventricular pseudoaneurysm. *Tex Heart Inst J* 2007; **34:** 47-51.
6. Zoffoli G, Mangino D, Venturini A, Terrini A, Asta A, Zanchettin C, et al. Diagnosing left ventricular aneurysm from psudo-aneurysm: a case report and a review in literature. *J Cardiothorac Surg* 2009; **4:** 11.
7. Stoddard MF, Dawkins RP, Longaker RA, Shih A. Transesophageal echocardiography in the detection of left ventricular pseudoaneurysm. *Am Heart J* 1993; **125:** 534-9.
8. Raquel M, Tegtmeier T, Smith SA, Ognibene A. Left ventricular pseudoaneurysm presenting twenty-eight months after myocardial infarction. *Angiology* 1997; **48:** 177-81.
9. Tuan J, Kaivani F, Fewins H. Left ventricular pseudoaneurysm. *Eur J Echocardiogr* 2008; **9:** 107-9.
10. Cho MN, Mehta SK, Matulevicius S, Weinstein D, Wait MA, McGuire DK. Differentiating true versus pseudo left ventricular aneurysm. A case report and review of diagnostic strategies. *Cardiol Rev* 2006; **14:** 27-30.
11. Harrity P, Patel A, Bianco J, Subramanian R. Improved diagnosis and characterization of postinfarction left ventricular psudoaneurysm by cardiac magnetic resonance imaging. *Clin Cardiol* 1991; **14:** 603-6.
12. Prakash S, Garg N, Xie GY, Dellsperger KC. Giant left ventricular pseudoaneurysm. *J Cardiovasc Comput Tomogr* 2010, **4:** 284-5.
13. Beslic S, Beslic N, Beslic S, Sofic A, Ibralic M, Karovic J. Diagnostic imaging of traumatic. pseudoaneurysm of the thoracic aorta. *Radiol Oncol* 2010; **44:** 158-63.
14. Kim MN, Park SM, Kim SW, Lee KN, Kim JS, Kang EJ, et al. Progression of left ventricular pseudoaneurysm after an acute myocardial infarction. *J Cardiovasc Ultrasound* 2010; **18:** 161-4.
15. Mukhopadhayay S, Yusuf J, Mehta V, Nathani S, Goyal V. Pseudoaneurysm of the left ventricle in a young asymptomatic female. *Echocardiography* 2010; **27:** 329-31.
16. Gjikolli B, Hadzihasanovic B, Jaganjac S, Herceglija E, Niksic M, Hadzimehmedagic A, et al. Treatment of complicated case with subclavia steal syndrome and stenosis of common iliac artery. *Radiol Oncol* 2008; **42:** 1-12.
17. Higgins BC, Lipton MJ, Johnson AD, Peterson KL, Vieweg WVR. False aneurysms of the left ventricle. *Radiology* 1978, **127:** 21-7.
18. Masani F, Kato H, Sasagawa Y. An echocardiographic study of alcoholic cardiomyophaty after total abstinence. *J Cardiol* 1990, **20:** 627-34.

research article

Scatterogram: a method for outlining the body during lymphoscintigraphy without using external flood source

Mehdi Momennezhad[1], Seyed Rasoul Zakavi[1], Vahid Reza Dabbagh Kakhki[1], Ali Jangjoo[2], Mohammad Reza Ghavamnasiri[3], Ramin Sadeghi[1]

[1] Nuclear Medicine Research Center, Mashhad University of Medical Sciences, Mashhad, Iran
[2] Surgical Oncology Research Center, Mashhad University of Medical Sciences, Mashhad, Iran
[3] Cancer Research Center, Mashhad University of Medical Sciences, Mashhad, Iran

Received 13 January 2011
Accepted 27 January 2011

Correspondence to: Ramin Sadeghi, MD, Assistant Professor of Nuclear Medicine, Nuclear Medicine Research Center, Imam Reza Hospital, Mashhad University of Medical Sciences, Ebn Sina Street, Mashhad, Iran. Phone: +98 (511) 802 2729; Fax: +98 (511) 859 9359; E-mail: Sadeghir@mums.ac.ir

Disclosure: No potential conflicts of interest were disclosed.

Background. We evaluated the feasibility of outlining the body with scattered photons using a low dose intradermal injection of the radiotracer.

Patients and methods. Sixty breast cancer patients were included into the study. 30 minutes post radiotracer injection static lymphoscintigraphy images were acquired using low energy high resolution collimator in anterior and lateral views. For patients with 2-day protocol another set of images was taken 20 hours post-injection. Two photopeaks were used during imaging: 1-Tc-99m (130-150 keV) and 2- Scatter photons (60-120). The fusion image of these two images was constructed by NM-NM fusion workflow of the workstation. The usual body outline of the patients was also acquired in 20 cases using the external flood source without moving the patients from their positions.

Results. The early (30 minute image) scatterograms of the patients clearly showed the contour of the body. The 20 hour scatterograms were not as high quality as the corresponding early images. The constructed overlaid images showed the location of the axillary sentinel nodes and the body contours clearly for early scatterograms but not the delayed (20 hour) ones. The processing of the images for the reconstruction of overlaid scatterograms took the mean time of 10±5 seconds.

Conclusions. Imaging the scattered photons is feasible for the intradermal low dose injection of the radiotracers in order to outline the body contour. This imaging method does not increase the radiation exposure of the patients or operators and does not extend the time of imaging either.

Key words: breast cancer; scattered photons; body outlining; lymphoscintigraphy; intradermal injection; body contour

Introduction

Sentinel lymph node biopsy is considered as the standard method for axillary staging of breast cancer patients without clinically involved axilla which can significantly decrease the morbidity of these patients.[1,2] Lymphoscintigraphy with gamma cameras can show the sentinel lymph nodes and is recommended to be performed before surgery.[3] However, plain lymphoscintigraphy images do not show any anatomical detail or exact location of the sentinel nodes in axilla which are very important factors for surgery planning.[4] Skin pen marking[1], stereoscopic lymphoscintigraphy[5] and body outlining[6] are three solutions to deal with this problem. Several methods are in use for outlining the body contour during lymphoscintigrpahy imaging with their own advantages and drawbacks.[7] These include: (1) moving a small point source of Tc-99m around the edge of the patient manually[4,8]; (2) external sources of gamma rays such as Co-57 flood source[9] and Gd-153 line source[4]; (3) imaging the scattered photons of the injected radiotracer[10] and (4) intravenous injection of a small amount of Tc-99m-pertechnetate.[11]

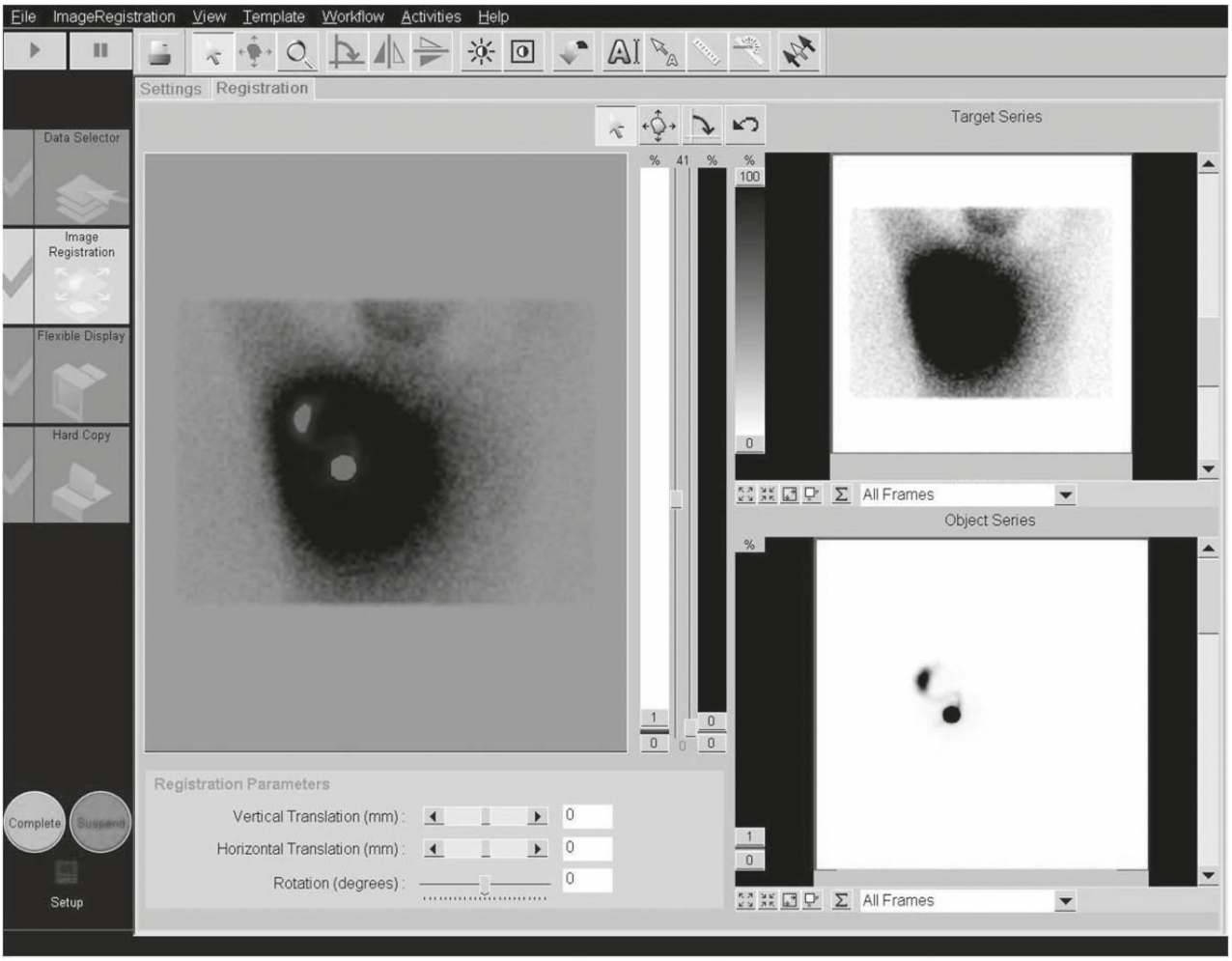

FIGURE 1. NM-NM fusion workflow. We used this workflow to construct the overlay image of the lymphoscintigraphy and scattered photons. The original images with Tc-99m photopeak and scatter photopeaks are shown on the right side of the image. The constructed overlay image is shown on the left side. Note clear visualization of the axillary sentinel node as well as the outline of the patient.

Imaging the scattered photons (which we call scatterogram) is an easy way to outline the body during lymphoscintigraphy imaging without any additional radiation exposure to patients and technologists. This method has been previously described by Fujii *et al.*[10,12] for breast cancer patients using peritumoral injection of 111 MBq radiotracer. We routinely use intradermal injection of 18.5-37 MBq Tc-99m-antimony sulfide colloid for sentinel lymph node mapping.[1] In the current study we evaluated the feasibility of outlining the body with scattered photons for this protocol of sentinel lymph node biopsy.

Patients and methods

Sixty female patients with the diagnosis of breast cancer without clinically involved axilla were included into the study. The intradermal injection of Tc-99m-antimony sulfide colloid (18.5 MBq or 37 MBq for 1 day and two-days protocols respectively) was used in a peri-areolar fashion. Static lymphoscintigraphy images were acquired 30 minutes post-injection using a dual head variable angle gamma camera (E.CAM Siemens) equipped with low energy high resolution collimator in anterior and lateral views (5 minutes/image and 128×128 matrix). For patients with 2-day protocol another set of images was taken 20 hours post-injection. Two photopeaks were used during imaging: 1-Tc-99m photopeak (130-150 keV) and 2- Photopeak for scatter photons (60-120). The outputs of each photopeaks were saved as separate images in the computer. The fusion image of these two images (lymphoscintigraphy with Tc-99m photopeak and the scatterogram) was constructed by NM-NM fusion workflow of the workstation after normaliz-

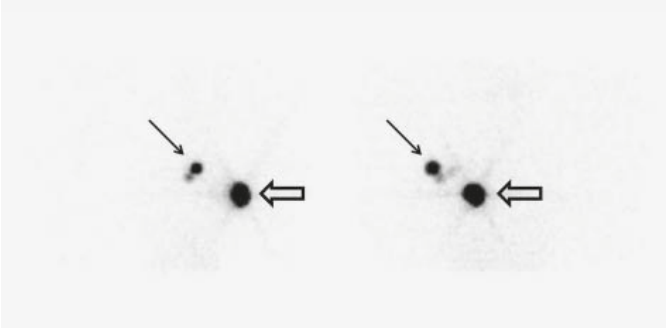

FIGURE 2. Anterior (right) and Lateral (left) lymphoscintigraphy images of a patient. Note the injection site (hollow arrows) as well as sentinel nodes (arrows).

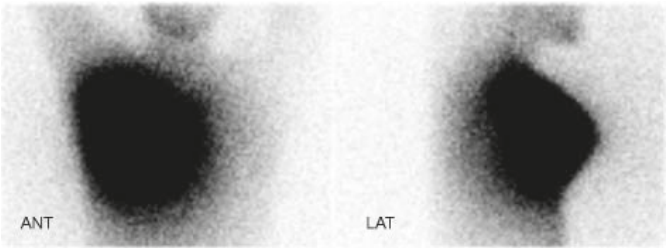

FIGURE 3. Anterior (left) and Lateral (right) scatter photon images of a patient acquired 30 minutes post-injection. Note clear visualization of body outline.

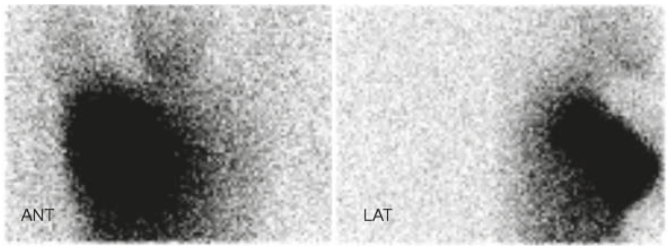

FIGURE 4. Anterior (left) and Lateral (right) scatter photon images of the patient shown on Figure 3. acquired 20 hours post-injection. Note poor quality of the images.

ing the intensity of the images to the sentinel node activity for the Tc-99m and the corresponding area for the scatterogram images. The images were simply overlaid on each other (Figure 1). The usual body outline of the patients was also acquired in 20 cases using external flood source without moving the patients from their positions. The resulting overlaid images were compared with the usual lymphoscintigraphy as well as outline images of the patients considering the quality of body outlining and anatomical location of the sentinel node in the axilla by two nuclear medicine specialists.

After the completion of the imaging, the patients were sent to the surgery ward for usual axillary sentinel node mapping with gamma probe as well as blue dye injection.

TABLE 1. Characteristics of the patients

Total number of patients	60
Age	34±3
Tumor size	2.2±1.2
Tumor location	
Upper outer	25
Upper inner	15
Lower outer	7
Lower inner	8
Central	5
Histological type	
Invasive ductal	45
Invasive lobular	15
Biopsy type	
Excisional	20
Core needle	40
Time of surgery	
One-day protocol	22
Two-day protocol	38

Results

Characteristics of the patients are shown in Table 1. Lymphoscintigraphy images showed at least one axillary sentinel node in all patients (Figure 2). The early (30 minute image) scatterograms of the patients clearly showed the contour of the body (Figure 3). The 20 hour scatterograms were not as high quality as the corresponding early images and the body contours could not be clearly identified on these images (Figure 4). The constructed overlaid images showed the location of the axillary sentinel nodes and the body contours clearly for early scatterograms but not the delayed (20 hour) ones (Figure 1). In comparison with the corresponding outline images of the patients (using external flood source), no discordance was found regarding the body contour of the patients (Figure 5). No extra-axillary lymph drainage was noticed in our patients.

The processing of the images for the reconstruction of overlaid scatterograms took the mean time of 10±5 seconds.

Discussion

As mentioned before several methods are in use for outlining the body contour during lymphoscintigraphy imaging. Providing the outline of the body can help the surgeons for better planning of the surgery with resulting the decrease in patients' morbidity.[13,14]

The injection of small dose of Tc-99m-Pertechnetate to the patients can delineate the body outline as described by Klutmann *et al*. However, this method imposes an additional injection to the patients and also increases the radiation exposure.[11]

Manual outlining of the body using a Tc-99m point source and moving it around the patient's edge is another way of body outlining. However, the images by this method are of low quality and still there is the additional radiation exposure to the patients and technologists.[4]

Using external gamma sources such as Co-57 and Gd-153 is another option. Despite using several methods for decreasing the radiation exposure[7,9], Co-57 flood source poses additional radiation to the patients and personnel.[4] Although additional radiation to the patients is lower with Gd-153 line sources[4], acquiring body outline image with this method extends the time of examination which can interfere with the operation room scheduling. This is also true for all the methods mentioned above.[10]

The scattered photons of Tc-99m gamma rays are mainly the results of Compton scattering. As described by Fujii *et al*., these photons occur everywhere in the body of the patients and imaging of these photons can show the contour of the body fairly well.[10] We used the same method as described by Fujii *et al*. However, they used 111 MBq of the tracer in the peri-tumoral fashion.[10] We use the intradermal injection of 18.5-37 MBq of the radiotracer for sentinel node mapping which produces less scattered photons compared to the Fujii *et al.* protocol. To obviate this problem we used the energy window of 60-120 keV for imaging of the scattered photons which is wider than the one used by Fujii *et al.* (70-110 keV).

Our study showed the same favourable results as the previous ones by a Fujii group. However, the images taken 20 hours post-injection were not of good quality at all which was due to scarcity of the scattered photon at the time of imaging.

One disadvantage of outlining the body with scattered photons is the non-homogenous distribution of these photons across the body of the patients. The scattered photons are densely distributed near the injection site and their density gradually decreases as the distance from the injection site increases.[12] Because of this non-homogenous distribution of the scattered photons, simple summation of acquired images is not usually feasible since the sentinel node would be obscured and the exact location can not be identified. This is usually more problematic when the injection site is too close to the sentinel node location in the axilla.[12] Fujii *et al.* developed a processing method to obviate this problem by dividing the primary photon image counts by the scattered photon image counts for each pixel after the addition of some constant counts to each pixel of the acquired image.[12] These processing step was done for the compensation of count difference between two set of images. We used the NM-NM fusion workflow of E.CAM workstation to simply overlay the primary and scattered photon images after normalization of the images to the sentinel node counts on the primary photon images and the corresponding location in the axilla on the scattered photon ones. As both images were normalized to their corresponding optimized counts, the problem of the sentinel lymph node masking by the high activity of the injection site would be solved since the processing of each set of image was individualized and the optimal

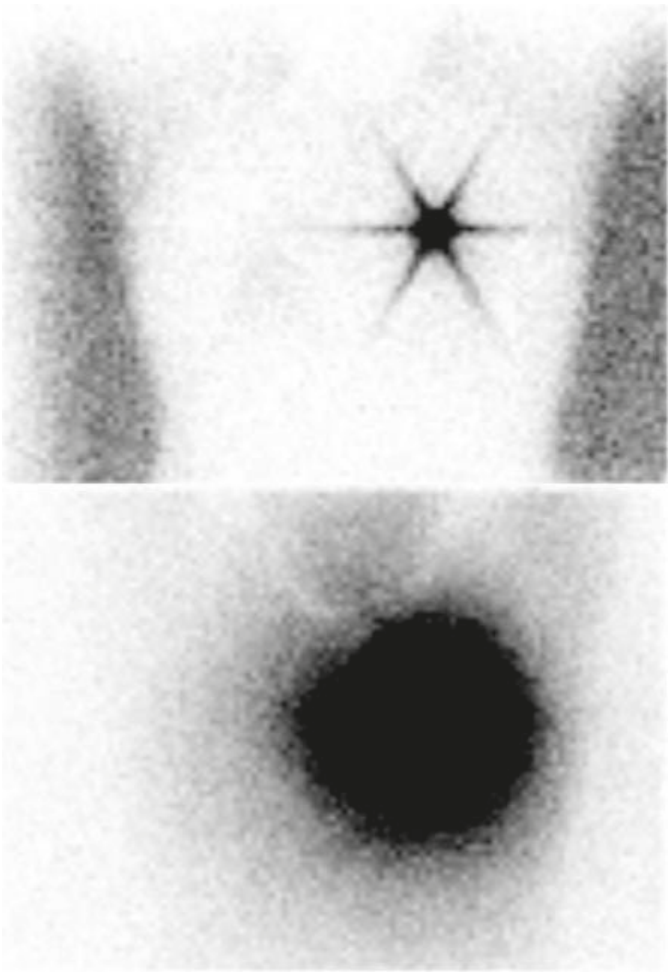

FIGURE 5. Body outline (top) and scatterogram (bottom) images of a patient. Note Concordance of body outlines in these two sets of image.

image for each patient could be reconstructed. Although Krynyckyi *et al.* considered this additional processing a drawback[7], due to the simultaneous acquisition of both primary and scattered photons, there was no need for co-registration of the images and processing step could be done in a short time.

Conclusions

Our study showed that imaging the scattered photons (scatterogram) during lymphoscintigrpahy could be a useful method for outlining the body contour of the patients and was feasible for the intradermal low dose injection of the radiotracers. This is especially true when the imaging is performed early after the injection of the tracer. This imaging method does not increase the radiation exposure of the patients or operators and does not extend the time of imaging either.

Acknowledgements

This study was financially supported by vice chancellery of research of Mashhad University of Medical Sciences with the approval number of 87623.

References

1. Abdollahi A, Jangjoo A, Dabbagh Kakhki VR, Zakavi SR, Memar B, Forghani MN, et al. Factors affecting sentinel lymph node detection failure in breast cancer patients using intradermal injection of the tracer. *Rev Esp Med Nucl* 2010; **29:** 73-7.
2. Goyal A, Newcombe RG, Chhabra A, Mansel RE. Morbidity in breast cancer patients with sentinel node metastases undergoing delayed axillary lymph node dissection (ALND) compared with immediate ALND. *Ann Surg Oncol* 2008; **15:** 262-7.
3. Goyal A, Newcombe RG, Mansel RE, Chetty U, Ell P, Fallowfield L, et al. Role of routine preoperative lymphoscintigraphy in sentinel node biopsy for breast cancer. *Eur J Cancer* 2005; **41:** 238-43.
4. Clarke E, Notghi A, Harding K. Improved body-outline imaging technique for localization of sentinel lymph nodes in breast surgery. *J Nucl Med* 2002; **43:** 1181-3.
5. Tanaka C, Fujii H, Ikeda T, Jinno H, Nakahara T, Suzuki T, et al. Stereoscopic scintigraphic imaging of breast cancer sentinel lymph nodes. *Breast Cancer* 2007; **14:** 92-9.
6. Krynyckyi BR, Miner M, Ragonese JM, Firestone M, Kim CK, Machac J. Technical aspects of performing lymphoscintigraphy: optimization of methods used to obtain images. *Clin Nucl Med* 2000; **25:** 978-85.
7. Krynyckyi BR, Kim CK, Goyenechea M, Machac J. Methods to outline the patient during lymphoscintigraphy. *J Nucl Med* 2003; **44:** 992; 992-3.
8. Buscombe J, Paganelli G, Burak ZE, Waddington W, Maublant J, Prats E, et al. Sentinel node in breast cancer procedural guidelines. *Eur J Nucl Med Mol Imag* 2007; **34:** 2154-9.
9. Krynyckyi BR, Sata S, Zolty I, Kim CK, Knesaurek K. Reducing exposure from 57Co sources during breast lymphoscintigraphy by optimizing energy windows and other suggested enhancements of acquisition and the display of images. *J Nucl Med Technol* 2004; **32:** 198-205.
10. Fujii H, Yamashita H, Nakahara T, Ikeda T, Kitagawa Y, Iwasaki R, et al. Outlining the body contours with scattered photons in lymphoscintigraphy for sentinel nodes. *Ann Nucl Med* 2000; **14:** 401-4.
11. Klutmann S, Bohuslavizki KH, Hoft S, Kroger S, Brenner W, Tinnemeyer S, et al. Lymphoscintigraphy with double tracer technique in carcinomas of the head-neck region. *Laryngorhinootologie* 1997; **76:** 740-4.
12. Fujii H, Ikeda T, Jinno H, Kitagawa Y, Yamashita H, Seki S, et al. Lymphoscintigraphy for the visualization of sentinel lymph nodes and body contour. *Breast Cancer* 2004; **11:** 250-5.
13. Rucigaj TP, Leskovec NK, Zunter VT. Lymphedema following cancer therapy in Slovenia: a frequently overlooked condition? *Radiol Oncol* 2010; **44:** 244-8.
14. Krynyckyi BR, Shafir MK, Kim SC, Kim DW, Travis A, Moadel RM, et al. Lymphoscintigraphy and triangulated body marking for morbidity reduction during sentinel node biopsy in breast cancer. *Int Semin Surg Oncol* 2005; **2:** 25.

research article

Usefulness of low iodine diet in managing patients with differentiated thyroid cancer - initial results

Margareta Dobrenic, Drazen Huic, Marijan Zuvic, Darko Grosev, Ratimir Petrovic, Tatjana Samardzic

Department of Nuclear Medicine and Radiation Protection, University Hospital Center Zagreb, Zagreb, Croatia

Received 28 December 2010
Accepted 3 May 2011

Correspondence to: Margareta Dobrenić, MD, Department of Nuclear Medicine and Radiation Protection, University Hospital Center Zagreb, Kispaticeva 12, 10 000 Zagreb, Croatia. Phone: +385 1 2388587; Fax: +385 1 2376040; E-mail: margareta.dobrenic@gmail.com

Disclosure: No potential conflicts of interest were disclosed.

Background. Low iodine diet (LID) is recommended in patients with differentiated thyroid cancer before radioiodine administration. Patients with increased thyroglobulin (Tg) level, but negative ^{131}I whole body scan present diagnostic and therapeutic dilemma. This study was designed to evaluate the benefit of a two-week LID in patients with elevated serum Tg levels and negative ^{131}I whole body scans.

Patients and methods. For the impact assessment of two-week LID on radioiodine tissue avidity, radioiodine scans before and after LID were compared. Sixteen patients with serum Tg > 2 μg/L, negative Tg-antibodies, and negative radioiodine scans underwent two-week LID before the ^{131}I administration. Fourteen patients underwent diagnostic scanning and two patients received radioiodine therapy. Iodine concentration in the morning urine specimens were measured in each patient, a day before and 15th day after starting LID.

Results. Following self-managed LID, patients were able to significantly reduce their iodine body content by 50% (range 28-65%, p<0,001). 13 patients (82%) accomplished mild iodine deficiency (50-99 μg/L) and one patient (6%) achieved targeted moderate iodine deficient state (<50 μg/L). All diagnostic post-LID scans were negative. Both post-therapy ^{131}I scans showed radioiodine accumulation outside of normal ^{131}I distribution (neck region and diffuse hepatic uptake). This study demonstrated that two-week LID is effective way to decrease total body iodine content, although without a visible effect on post-LID diagnostic ^{131}I scans.

Conclusions. A more stringent dietary protocol and longer iodine restriction period are probably needed to achieve targeted moderate iodine deficiency in patients preparing for ^{131}I administration. This might result in higher radioiodine avidity of thyroid remnant/metastases.

Key words: low iodine diet; urine iodine concentration; differentiated thyroid cancer; radioiodine

Introduction

A follow-up of patients with differentiated thyroid cancer (DTC) is a lifelong process. The goals of monitoring after the initial therapy are to maintain the adequate thyroid hormone therapy and to detect persistent or recurrent thyroid cancer. When used at the same time, serum thyroglobulin (Tg) levels measurement and ^{131}I whole body scanning offer best possibilities in the patients' follow-up.[1] Serum Tg is a tumour marker and radioiodine scans localize tumour sites. To enhance ^{131}I uptake in whole body scans, thyrotropin (TSH) levels should be above 30 mU/L prior to ^{131}I administration for either diagnostic or therapeutic purposes.[2] This could be achieved by a withdrawal of thyroid hormone therapy, resulting in symptomatic hypothyroidism before and during the testing period. Alternative to the thyroid hormone withdrawal is an administration of recombinant human TSH (rh-TSH) in euthyroid patients.[3]

When ^{131}I scanning or therapy is planed, patients are also instructed to follow a low iodine diet (LID), which basically means avoiding the iodine-rich food and iodine-containing medications.[4] LID is designed to decrease the total body stable iodine

concentration prior to radioiodine administration. Pluijmen *et al.* demonstrated the increase of radioiodine uptake by 65% in thyroid remnant and also longer effective half-life of ^{131}I, both of which contributed to the increase of the absorbed radiation dose.[5] Most centres advise a two-week low iodine diet prior to the ^{131}I administration.[4,6]

Urinary iodine excretion is a good marker of the recent dietary iodine intake. According to the World Health Organization's report, profile of iodine concentrations in the morning urine specimens provides an adequate assessment of the recent dietary iodine intake.[7] Furthermore, according to the same report, urinary iodine concentration less than 50 μg/L reflects a moderate iodine deficiency, while urinary iodine concentration >50 μg/L and <99 μg/L indicates a mild iodine deficient state.

Patients with elevated serum Tg level and negative ^{131}I whole body scan present a diagnostic and a therapeutic challenge. One of the possibilities for such a finding is that neoplastic thyroid tissue is still capable to produce thyroglobulin but is unable to accumulate ^{131}I, suggesting tumour dedifferentiation.[8] The other possibility is that thyroid cancer metastases/remnant tissue is blocked with stable iodine. The identification of the Tg production site may dictate appropriate treatment modalities, for instance, surgery in the case of lymph node metastases and resectable distant lesions, or ^{131}I therapy in radioiodine-avid metastases and thyroid remnant tissue.

The aim of this study was to evaluate the influence of decreased total body iodine level on radioiodine avidity of possible thyroid remnants, tumour recurrences or metastases after a two-week LID.

Methods

Patients

Sixteen patients (11 women, 5 men, median age 55) with DTC who fulfilled the criteria of serum Tg concentration above 2 μg/L, negative thyroglobulin-antibodies (TgAt<20 U/mL) and negative ^{131}I whole body scan were selected for this study. All patients underwent total thyroidectomy and ^{131}I thyroid remnant ablation as an initial therapy. Ten patients (63%) had papillary and 6 patients (37%) had follicular cancer. A postsurgical ^{131}I administration was performed in all patients in hypothyroid state with 888-5550 MBq (24-150 mCi) 4-6 weeks after the surgery. Applied ^{131}I activity depended on tumour size and initial cancer extension. In the follow-up all patients had negative ^{131}I whole body scans, but in seven patients the other diagnostic studies (computed tomography, chest x-ray and fine needle aspiration (FNA) cytology) suggested recurrent thyroid cancer. In five of them small nodules in lungs were found and in one patient bone lesions were suspected. One patient had lymph node metastasis in the neck region (proven by FNA cytology) but was not willing to the surgical treatment. Trying to find out whether there is any uptake of radioiodine, the same patients were scheduled for control ^{131}I whole body scans 12-18 months after the last scanning, but now after two-week LID. All of them were withdrawn from L-thyroxin therapy for four weeks prior to ^{131}I scanning. The serum Tg concentration was measured with elevated TSH (TSH>30 mU/L in all patients).

All fourteen patients who received diagnostic activity of ^{131}I had serum Tg level between 2 and 6 μg/L before LID. Since the empiric ^{131}I therapy is justified in patients with Tg levels > 10 μg/L and negative ^{131}I whole body scan[9], two of our patients underwent the empiric radioiodine therapy (serum Tg value was 22.4 μg/L in one patient and 24.9 μg/L in another). In those patients gradually rising serum Tg levels were observed after the initial

TABLE 1. Epidemiological and clinical features of patients

	Patients (N=16)
Age (yr)	
Median	55
Range	43 – 69
Sex	
Female	11 (69%)
Male	5 (31%)
Histological type	
Papillary	10 (63%)
Follicular	6 (37%)
Peak TSH (mU/L) (Patients N=12)	
Median	72.3
Range	46.5 – 99.7
TSH> 100 mU/L (Patients N=4)	
Serum Tg concentration (μg/L)	
Median	5.0
Range	2.5 – 55.9
Administrated activity of ^{131}I (MBq)	185 (diagnostic)
	3700, 7400 (therapy)
Range	185 – 7400

TABLE 2. Low iodine diet – recommendations by University Hospital Center Zagreb

Avoid the following food
Iodized salt, sea salt and salty food
Many prepared and/or cured meat (ham, bacon, sausage)
All dairy products (milk, cheese, cream, sour cream, yogurt, butter, ice cream)
Egg yolk, commercial bakery products, chocolate, dried fruit, canned vegetables, beans
Sea food and sea products (fish, shellfish, crawfish, calamari, black fish, octopus, seaweeds)
Food containing red food dyes (candies, liqueurs, cocktails)
Iodine-containing vitamins and food supplements (check the label and ingredients and discontinue completely if iodine is included)
Medications: Betadine, Rocaltrol 0.5μg (use Rocaltrol 0.25 μg instead)
Food that is fine to eat
Fresh fruit and vegetable (but not too much spinach and broccoli), washed well
Vegetable can be prepared with vegetable oil and no iodized salt
Fresh no cured meat from the butcher, vegetable oil, egg white
Home-made bread (without iodized salt, milk, butter or egg yolks), pasta (without egg yolks)
Sugar , honey, clear fruit juice, tea, coffee (without milk and cream)
Canned peaches, pears and pineapples

treatment. There are not any data about receiving iodinated contrast media in the six months prior to the diagnostic or therapeutic ^{131}I administration. Epidemiological and clinical characteristics of the selected patients are summarized in Table 1.

Low iodine diet

Low iodine diet was explained to the patients and they were sent home with a list of dietary recommendations (Table 2). Patients have been told to follow LID for two weeks prior to the ^{131}I administration.

Urine iodine

Two morning urine specimens were obtained from each patient to assure the adequate diet preparation has been achieved. The first urine sample was taken a day before starting a LID and the second sample after a two-week LID performance, a few hours before the ^{131}I application. Both specimens were immediately deep frozen for further determinations of urinary stable iodine. The determination of urinary iodine concentration was based on the manual spectrophotometric measurement of Sandell-Kolthoff reduction reaction catalysed by iodine.[10-12] Spectrophotometer Camspect M350 Double Beam was used. Sensitivity of the method is 5 μg of iodine/L. WHO recommends the expression of urinary iodine concentration as a simple iodine concentration (μg/L), without the urinary creatinine measurement or 24 h urine collection.[7] Final results were expressed as iodine concentration (μg/L).

Dietary efficacy

Categories of iodine depletion were based upon WHO's criteria of the iodine nutrition status.[7] Urinary iodine concentration less than 50 μg/L reflects a moderate iodine deficient state and was the aimed value in this study. Urinary iodine concentration >50 μg/L and <99 μg/L indicates a mild iodine deficient status and is suboptimal, but still an adequate preparation for the radioiodine administration. Urinary iodine concentration >100 μg/L and < 199 μg/L represents the adequate iodine nutrition status.

Radioiodine (^{131}I) scintigraphy

Gamma camera imaging of ^{131}I distribution in patients was performed using either DIACAM (Siemens Gammasonics, Inc.,Hoffman Estates, IL) single-head camera or SYMBIA E (Siemens Gammasonics, Inc.,Hoffman Estates, IL) dual-head camera. Both cameras have similar characteristics: rectangular field of view (53.3x38.7 cm), 9.5 mm NaI (Tl) detector crystal thickness and high-energy collimators. Patient scintigraphy acquisitions included: a whole body planar anterior scan (acquisition matrix: 256 x 1024), and static anterior scan of the neck and the thorax region with a preset number of 150 000 counts.

At the same day of the ^{131}I administration, the morning urine sample for the urinary iodine concentration measurement was taken. Fourteen patients who underwent diagnostic post-LID radioiodine scans received 185 MBq (5 mCi) of ^{131}I activity each, and acquisitions were performed 48h after the radioiodine administration. Two patients with Tg level higher than 22 μg/L have been scheduled for radioiodine therapy and received 3700 MBq (100 mCi) and 7400 MBq (200 mCi) of ^{131}I, respectively. Post-therapy scans following LID were made 72 h after the radioiodine administration.

Radioiodine scans were assessed visually.

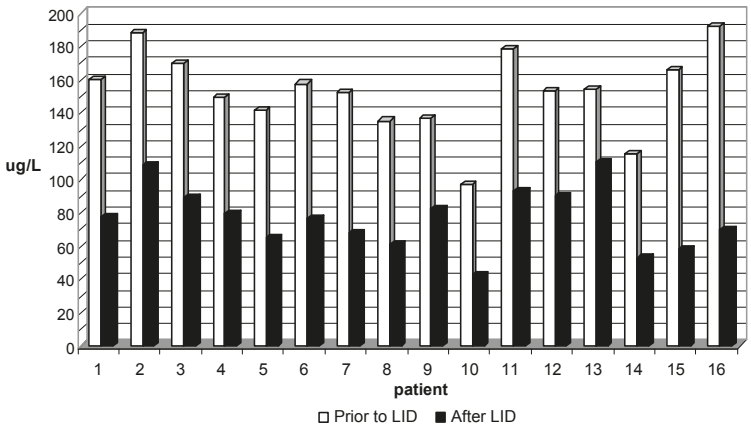

FIGURE 1. Urine iodine concentration (μg/L) for each patient prior to and after low iodine diet (LID).

Statistical analysis

T-test: paired two sample for means was used to test the difference between groups. A statistical result was considered significant if $p< 0.001$.

Results

Dietary performance

Urine iodine concentration values based on the single morning urine sample are presented in Figure 1 and Table 3. Fifteen patients (94%) had an adequate iodine intake prior to LID and, therefore were optimally iodine nourished. One patient (6%) was mild iodine deficient before LID. Following self-managed LID, patients were able to significantly reduce their iodine body content by 50% (mean±SD: 50±9, range: 28-65, $p<0.001$). 88% of patients were iodine deficient after two-week LID. 82% of patients (n=13) accomplished mild iodine deficiency (50-99 μg/L) and one patient (6%) achieved a targeted moderate iodine deficient state (<50 μg/L). Two patients (12%) had the iodine sufficient status (>100 μg/L) even after two-week low iodine diet preparation.

Post-low iodine diet (post-LID) radioiodine scans

Fourteen patients underwent diagnostic ^{131}I scan after two-week LID and all post-LID radioiodine scans were negative. Six of those patients had morphological findings suggestive of recurrent thyroid cancer in neck lymph node, lungs and bones. Patients with lung and bone metastases were mild iodine deficient after LID. The patient with a neck lymph node metastasis was sufficient iodine nourished even after two-week LID performance. On the other hand, on both post-therapy ^{131}I scans some radioiodine accumulation outside of the normal ^{131}I distribution was visible. The patient who received 3700 MBq of ^{131}I had focal radioiodine accumulation in the neck region. He was the only one who had the aimed moderate iodine deficient status after LID and, therefore, was optimally prepared for the ^{131}I administration. His serum Tg value prior to LID and the empiric ^{131}I therapy was 22.4 μg/L (Figure 2).

The patient with small pulmonary nodules seen on computed tomography images had a diffuse increased ^{131}I uptake in liver after the radioiodine therapy with 7400 MBq. There was no focal or diffuse accumulation of radioiodine seen in lungs. This patient was mild iodine deficient after LID and, therefore, was suboptimal prepared for the radioiodine administration. His serum Tg level before LID and empiric radioiodine therapy was 24.9 μg/L (Figure 3).

Discussion

In our study patients following a self-managed two-week LID significantly reduced their total iodine body content by 50%. Iodine deficient status accomplished 88% (n=14) of patients (82% of them achieved mild iodine deficiency, and 6% patients had gained moderate iodine deficient state). Two patients (12%) had the iodine sufficient status (>100 μg/L) even after the two-week LID preparation. According to Park *et al.*[4], 78% of patients were able to achieve moderate iodine deficiency (<50 μg/L) after two-week LID. Tomoda *et al.*[6] showed that 70% of patients reduced their urinary iodine concentration to less than 100 μg/L after two-week LID, and 35% patients were moderate iodine deficient. Possible reasons for discrepancy among data could be different regulations among countries regarding food supplementation with iodine and various dietary habits. In accordance with the legislative, all salt on the Croatian market must be iodized with 15-23 mg KI/kg NaCl.[13] Thus, when a discontinuance of dietary iodine intake is recommended, patients have no choice but to eat unsalted food.

In our study, all fourteen patients who received ^{131}I in diagnostic purposes had negative radioiodine post-LID whole body scans. All of them were mild iodine deficient or even had sufficient iodine status after two week of LID. Diffuse lung lesions in five patients, seen on computed tomography images, were small, up to 5 mm in diameter, and

TABLE 3. Urine iodine concentration (μg/L)

	Mean ± SD	Median	Range	
Urine iodine concentration prior to low iodine diet	153.1 ± 24.8	154.0	97.1 – 192.4	p<0.001
Urine iodine concentration after low iodine diet	76.6 ± 19.0	77.2	42.5 – 110.4	

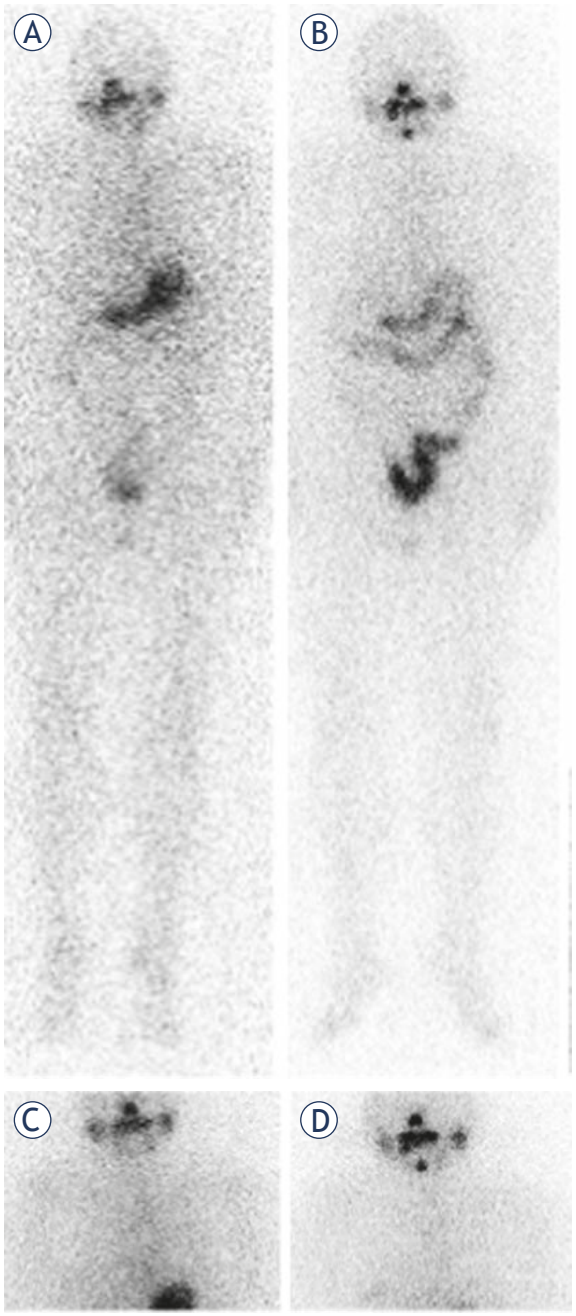

FIGURE 2. Radioiodine scans of the patient who received 3700 MBq (100 mCi) of ^{131}I. The ^{131}I uptake is visible in the neck region. Prior to a low iodine diet (LID), the patient had urinary iodine concentration of 97.1 μg/L, and post-LID value was 42.5 μg/L. Anterior whole body scans (A) prior to LID and (B) post LID; static scans of the neck and the thorax region (C) prior to LID and (D) post LID.

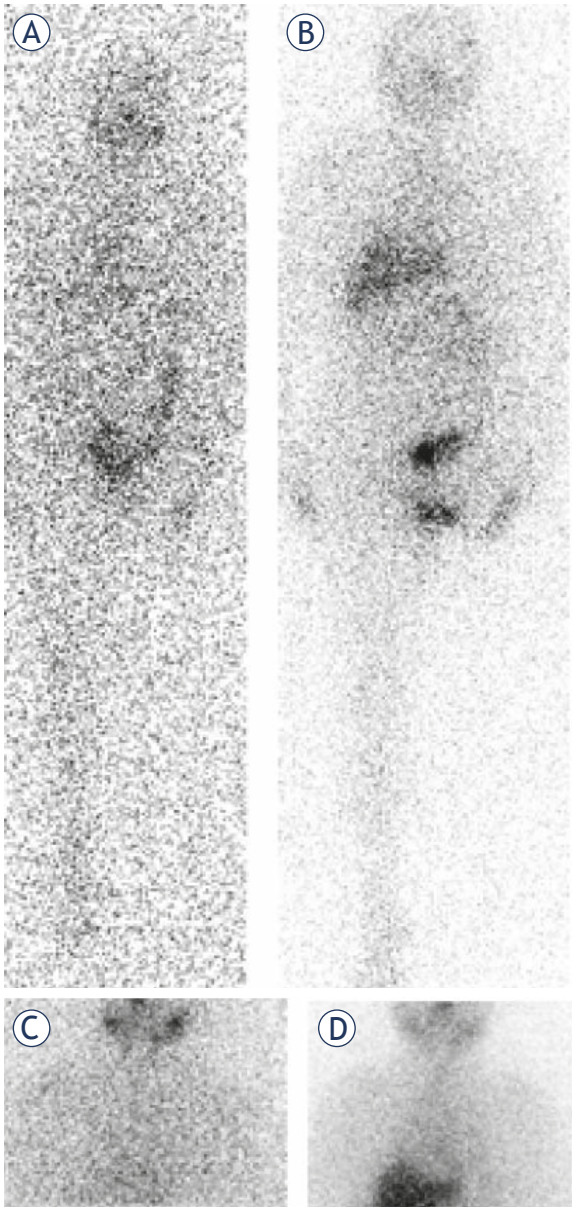

FIGURE 3. Radioiodine scans in the patient who underwent therapy with 7400 MBq (200 mCi) of ^{131}I. This patient had small pulmonary nodules seen on computed tomography images performed 7 months before LID. A diffuse radioiodine uptake is seen in liver. Focal accumulation of ^{131}I was not visible. Prior to LID, this patient had urinary iodine concentration of 169.6 μg/L, and post-LID value was 89.0 μg/L. Anterior whole body scans (A) prior to LID and (B) post LID; static scans of the neck and the thorax region (C) prior to LID and (D) post LID.

could be too small to be evident on radioiodine scans. Bone lesions in one patient, seen on computed tomography images, were also tiny, probably too small to be visualized on radioiodine scans. A neck lymph node metastasis in the patient who refuses the surgical treatment contains cystic tissue and, therefore, could not be visible on ^{131}I scans. Post-therapy scans showed the increased diffuse radioiodine uptake in liver in one patient and focal ^{131}I accumulation in the neck region in another one.

There are different data regarding to significance of the diffuse hepatic uptake seen on ^{131}I whole body scans. Chung *et al*.[14] reported the correlation between the diffuse hepatic radioiodine uptake and the thyroid remnant or metastases. Other authors did not find any connection between the thyroid remnant or recurrence and the diffuse hepatic ^{131}I uptake.[15,16] Omür *et al*.[16] also find a positive correlation between the diffuse ^{131}I uptake in liver and administrated ^{131}I activity, increased levels of serum hepatic enzymes (AST, ALT) and hepatosteatosis.

Our patient received radioiodine therapy with 7400 MBq and the ^{131}I activity was determined on an empirical basis, what is frequent at clinical praxis.[17] The patient had hepatosteatosis and two hepatic hypovascular lesions, 7 and 10 mm in diameter, but normal serum AST and ALT levels. Due to the diffuse uptake in lungs seen on the post-ablation ^{131}I whole body scan, he underwent the radioiodine therapy with 5550 MBq 10 years ago. All diagnostic radioiodine scans afterward were negative with gradually rising serum Tg levels. Hepatosteatosis and high administered activity remained only possible explanations for our patient's radioiodine liver uptake.

Beside the ablation therapy with 1480 MBq of ^{131}I five years ago and three negative radioiodine diagnostic scans afterwards, the patient who received 3700 MBq of radioiodine after LID did not receive any other ^{131}I therapy. This patient achieved targeted moderate iodine deficiency, and positive finding in the neck region could be a result of thyroid remnant ^{131}I avidity after two-week LID. In the further follow-up, no other morphological findings suggestive of thyroid cancer recurrence were found. Nevertheless, sensitivity of radioiodine whole body scans for detecting radioiodine avid tissue might be also improved following the administration of a high ^{131}I activity.

To the best of our knowledge, there are no studies in literature related to the impact of a LID on the diagnostic or the therapeutic ^{131}I administration in patients with elevated serum Tg levels and negative ^{131}I whole body scans. Studies demonstrating the efficacy of a LID on postsurgical ^{131}I ablation therapy are contradictory. When using the criteria of no visible uptake in the neck region and negative Tg level, Pluijmen *et al*.[5] found a significantly higher ablation rate in patients performing a two-week LID compared to the control group (65% *vs.* 48%). On the other hand, Morris *et al*.[18] showed no significant difference of ablation rate between two-week LID patients and those performing a regular diet (68.2% *vs*. 62.0%).

Apart from iodine contamination, radioiodine scan can be negative due to the dedifferentiation of tumour which still can produce Tg, but lost its ability to accumulate iodine, microscopic metastases which are too small to be visualized, and mutation of NIS (potassium/iodine symporter) in thyroid/tumour cells.[19] All these facts might be responsible for ^{131}I negative scans in our patients, in spite of relatively effective LID. A rather small number of the patients and the comparison of diagnostic and therapeutic scans in two patients are clear limitations of our study. Nevertheless, encouraged with the achieved reduction of total body iodine content after LID we decided to continue with a more rigorous diet, trying, as much as we can, to exclude the influence of stable iodine on the ^{131}I uptake.

Conclusions

Our study demonstrated that two-week LID in patients with DTC was an effective way to reduce total body iodine content. Non iodized salt availability, a more stringent dietary protocol and a longer iodine restriction period are probably necessary to achieve the targeted moderate iodine deficient state in patients preparing for the ^{131}I administration.

References

1. Pacini F, Schlumberger M, Dralle H, Elisei R, Smith JW, Wiersinga W. The European Thyroid Cancer Taskforce. European concensus for the management of patients with differentiated thyroid carcinoma of the follicular epithelium. *Eur J Endocrinol* 2006; **154:** 787-803.

2. Schlumberger M, Charbord P, Fragu P, Lumbroso J, Parmentier C, Tubiana M. Circulating thyroglobulin and thyroid hormones in patients with metastases of differentiated thyroid carcinoma: relationship to serum thyrotropin levels. *J Clin Endocrinol Metab* 1980; **51:** 513-9.

3. Ladenson PW, Bravermann LE, Mazzaferi ME, Brucker-Davis F. Comparison of administration of recombinant human thyrotropin with withdrawal of thyroide hormone for radioactive scanning in patients with thyroid cancer. *N Engl J Med* 1997; **337:** 888-96.

4. Park JT, Hennessey JV. Two-week low iodine diet is necessary for adequate outpatient preparation for radioiodine rhTSH scanning in patients taking levothyroxine. *Thyroid* 2004; **14:** 57-63.

5. Pluijmen M, Eustatia-Rutten C, Goslings BM, Stokkel MP, Pereira Arias AM, Diamant M, et al. Effects of low-iodide diet on post surgical radioiodide ablation therapy in patients with differentiated thyroid carcinoma. *Clin Endocrinol* 2003; **58:** 428-35.
6. Tomoda C, Uruno T, Takamura Y, Ito Y, Miya A, Kobayashi K, et al. Reevaluation of stringent low iodine diet in outpatient preparation of radioiodine examination and therapy. *Endocr J* 2005; **52**: 237-40.
7. WHO, UNICEF, ICCIDD. *Assessment of the Iodine Deficiency Disorders and Monitoring Their Elimination*. World Health Organisation, 2001. WHO Document WHO/NHD/01.1
8. Schlumberger M, Mancusi F, Baudin E, Pacini F. ^{131}I therapy for elevated thyroglobulin levels. *Thyroid* 1997; **7:** 273-6.
9. Chao M. Management of differentiated thyroid cancer with rising thyroglobulin and negative diagnostic radioiodine whole body scan. *Clin Oncol (R Coll Radiol)* 2010; **22:** 438-47.
10. Benotti J, Benotti N, Pino S, Gardyna H. Determination of total iodine in urine, stool, diets and tissue. *Clinical Chem* 1965; **11:** 932-6.
11. Yates J S, Thomas H C. Kinetics of the iodide-catalyzed reaction betwen cerium (IV) and arsenic (III). *JACS* 1956; **78:** 3950-3.
12. Jooste PL, Strydom E. Methods for determination of iodine in urine and salt**.** *Best Pract Res Clin Endocrinol Meta*b 2010; **24**: 77-88.
13. *The Instructions for Table Salt Iodinesation.* The Official Gazette No 8, 09.10.1996.
14. Chung JK, Lee YJ, Jeong JM, Lee DS, Lee MC, Cho BY, et al. Clinical significance of hepatic visualization on iodine-131 whole-body scan in patients with thyroid carcinoma. *J Nucl Med* 1997; **38:** 1191-5.
15. Tatar FA, Morita E, Ituarte PH, Cavalieri RR, Duh QY, Price DC, et al. Association between residual thyroid carcinoma and diffuse hepatic uptake of 131I following radioiodine ablation in postoperative total thyroidectomy patients. *World J Surg* 2001; **25:** 718-22.
16. Omür O, Akgün A, Ozcan Z, Sen C, Ozkiliç H. Clinical implications of diffuse hepatic uptake observed in postablative and post-therapeutic I-131 scans. *Clin Nucl Med* 2009; **34:** 11-4.
17. Mowlavi AA, Fornasier MR, de Denaro M. Thyroid volume's influence on energy deposition from 131I calculated by Monte Carlo (MC) simulation. *Radiol Oncol* 2011; **45(2):** 143-6.
18. Morris LF, Wilder MS, Waxmann AD, Braunstein Gd. Reevaluation of the impact of a stringent low-iodine diet on ablation rates in radioiodine treatment of thyroid carcinoma. *Thyroid* 2001; **11:** 749-55.
19. Ma C, Kuang A, Xie J, Ma T. Possible Explanations for Patients with Discordant Findings of Serum Thyroglobulin and ^{131}I Whole-Body Scanning. *J Nucl Med* 2005; **46:** 1473-1480.

research article

Knockdown of *stat3* expression by RNAi inhibits *in vitro* growth of human ovarian cancer

Shu-Hua Zhao[1], Fan Zhao[1], Jing-Ying Zheng[1], Li-Fang Gao[2], Xue-Jian Zhao[2], Man-Hua Cui[1]

[1] Second Clinical Hospital of Jilin University, Changchun, China
[2] Department of Pathophysiology, School of Basic Medical Sciences, Jilin University, Changchun, China

Received 28 January 2011
Accepted 10 March 2011

Correspondence to: Man-Hua Cui, Second Clinical Hospital of Jilin University, Changchun 130041, China. E-mail: Mercury098@mspil.edu.cn

Disclosure: No potential conflicts of interest were disclosed.

Background. The aim of the study was to investigate the suppressive effects of pSilencer2.1-U6-siRNA-*stat3* recombinant plasmids on the growth of ovarian cancer *in vitro*.

Material and methods. Three pairs of DNA template (*stat3*-1, *stat3*-2, *stat3*-3) specific for different target sites on *stat3* mRNA were synthesized to reconstruct pSilencer2.1-U6-siRNA-*stat3*s, which were transfected into SKOV3 cells. The expressions of STAT3, BcL-2, cyclin D1 and C-myc in these cells were detected by Western blot and Northern blot. The cell cycle and the growth were determined by flow cytometry (FCM) and MTT assay, respectively. Cell apoptosis was determined by TUNEL staining.

Results. Of the three siRNAs, only siRNA targeting *stat3*-3 markedly suppressed the protein expression of *stat3* in SKOV3 cells; MTT assay and FCM showed that transfection of *stat3*-3 siRNA could significantly suppress the growth of SKOV3 cells and arrest the cell cycle *in vitro*. TUNEL staining also showed massive apoptosis in SKOV3 cells transfected with *stat3*-3 siRNA.

Conclusions. pSilencer2.1-U6-siRNA-*stat3*-3 can significantly inhibit the STAT3 expression in human ovarian cancer cells resulting in the inhibition of the cancer growth and the increase of apoptosis of cancer cells.

Key words: RNA interference; *stat3*; SKOV3 cells; ovarian cancer; apoptosis

Introduction

Ovarian cancer, such as serous carcinoma, mucinous carcinoma, endometrioid carcinoma, metastatic carcinoma etc., is one of the common gynecological malignant tumors with high mortality. It is highly malignant and its incidence is increasing.[1] Although great advances have been achieved in the radiotherapy and chemotherapy of ovarian cancer, the 5-year survival rate of ovarian cancer is not improved significantly.[2] Further understanding of the molecular mechanisms underlying the proliferation, differentiation and survival of gynecological cancer cells is critical for the development of optimal therapeutic modalities. Although the molecular changes in the development of ovarian cancer are not completely understood, a lot of genes have been found to be involved in the occurrence and development of gynecological cancers.[3,4] Thus, these genes may be useful targets in the development of specific antitumor therapeutic strategies. Studies have demonstrated the signal transducers and activators of transcription 3 (STAT3) signaling pathway plays a key role in the carcinogenesis by promotion of proliferation, differentiation and cell cycle progression, as well as the inhibition of apoptosis.[5,6] The constitutive activation of STAT3 is implicated in a variety of cancer cell lines[7-11], which suggests *stat3* may be an important molecular target for the anti-tumor therapy. Recent studies demonstrate the blockade of STAT3 expression in human cancer cells that suppresses the *in vitro* proliferation of cancer cells and the *in vivo* tumorigenicity. Attempts to suppress STAT3 expression have been made using tyrosine kinase inhibitors[12,13], antisense oligonucleotides[14], decoy oligonucleotides[15], dominant-negative STAT3 protein[16,17] and RNA interference (RNAi).[18,19] *In vitro* studies have shown that the inhibition of STAT3 activity in human cancer cells can induce the ap-

optosis and/or the growth arrest. In human head and neck squamous carcinoma cells, prostate cancer cells, and laryngeal cancer cells, blocking of *stat3* by decoy oligonucleotides or antisense oligonucleotides or siRNA abrogates the production of transforming growth factor (TGF) and suppresses the oncogenic growth of these cells.[15] Furthermore, some studies have revealed some apoptosis-related genes, such as Bcl-xL, C-myc and cyclin D1, etc, that are involved in the STAT3 blockage induced suppression of cancer cell growth.

RNAi is triggered by the presence of double-stranded RNA (dsRNA) in cells and results in rapid degradation of targeted mRNA with homology to double strand RNA leading to potent and selective silencing of genes. RNAi provides a novel approach to inhibit gene expression, and to date, RNAi with siRNA has been applied as a functional genomic tool.[20]

In the present study, siRNA targeting *stat3* gene was synthesized and siRNA-*stat3* expression vectors were constructed with pSilencer 2.1-U6, which was then used to transfect human ovarian cancer cells (SKOV3 cells) aiming to inhibit the STAT3 expression and induce apoptosis of cancer cells. SKOV3 cells transfected with siRNA-*stat3* were subcutaneously injected into nude mice and the growth and the apoptosis of ovarian cancer cells were observed.

Materials and methods

Immunohistochemistry for stat3 in the ovarian cancer

Twenty-five ovarian cancer samples and twenty fresh normal ovary tissues were collected for the determination of STAT3 expression. These tissues were embedded in paraffin and cut into 5-μm sections. After deparaffinization, the endogenous peroxidase was inactivated by 3% hydrogen peroxide in methanol for 10 min. The sections were treated with rabbit anti-human STAT3 polyclonal antibody (Santa Cruz, USA) and then with goat anti-rabbit IgG conjugated with horseradish peroxidase. The development was done at room temperature, using an avidin-biotin-peroxidase complex method (Vectastain Elite ABC kit; Vector Laboratories). The criteria for grading of STAT3 expression were as follows: negative (-): ≤5% positive cells; low (+): 5~25% positive cells; moderate (++): 25~50% positive cells; strong (+++): 50~100% positive cells).

Plasmid construction and determination

Three pairs of double stranded siRNA oligonucleotide against *stat3* (*stat3*-1, *stat3*-2 and *stat3*-3) were designed according to the sequence of human *stat3* gene (Genebank: NM003150). These oligonucleotides contain a sense strand with 19 nucleotides followed by a short spacer (TTCAAGAGA). The reverse complement of the sense strand has five thymines as a stop signal of RNA polymerase III transcription. The sequences of oligonucleotides were as follows:

stat3-1: 5′-GATTGACCTAGAGAC-CCACTTCAAGAGAGTGGGTCTCTAGGT-CAATCTTTTT-3′ (forward) and 5′-AATTAAAAAG ATTGACCTAGAGACCCACTCTCTTGAAGTG GTCTCTAGGTCAATCGGCC-3′ (reverse); *stat3*-2: 5′-GAGTCGAATGTTCTCTATCTT CAAGAGAGATAGAGAACATTCGA CTCTTTTT-3′ (forward); and 5′-AATTAAAAAGAG TCGAATGTTCTCTATCTCTCTTGAAGATAGA GAACATTCGACTCTGGCC-3′ (reverse); *stat3*-3: 5′-GCAGCAGCTGAACAACATGTTGTTCAGCTGC TGCT TTTT-3′ (forward), and 5′-AATTAAAAA GCAGCAGCTGAACAACATGTCTCTTGAACAT GTTGTTCAG CTGCTGCTGCGGCC-3′ (reverse).

These Oligos were annealed in the annealing buffer (100 mM K-actate, 30 mM HEPES-KOH [pH 7.4], 2 mM Mg-acetate, and the mixture was incubated at 90°C for 3 min and then at 37°C for 1 h) and cloned into the ***Hind*** III-***BamH*** I sites of pSliencer 2.1-U6 vectors[18] which can express hairpin siRNAs under the control of U6 promoter. The pSilencer2.1-U6 was linearized with the ***Hind*** III-***BamH*** I restriction enzymes. The products with the double-stranded **s**tructure were used to form a recombinant plasmid with T4 DNA ligase followed by annealing. A negative control scrambled siRNA (Ambion, USA), which has no evident homology to mouse or human *stat3* sequences, was also designed aiming to exclude non-specificity.

Cell culture and transfection

Human ovarian cancer cells (SKOV3 cells) were grown in Iscove's Modified Dulbecco's Medium (IMDM) (Invitrogen, USA) containing 10% fetal bovine serum (FBS). When the cell confluence reached 80~90%, SKOV3 cells were washed three times with serum-free medium and divided into three groups: mock group, pSi-scramble siRNA group and pSi-*stat3* siRNA group. LipofectAMINE 2000 (Invitrogen, USA) was used in the cell transfection,

and enhanced green fluorescent protein vector (pEGFP; BD Clontech, Inc; USA) was cotransfected with either pSilencer 2.1-U6-*stat3* siRNAs or pSilencer 2.1-U6-scrambled siRNA at a volume ratio of 1:20 to label the positive transfected cells. The transfection was performed for 5~20 h and then the medium was refreshed with medium containing 10% FBS followed by lysis for 24~72 h after the transfection.

mRNA quantification

Total RNA was extracted from tissues with Trizol (Invitrogen, USA) following the manufacturer's instructions. For Northern blot analysis, 20 μg of total RNA were separated by 1.2% agarose-formaldehyde gel, and blotted onto Hybridization-*N* membranes (Amersham Pharmacia Biotech, USA). Hybridization was performed using the express Hyb buffer (BD Clontech, USA) with ^{32}P-labeled cDNA of Survivin and actin as probes. Blots were exposed to Kodak MS film and then quantitated using a Molecular Dynamics Phosphorlmager.

Assay of growth and cell cycle in vitro

SKOV3 cells were incubated in 96-well plates. The cell proliferation was determined by 3-(4,5-dimethylthiazol-2-y1)-2,5-diphenyltetrazolium bromide (MTT; Sigma, USA) assay and the number of viable cells were counted with a hemocytometer at 72 h after the transfection. The absorbance at 570 nm (A_{570}) was determined with a microplate reader. The growth inhibition rate was calculated according to the following formula:

Growth inhibition rate (%) = $[(A_{570c}- A_{570e})/ A_{570c}]\times100\%$

A_{570c}: A_{570} in control group; A_{570e}: A_{570} in experimental group

For the assay of cell cycle, SKOV3 cells were transfected with siRNA-stat3s or siRNA-scrambled vectors. After 72 h of transfection, these cells were collected, washed with phosphate buffered saline (PBS) containing 4 mmol/L ethylenediaminetetraacetic acid (EDTA), and fixed in cold 70% ethanol followed by centrifugation. The supernatant was removed and cells were washed once with PBS containing 4 mmol/L EDTA. Cells were then re-suspended in PBS containing 4 mmol/L EDTA, 20 ml/L of propidium iodide (Sigma, USA), 0.2% Triton X-100, and 40 mg/L RNase A followed by incubation for at least 30 min at 4°C. The cell cycle was detected with a flow cytometer (FACScan, Becton Dickinson, USA) followed by the analysis with Cell Quest software. For the determination of apoptotic cells, 95 μl of floating cells were mixed with 0.1% AO/EB (acridine orange/ethidium bromide [Sigma, USA]) followed by the observation under a microscope.

In vivo growth of cancer cells

SKOV3 cells (3×10^6) were subcutaneously inoculated into the back of 18 nude mice. The tumor volume ($m_1^2\times m_2\times0.5236$, where m_1 represents the short axis and m_2 the longer axis) was measured every 2~3 d until the tumors reached about 50.56±36.45 mm^3 (by day 12) in volume. Then, these nude mice were randomized into three groups (n=6): (1) mock transfection group (PBS buffer alone); (2) scrambled vector group (20 μg/mouse); (3) pSilencer2.1-U6-*stat3*-siRNA group (20 μg/mouse). The plasmids were diluted in 50 μl of PBS and injected percutaneously into the tumors by using a syringe with a 27-gauge needle. Immediately after the injection, tumors were pulsed with an electroporation generator (ECM 830, BTX, USA). Pulses were delivered at a frequency of 1/sec and 150 v/cm for 50 ms. This process was repeated once a week, mice were sacrificed on day 33. The tumor volume was determined and then tumors were collected for H&E staining and terminal deoxynucleotidy1 transferase-mediated nick end labeling (TUNEL) assay.

HE staining and TUNEL assay

Serial sections of tumor tissues were fixed in formalin, stained with H&E, and processed for the routine histological examination. TUNEL assay was done by using the In Situ Cell Death Detection Kit (Roche, Switzerland). Paraffin-embedded tissues were cut into 3-μm sections, deparaffinized and hydrated according to the standard protocol. After the incubation with proteinase K (200 μg/ml) for 30 min at 21°C, the TUNEL reaction mixture containing bromodeoxyuridine triphosphate, terminal deoxynucleotidy1 transferase, and reaction buffer was added onto the sections which were incubated in a humidified chamber for 60 s at 37°C, followed by washing and incubation with a FITC-labeled anti-bromodeoxyuridine monoclonal antibody for 30 min at room temperature. The reaction was visualized under a fluorescence microscope. TUNEL-positive cells present green fluorescence. The apoptotic index was calculated as follows: apoptotic index = (number of apoptotic cells/ number of total cells) ×100%.

Statistical analysis

The statistical analysis was done with SPSS 13.0 statistic software package. The significance of the differences between various samples was determined using the student's two-tailed t test. The comparisons between medians were performed with the two-tailed Mann-Whitney test. A value of $P<0.05$ was considered statistically significant.

Results

Stat3 is over-expressed in ovarian cancer cells and ovarian cancer tissues

The STAT3 expression in normal ovarian tissue (n=20), ovarian cancer tissues (n=25) and ovarian cancer cells (SKOV3 cells) was determined by using immunohistochemistry. Normal ovarian tissues showed low to moderate expression of Stat3. In contrast, primary ovarian cancer tissues and ovarian cancer cells had moderate to high expression of STAT3 (Figure1). Immunohistochemistry revealed that *stat3* expressions in 85% of ovarian cancers were classified as ++ to +++, which were significantly different ($P<0.001$) from that in normal ovarian tissues (+).

Stat3-specific siRNA specifically reduces Stat3 expression in SKOV3 cells

Previous studies have provided strong evidence that siRNA specific to *stat3* gene can significantly suppress STAT3 protein expression.[18,19,21] To determine if STAT3 expression in the ovarian cancer can be suppressed via the gene-silencing effect of vector-based RNAi, the siRNAs targeting different sites of *stat3* gene were designed previously which inhibited STAT3 expression significantly in prostate cancer cells.[22] In the present study, SKOV3 cells were also transfected with siRNA and results showed only siRNA targeting *stat3*-3 could decrease the STAT3 expression significantly at both mRNA (Figure 2) and protein (Figure 3) levels when compared with scambled-siRNA. The siRNA targeting *stat3*-1 and *stat3*-2 had no significantly inhibitory effects on the mRNA and protein expressions of *stat3*.

Inhibition of stat3 suppresses expressions of BcL-2, cyclin D1, and c-Myc in SKOV3 cells

Constitutive activation of STAT3 induces the expressions of several genes including anti-apoptotic gene BcL-2, cyclin D1 and c-Myc which promote cell division. In order to determine whether these genes were involved in the Stat3-mediated apopto-

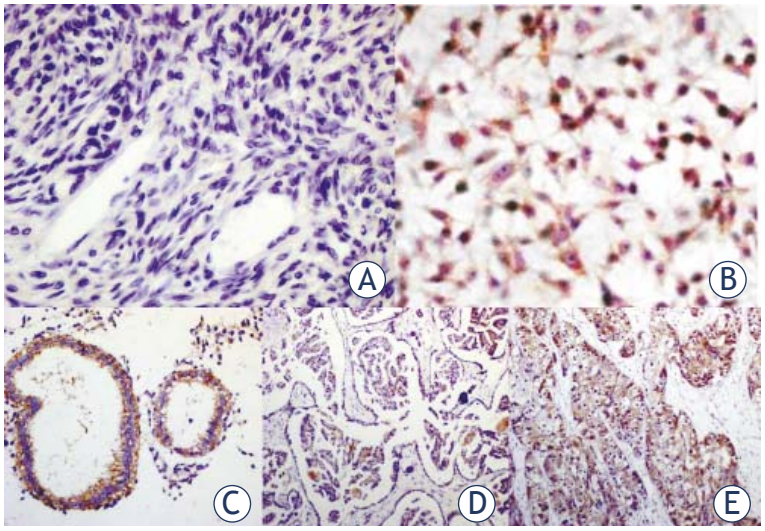

FIGURE 1. Expression of STAT3 in SKOV3 cells, ovarian cancer tissues, and normal ovarian tissue. A: normal ovarian tissue; B: SKOV3 cells; C: ovrian serous cystadenocarcinoma; D: ovarian mucinous cysadencarcinoma; E: clear-cell ovarian carcinoma.

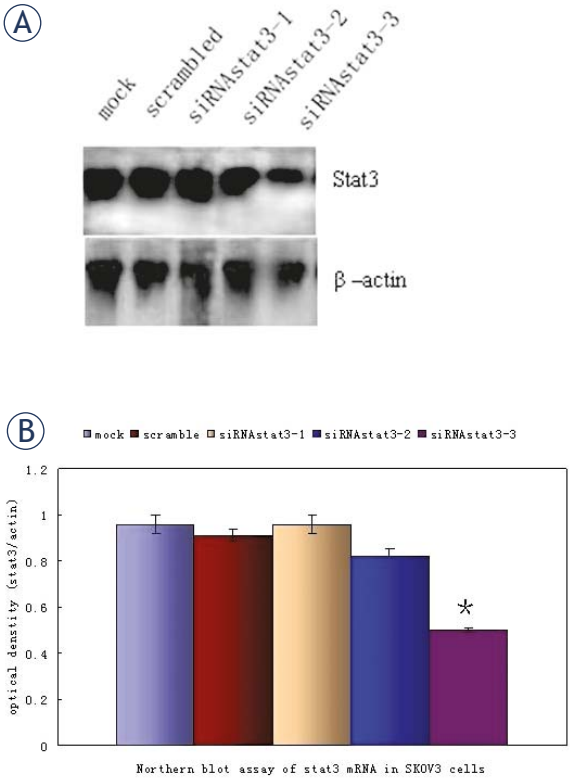

FIGURE 2. Northern blot assay of *stat3* mRNA in human ovarian cancer cell line. A: SKOV3 cells were treated with either 2 μg of pSliencer 2.1-U6 vector *stat3* siRNAs or scrambled siRNA vector for 72 h. B: Quantification of *stat3* mRNA expression from three separate experiments, which was normalized by that of β-actin. (*$P<0.05$ vs scrambled siRNA group).

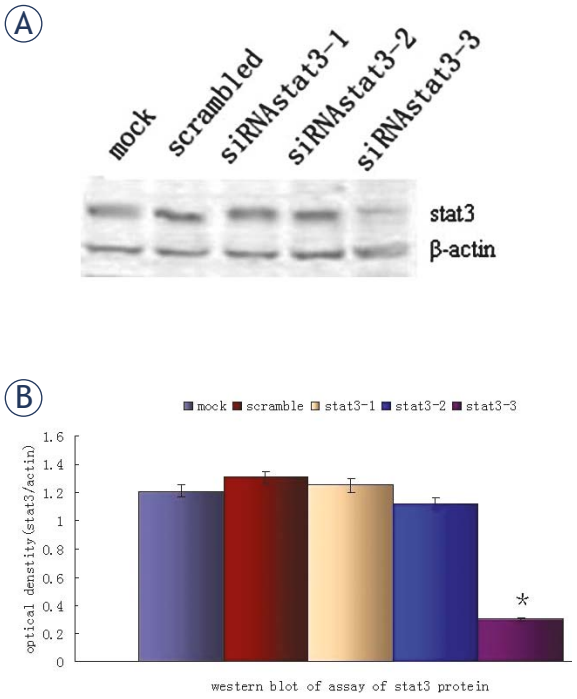

FIGURE 3. Western blot assay of STAT3 protein in human ovarian cancer cells. A: SKOV3 cells were treated with either 2 μg of pSliencer 2.1-U6 vector *stat3* siRNA or scrambled siRNA vector for 72 h. B: Quantification of STAT3 protein from three separate experiments, which was normalized by that of β-actin. (**P*<0.05 vs controls)

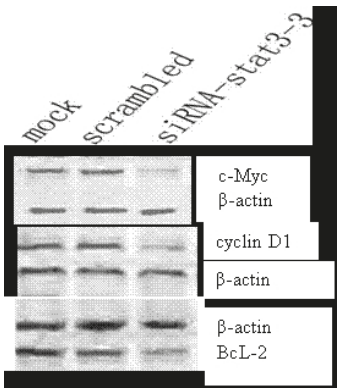

FIGURE 4. Western blot assay of c-Myc, cyclin D1 and BcL-2 in SKOV3 cells treated with either 2 μg of pSliencer 2.1-U6 *stat3-3* or scrambled siRNA vector for 72 h.

TABLE 1. Apoptosis of SKOV3 cells after transfection with siRNA-*stat3-3* (n=3) ±sd

Group	Apoptosis rate (%)
Mock	0.02 ± 0.00
Scrambed siRNA	2.49 ± 1.54
siRNA-Stat3-3	16.6 ± 3.43*

*P <0.05 vs. mock and scrambled groups.

sis blocking in SKOV3 cells, Western blot assay was performed. Figure 4 shows that the BcL-2, cyclin D1 and c-Myc were highly expressed in the scrambled-siRNA transfected cells, whereas the expression levels of these proteins were significantly decreased after the transfection with siRNA-*stat3*.

Stat3 siRNA inhibits in vitro growth and survival, induces apoptosis of SKOV3 cells and arrests SKOV3 cells in G1 phase

In order to determine whether *stat3*-siRNA had inhibitory effects on the growth of SKOV3 cells, MTT assay was conducted to determine the cell proliferation. Results showed the cells transfected with siRNA-*stat3* became less confluent and some cells were rounded and detached from the plates, when compared with cells transfected with scrambled vectors (Figure 5). AO/EB staining (nucleus condensation) was performed to detect the apoptotic cells. Results showed both early apoptotic and late apoptotic SKVO3 cells were seen in cells transfected with siRNA-*stat3*-3 (Figure 5). Flow cytometry revealed the apoptosis rate of siRNA-*stat3*-3 transfected cells was significantly higher than that of scrambled siRNA transfected cells (Table 1).

In vivo anti-tumor activity of stat3 siRNA

In order to evaluate the effects of *stat3*-siRNA on the ovarian cancer growth *in vivo*, *stat3*-siRNA was injected into ovarian cancer bearing nude mice. Mice were subcutaneously inoculated with 3×10^6 SKOV3 cells and the tumors were palpable at the sites of injection on day 12. Then, the mice were intra-tumorally injected with PBS, scrambled-siRNA or siRNA-*stat3*-3. This process was repeated at days 19 and 26, and animals were killed on day 33. The mean tumor volume in mice treated with scrambled siRNA was 767.65±100.23 mm^3, and that in mice treated with siRNA *stat3*-3 was 298.23±19.89 mm^3, showing the significant difference in tumor volume between these two groups. However, there was no marked difference between mice transfected with scrambled-siRNA and those treated with buffer (*P*>0.05) (Figure 6). To determine the mechanism of suppressed cancer growth *in vivo*, tumors were collected for H&E staining and TUNEL staining. Results showed siRNA-*stat3*-3 transfected cells underwent massive apoptosis with sparsely

dispersed chromatin and necrotic tissue (Figure 6) and several TUNEL-positive cells or cell clusters (Figure 6), which was seldom found in the other two groups. These findings demonstrate the intratumoral administration of *stat3*-3 siRNA exerts potent suppressive effects on the cancer growth.

Discussion

Under physiological conditions, STAT3 activation is a rapid process and activated STAT3 has short half life. The study has demonstrated *stat3* plays an important role in maintaining physiological functions of cells. STAT3 is a critical element in the epidermal growth factor receptor (EGFR), interleukin-6 (IL-6)/Janus kinase (JAK) and other carcinogenic tyrosine kinase signaling pathways. Evidence reveals STAT3 is expressed in a variety of human malignancies, including leukemia, multiple myeloma, multiple melanoma, squamous cell carcinoma of the head and neck (SCCHN), breast cancer, prostate cancer, ovarian cancer and lung cancer. The activated *stat3* plays crucial roles in the occurrence, growth, apoptosis inhibition of cancer cells.[23-25] Rosen *et al.*[26] indicated the persistent activation of STAT3 signal transduction was very important in the occurrence of ovarian cancer and could promote the cell proliferation resulting in occurrence of cancers. The persistent activation of STAT3 helps the cancer development, and a high expression of STAT3 also indicates a poor prognosis of the cancer. Therefore, *stat3* can be used as a novel target for the anti-cancer therapy and may become a novel cancer marker.

Our results showed the STAT3 expression was significantly increased in human ovarian cancer when compared with that in normal ovary tissues. Among the three pairs of double stranded siRNA oligonucleotide against *stat3*, only siRNA targeting *stat3*-3 could markedly inhibit the STAT3 expression in SKOV3 cells demonstrated by Western Blot and Northern Blot. Then, siRNA-*stat3*-3 was used to transfect SKOV3 cells for further experiments. Results revealed transfection with siRNA-*stat3* significantly decreased the expressions of BcL-2, cyclin D1 and c-Myc in SKOV3 cells. In addition, *stat3* siRNA inhibits the *in vitro* growth and survival, induces apoptosis of SKOV3 cells and arrests $SKOV_3$ cells in G1 phase. Furthermore, the anti-tumor effects of *stat3* siRNA were also confirmed in ovarian cancer bearing nude mice. Taken together, these findings demonstrated the *in vitro* and *in vivo* anti-tumor effects of *stat3* siRNA.

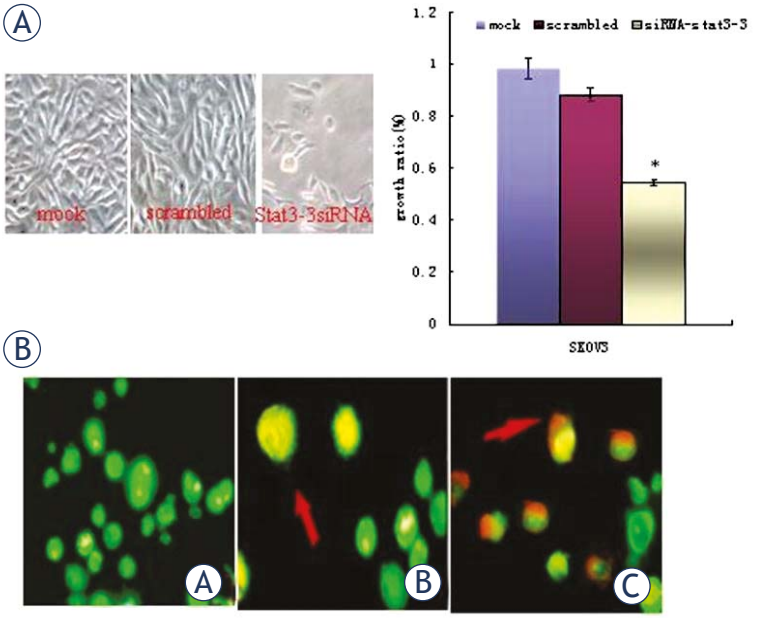

FIGURE 5. siRNA-Stat3-3 transfection significantly inhibited the growth of SKOV3 cells and induced apoptosis (A) transfection with *stat3*-3 siRNA for 72 h inhibited the growth of cancer cells (×400). B: Representative fluoromicrographs of apoptosis detected by AO/EB assay in control and *stat3*-3-siRNA–treated cells. C: SKOV3 cells (D) red arrow indicates early apoptotic cells; (E) red arrow indicates late apoptotic cells.

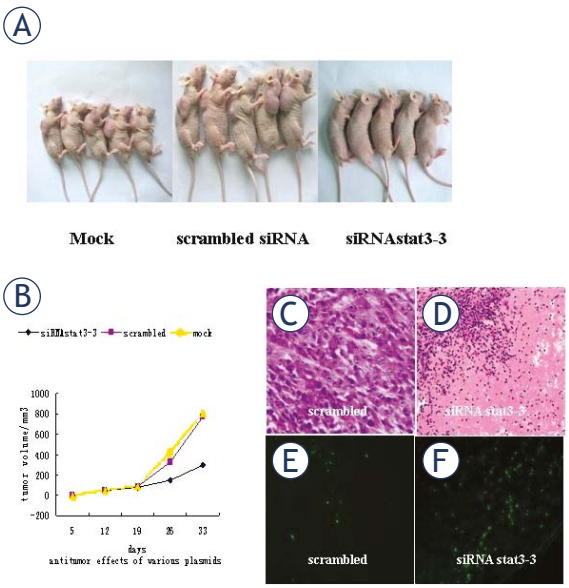

FIGURE 6. Intratumoral electroinjection of Stat3-3 siRNA resulted in significant inhibition of cancer growth and induced apoptosis of cancer cells *in vivo*. (A) Mice treated with scrambled vectors had visible cancers, whereas mice treated with 20 μg of *stat3*-3siRNA vectors had reduced tumor volumes. (B) Growth curves of cancer cells treated with *stat3*-3 siRNA. Mice were inoculated subcutaneously with SKOV3 cell. On day 12, the mean volume of palpable cancers reached 50.56±36.45 mm^3 (n=6) at the sites of injection. Then, these mice were injected intratumorally with buffer, *stat3*-3 siRNA or scrambled siRNA. Injection was repeated on days 19 and 26, and the tumor sizes were determined on days 0, 5, 12, 19, 26 and 33. (Mean±SEM. n=6, $P<0.01$). (C, D) HE staining (100×). (E, F) TUNEL staining (200×).

Our results were similar to that of Cai *et al*.[27] in which they also found the anti-tumor effects of *stat3* siRNA *in vitro* and *in vivo*. However, in the present study, we designed three pairs of double stranded siRNA oligonucleotide against *stat3*, and the most effective siRNA in the inhibition of STAT3 expression was selected. In addition, the suppressed expression of *stat3* was confirmed by Western Blot and Northern Blot at protein and mRNA levels, respectively. In the *in vivo* experiment, we detected not only changes of the tumor size but also the apoptosis of cancer cells in the tumors. In 2008, Huang *et al.* applied shRNA to knockdown *stat3* expression in CAOV3 ovarian cancer cell line demonstrating similar results.[28] Their results suggest RNA interference is an effective and feasible strategy to down-regulate *stat3* expression in the treatment of ovarian cancer.

Bcl-2 is the founding member of the Bcl-2 family of apoptosis regulator proteins. The Bcl-2 gene has been implicated in a number of cancers. It is also thought to be involved in resistance to the conventional cancer treatment.[29] Cyclin-D1, in humans is encoded by the CCND1 gene, that belongs to the highly conserved cyclin family whose members are characterized by a dramatic periodicity in protein abundance throughout the cell cycle. Mutations, amplification and over-expression of CCND1 gene, which alters the cell cycle progression, are observed frequently in a variety of tumors and may contribute to tumorigenesis.[30] c-Myc protein is a transcription factor that activates the expression of a great number of genes through binding on consensus sequences and recruiting histone acetyltransferases (HATs). Myc gene is a very strong proto-oncogene and very often found to be up-regulated in many types of cancers.[31] Based on the results of the present study, we speculated that the anti-tumor effects of siRNA targeting *stat3* may be related to the cell cycle arrest and promotion of the apoptosis of cancer cells.

In summary, our results indicate *stat3* siRNA treatment can significantly inhibit the growth of ovarian cancer cells and promote their apoptosis. Thus, we postulate that STAT3 can be used as a therapeutic target for ovarian cancer patients and RNA interference with siRNA targeting *stat3* may become an effective strategy for the treatment of ovarian cancer.

References

1. Klint A, Tryggvadóttir L, Bray F, Gislum M, Hakulinen T, Storm HH, et al. Trends in the survival of patients diagnosed with cancer in female genital organs in the Nordic countries 1964-2003 followed up to the end of 2006. *Acta Oncol* 2010; **49:** 632-43.
2. Lenhard SM, Bufe A, Kümper C, Stieber P, Mayr D, Hertlein L, et al. Relapse and survival in early-stage ovarian cancer. *Arch Gynecol Obstet* 2009; **280:** 71-7.
3. Zhang Z, Zhou B, Zhang J, Chen Y, Lai T, Yan L, et al. Association of interleukin-23 receptor gene polymorphisms with risk of ovarian cancer. *Cancer Genet Cytogenet* 2010; **196:** 146-52.
4. Shih IeM, Davidson B. Pathogenesis of ovarian cancer: clues from selected overexpressed genes. *Future Oncol* 2009; **5:** 1641-57.
5. Darnell JE Jr. STATs and gene regulation. *Science* 1997; **277:** 1630- 5.
6. Lu Y, Fukuyama S, Yoshida R, Kobayashi T, Saeki K, Shiraishi H, et al. Loss of SOCS3 gene expression converts STAT3 function from anti-apoptotic to pro-apoptotic. *J Biol Chem* 2006; **281:** 36683-90.
7. Garcia R, Yu CL, Hudnall A, Catlett R, Nelson KL, Smithgall T, et al. Constitutive activation of STAT3 in fibroblasts transformed by diverse oncoproteins and in breast carcinoma cells. *Cell Growth Differ* 1997; **8:** 1267-76.
8. Garcia R, Bowman TL, Niu G, Yu H, Minton S, Muro-Cacho CA, et al. Constitutive activation of STAT3 by the Src and JAK tyrosine kinases participates in growth regulation of human breast carcinoma cells. *Oncogene* 2010; **20:** 2499-513.
9. Buettner R, Mora LB, Jove R. Activated STAT signaling in human tumors provides novel molecular targets for therapeutic intervention. *Clin Cancer Res*. 2002; **8**: 945-54.
10. Takemoto S, Mulloy JC, Cereseto A, Migone TS, Patel BK, Matsuoka M, et al. Proliferation of adult T cell leukemia/lymphoma cells is associated with the constitutive activation of JAK/STAT proteins. *Proc Natl Acad Sci USA* 1997; **94:** 13897-902.
11. Gouilleux-Gruart V, Gouilleux F, Desaint C, Claisse JF, Capiod JC, Delobel J, et al. STAT-related transcription factors are constitutively activated in peripheral blood cells from acute leukemia patients. *Blood* 1996; **87:** 1692-7.
12. Levitzki A. Tyrosine kinases as targets for cancer therapy. *Eur J Cancer* 2002; **38:** S11-8.
13. Blaskovich MA, Sun J, Cantor A, Turkson J, Jove R, Sebti SM. Discovery of JSI-124 (cucurbitacin I), a selective Janus kinase/signal transducer and activator of transcription 3 signaling pathway inhibitor with potent antitumor activity against human and murine cancer cells in mice. *Cancer Res* 2003; **63:** 1270-9.
14. Bromberg J, Darnell JE Jr. The role of STATs in transcriptional control and their impact on cellular function. *Oncogene* 2000; **19:** 2468-73.
15. Leong PL, Andrews GA, Johnson DE, Dyer KF, Xi S, Mai JC, et al. Targeted inhibition of STAT3 with a decoy oligonucleotide abrogates head and neck cancer cell growth. *Proc Natl Acad Sci USA* 2003; **100:** 4138-43.
16. Ni Z, Lou W, Leman ES, Gao AC. Inhibition of constitutively activated STAT3 signaling pathway suppresses growth of prostate cancer cells. *Cancer Res* 2000; **60:** 1225-8.
17. Zhang J, Shen B, Li Y, Sun Y. STAT3 exerts two-way regulation in the biological effects of IL-6 in M1 leukemia cells. *Leuk Res* 2001; **25:** 463-72.
18. Lee SO, Lou W, Qureshi KM, Mehraein-Ghomi F, Trump DL, et al. RNA interference targeting STAT3 inhibits growth and induces apoptosis of human prostate cancer cells. *Prostate* 2004; **60:** 303-9.
19. Konnikova L, Kotecki M, Kruger MM, Cochran BH. Knock-down of STAT3 expression by RNAi induces apoptosis in astrocytoma cells. *BMC Cancer* 2003; **3:** 23.
20. Mesojednik S, Kamensek U, Cemazar M. Evaluation of shRNA-mediated gene silencing by electroporation in LPB fibrosarcoma cells. *Radiol Oncol* 2008; **42:** 82-92.
21. Grandis JR, Zheng Q, Drenning SD. Epidermal growth factor receptor-mediated *stat3* signaling blocks apoptosis in head and neck cancer. *Laryngoscope* 2000; **110:** 868-74.

22. Gao L, Zhang L, Hu J, Li F, Shao Y, Zhao D, et al. Down-regulation of signal transducer and activator of transcription 3 expression using vector-based small Interfering RNAs suppresses growth of human prostate tumor in vivo. *Clin Cancer Res* 2005; **11:** 6333-41.

23. Fernandes A, Hamburger AW, Gerwin BI. ErbB-2 kinase is required for constitutive STAT3 activation in malignant human lung epithelial cells. *Int J Cancer* 1999; **83:** 564-70.

24. Nagpal JK, Mishra R, Das BR. Activation of Stat3 as one of the early events in tobacco chewing-mediated oral carcinogenesis. *Cancer* 2002; **94:** 2393-400.

25. Hsieh FC, Cheng G, Lin J. Evaluation of potential Stat3-regulated genes in human breast cancer. *Biochem Biophys Res Commun* 2005; **335:** 292-99.

26. Rosen DG, Mercado-Uribe I, Yang G, Bast RC Jr, Amin HM, Lai R, et al. The role of constitutively active signal transducer and activator of transcription 3 in ovarian tumorigenesis and prognosis. *Cancer* 2006; **107:** 2730-40.

27. Cai L, Zhang G, Tong X, You Q, An Y, Wang Y, et al. Growth inhibition of human ovarian cancer cells by blocking STAT3 activation with small interfering RNA. *Eur J Obstet Gynecol Reprod Biol* 2010; **148:** 73-80.

28. Huang F, Tong X, Fu L, Zhang R. Knockdown of STAT3 by shRNA inhibits the growth of CAOV3 ovarian cancer cell line in vitro and in vivo. *Acta Biochim Biophys Sin (Shanghai)* 2008; **40:** 519-25.

29. Ciardiello F, Tortora G.. Inhibition of bcl-2 as cancer therapy. *Ann Oncol* 2002; **13:** 501-2.

30. Hayakawa Y, Hirata Y, Nakagawa H, Sakamoto K, Hikiba Y, Kinoshita H, et al. Apoptosis signal-regulating kinase 1 and cyclin D1 compose a positive feedback loop contributing to tumor growth in gastric cancer. *Proc Natl Acad Sci USA* 2011; **108:**780-5.

31. Bressin C, Bourgarel-Rey V, Carré M, Pourroy B, Arango D, Braguer D, et al. Decrease in c-Myc activity enhances cancer cell sensitivity to vinblastine. *Anticancer Drugs* 2006; **17:** 181-7.

research article

Pipette tip with integrated electrodes for gene electrotransfer of cells in suspension: a feasibility study in CHO cells

Matej Rebersek, Masa Kanduser, Damijan Miklavcic

University of Ljubljana, Faculty of Electrical Engineering, Ljubljana, Slovenia

Received 1 June 2011
Accepted 22 June 2011

Correspondence to: Prof. Damijan Miklavčič, PhD, University of Ljubljana, Faculty of Electrical Engineering, Tržaška 25, SI-1000 Ljubljana, Slovenia. Phone: +386 1 4768 456; Fax: +386 1 4264 658; E-mail: damijan.miklavcic@fe.uni-lj.si

Disclosure: No potential conflicts of interest were disclosed.

Background. Gene electrotransfer is a non-viral gene delivery method that requires successful electroporation for DNA delivery into the cells. Changing the direction of the electric field during the pulse application improves the efficacy of gene delivery. In our study, we tested a pipette tip with integrated electrodes that enables changing the direction of the electric field for electroporation of cell suspension for gene electrotransfer.

Materials and methods. A new pipette tip consists of four cylindrical rod electrodes that allow the application of electric pulses in different electric field directions. The experiments were performed on cell suspension of CHO cells in phosphate buffer. Plasmid DNA encoding for green fluorescent protein (GFP) was used and the efficiency of gene electrotransfer was determined by counting cells expressing GFP 24 h after the experiment.

Results. Experimental results showed that the percentage of cells expressing GFP increased when the electric field orientation was changed during the application. The GFP expression was almost two times higher when the pulses were applied in orthogonal directions in comparison with single direction, while cell viability was not significantly affected.

Conclusions. We can conclude that results obtained with the described pipette tip are comparable to previously published results on gene electrotransfer using similar electrode geometry and electric pulse parameters. The tested pipette tip, however, allows work with small volumes/samples and requires less cell manipulation.

Key words: electrodes; gene electrotransfer; pipette tip, CHO cell line

Introduction

Gene electrotransfer is a non-viral method used to transfer DNA molecules into living cells by means of high-voltage electric pulses.[1-6] It is proven to be effective *in vitro*[7] and it has great potential for *ex vivo* transfection.[8] In comparison to viral methods it is safer[9] but less efficient *in vivo*.[10,11] However, being extensively investigated, gene electrotransfer is becoming a promising non-viral gene therapy method.[12-17] For *in vitro* and *ex vivo* experiments higher transfection yield can be achieved by optimizing electroporation medium, DNA preparation and its concentration, and parameters of electric pulses. The transfection yield obtained by gene electrotransfer *ex vivo* for hematopoietic and stem cells is still a problem, therefore, further optimisation of the protocol is needed.[18,19] One of the possible optimization options lies in increasing the area of cell membrane that is competent for the uptake of the plasmid DNA.

Study of Golzio *et al.* in 2002 demonstrated for the first time that during electric pulse application complex between DNA and permeabilized cell membrane was formed. The complex is formed only on the side of the cell facing anode indicating that DNA molecule only enters the cell on the membrane facing anode, therefore, changing the direction of the electric field results in the increase of the membrane area that is competent for DNA entry into the cell.[20] Afterwards, it was demonstrated that changing the electric field direction during electric pulse delivery improved the efficiency of gene electrotransfer *in vitro*.[21-24]

The aim of our research was to improve the design of electrodes that allow the application of electric pulses in different directions for electroporation of cell suspensions. We designed and tested a new pipette tip with integrated electrodes that could be used for improved gene electrotransfer *in vitro* and *ex vivo* for hematopoietic and stem cells.

Materials and methods

Cell cultures

Chinese hamster ovary CHO cells (European Collection of Cell Cultures) were grown in a nutrient mixture Ham's F12 (PAA, Austria) supplemented with 2 mM L-glutamine (Sigma-Aldrich, Germany), 10% foetal bovine serum (Sigma-Aldrich, Germany) and antibiotics Penicillin/Streptomycin and Gentamicin (PAA, Austria). Cells were kept at 37°C in a humidified 5% CO_2 atmosphere in the incubator for 3 to 4 days. Cell suspension was prepared by trypsinization of 90% confluent cell culture that was centrifuged for 5 minutes at 4°C. Cell pellet was resuspended in isoosmolar phosphate buffer with pH 7.4 consisting of 10 mM Na_2HPO_4/NaH_2PO_4, 1 mM $MgCl_2$ and 250 mM sucrose.

Gene electrotransfer protocol

Cells were exposed to the electric field in the pipette tip with integrated electrodes connected to a high-voltage prototype generator. The pipette tip with integrated electrodes for electroporation of cell suspension consists of four cylindrical rod electrodes and allows the application of relatively homogeneous electric field in different directions (Figure 1A,B,C). The electrodes are made of 90% platinum / 10% iridium; their diameter is 1.4 mm, adjacent electrodes are 1 mm apart, and opposite electrodes are 2 mm apart. The electrodes are glued into the plastic tip in parallel and their applicable length is 30 mm, so that the maximal treatable volume of cell suspension could be 140 µl. Numerical calculations of electric field distribution for four cylindrical rod electrodes were presented in our previous publication[22] and could be scaled down to smaller geometry in the presented pipette tip. The tip and the generator were developed at Laboratory of Biocybernetics, Faculty of Electrical Engineering, University of Ljubljana described in detail in patent[25] and previous publication.[22]

In our experiment, four different electric field protocols were used (Figure 1D): single polarity (SP), both polarities (BP), orthogonal single polarity (OSP) and orthogonal both polarities (OBP). In each electric field protocol 8 electric pulses were used in total. When SP electric field protocol was used, 8 pulses were applied in one direction between two opposite electrodes only. When BP electric field protocol was used, both polarities electric pulses were applied between two electrodes, 4 pulses in each direction. When OSP electric field protocol was used, single polarity electric pulses were applied between two orthogonal pairs of electrodes, 4 pulses in each direction. And when OBP electric field protocol was used, both polarities electric pulses were applied between two orthogonal pairs of electrodes, 2 pulses in each direction. Besides cells treated with different electric pulse protocols, cells not treated with electric pulses were used as control.

The pipette tip was sterilised before experiments in 70% ethanol for 10 minutes and rinsed thoroughly in sterile pulsing buffer before the first sample was treated and then the tip was rinsed each time before new electric field protocol was applied. For each parameter 100 µl of cell suspension was aspirated into the tip. In preliminary experiments electric pulse amplitude in the range from 80 to 300 V were tested and for further experiments 200 and

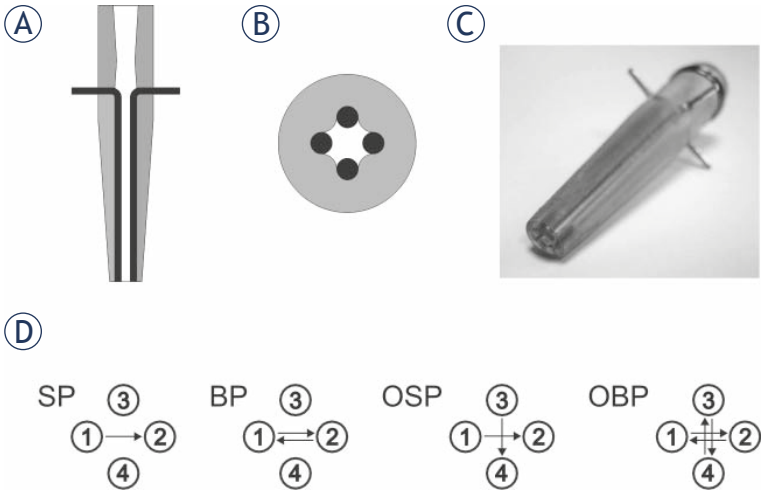

FIGURE 1. Pipette tip and electric field protocols. Vertical (A) and horizontal (B) cross section and photograph (C) of pipette tip with integrated electrodes. In the cross section grey colour is used for the plastic housing and black for the electrodes. Electric field protocols (D): in single polarity (SP) 8 electric pulses were applied in one direction between electrodes 1 and 2 (8 pulses in one direction), in both polarities (BP) 8 electric pulses were applied in both directions between electrodes 1 and 2 (4 pulses in each direction), in orthogonal single polarity (OSP) 8 electric pulses were applied in one direction between electrodes 1 and 2, and 3 and 4 (4 pulses in each direction), and in orthogonal both polarities (OBP) 8 electric pulses were applied in both directions between electrodes 1 and 2, and 3 and 4 (2 pulses in each direction).

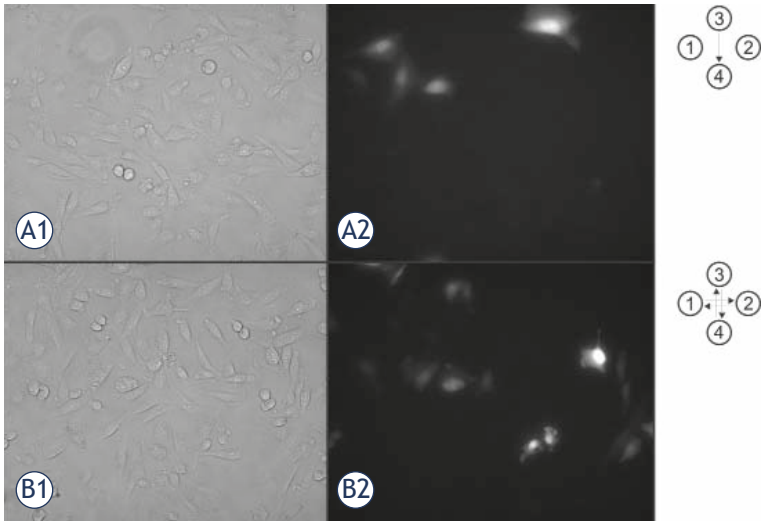

FIGURE 2. Phase contrast (A1 and B1) and fluorescence images (A2 and B2) of CHO cells 24 h after exposure to electric pulses at 20x objective magnification. Cells were exposed to 8 rectangular pulses with amplitude 225 V. The distance between the applied electrodes was 2 mm. Two electric field protocols are presented: single polarity (SP, A1 in A2), and orthogonal both polarities (OBP, B1 and B2). Only efficiently transfected cell express green florescence due to expression of GFP plasmid that was introduced into the cell by electric pulses (A2 and B2).

225 V were selected. Treated cells were exposed to 8 electric pulses with amplitude 200 V or 225 V, distance between the applied electrodes was 2 mm, pulse duration 1 ms and repetition frequency of 1 Hz regardless of the electric field protocol that was used *i.e.* 8 pulses in one direction for SP, 4 pulses in each direction for BP and OSP, and 2 pulses in each direction for OBP.

The efficiency of gene delivery was measured with the expression of reporter gene green fluorescent protein (GFP) 24 hours after gene delivery. Plasmid DNA pEGFP-N1 encoding for GFP was prepared with Endofree Plasmid mega kit (Qiagen, USA). The plasmid DNA was added to cell suspension that contained 5×10^5 cells/ml so that the final plasmid concentration was 10 µg/ml.[26] The mixture was then incubated for 2-3 minutes at room temperature. For electroporation 100 µl of cell suspension was aspired into the pipette tip and different electric pulse protocols were applied. After the pulse application treated cells were incubated for 5 minutes at 37°C to allow cell membrane resealing. Cells were then plated in a nutrient mixture Ham's F12 supplemented with 2 mM L-glutamine, 10% foetal bovine serum and then grown for 24 hours in cell culture medium to allow GFP expression.

Efficiency of transfection was determined as the percentage of cells expressing GFP. Cells were observed by fluorescent microscopy (Zeiss 200, Axiovert, ZR Germany). Excitation light for GFP detection was 488 nm (monochromator system PolyChrome IV, Visitron, Germany) and emission was 508 nm (Chroma, Rockingham, USA). Besides fluorescent images for each experimental condition phase contrast images were acquired by MetaMorph imaging system (Visitron, Germany) at 20x objective magnification. At least 5 randomly chosen images were recorded and analysed per each experimental condition. The cells were counted manually and the transfection efficiency was determined by the ratio between the number of fluorescent cells that express GFP and the total number of cells present in a phase contrast image. The approximate number of cells counted per each image was 300. The short term cell survival was determined 24 hours after the electric pulse treatment as the ratio between the number of cells present in the control and the number of cells counted in the treated sample exposed to electric pulses. For each experimental protocol at least three independent experiments were performed. Results are presented as mean values ± standard deviation.

Statistics

Statistical tests One way analysis of variance (One Way ANOVA) were performed on all results (SigmaStat 3.1, Systat, USA). Bonferroni t-test was performed on results if there was indication of a statistically significant difference between different electric field protocols used.

Results and discussion

The aim of our research was to design and test the new pipette tip with integrated electrodes and to evaluate the efficacy of the pipette tip for gene electrotransfer for 4 different electric field protocols. Experimental results are presented in Figures 2 and 3. In Figure 2 phase contrast and fluorescence micrographs of CHO cells expressing GFP 24 hours after the electric pulse application are presented. The upper row represents cells treated with electric pulses of single polarity (SP) while the bottom row shows cells treated with pulses applied in orthogonal positions of electrodes and in both pulse polarities (OSP). Figure 3 shows cell viability and percentage of cells expressing GFP observed 24 hours after the treatment of cell suspension with electric pulses in the pipette tip with integrated electrodes. The cells were treated with 8 electric pulses regardless of the electric field protocol that was used. We

have presented the results for 200 V and 225 V (d = 2 mm) as with these voltages the transfection yield was the highest. With lower voltages the percentage of transfected cells was lower and with higher voltages cell viability decreased while the differences between pulse protocols remained (data not shown). In Figure 3A it can be seen that the cell viability was not significantly affected by changing the electric field direction during the application of electric pulses. For cell viability statistical test One way ANOVA indicated that there was no statistically significant difference between the electric field protocols (P = 0.093 for 200 V and P = 0.798 for 225 V, d = 2 mm). The percentage of cells expressing GFP increased when the electric field direction was changed during the application of electric pulses (Figure 3B). Average percentage of cells expressing GFP was approximately two times higher when the pulses were applied in orthogonal directions of both polarities (OBP) in comparison with single direction and polarity (SP). For gene electrotransfer One Way ANOVA indicated that there was a statistically significant difference between the electric field protocols for 225 V (P = 0.005) but not for 200 V (P = 0,237). For 225 V Bonferroni t-test indicated that there was a statistically significant difference when we compared orthogonal both polarities (OBP) versus single polarity (SP) electric field protocol (P = 0.008) and orthogonal both polarities (OBP) versus both polarities (BP) electric field protocol (P = 0.042). Also the comparison of orthogonal single polarity (OSP) versus single polarity (SP) electric field protocol gave statistically significant difference (P = 0.05) while for other combinations the difference was not statistically different (P > 0.05).

Experimental results obtained with the pipette tip with integrated electrodes for electroporation of cell suspension show that the percentage of cells expressing GFP increases when the electric field direction was changed during the application of electric pulses whereas the cell viability was not affected. The results are in accordance with previously published results using similar electrode geometry and electric pulse parameters[21,22] indicating that the new pipette tip can be successfully used for gene electrotransfer. The advantage of this new pipette tip is easier and quicker cell handling during the electroporation experiment, and better control of the volume of cell suspension exposed to electric field in comparison with electrode design described in our previous paper.[22] Previous design was suitable for the electroporation of plated cells and presented some drawbacks when used for cell suspensions. Cell suspension was applied as a droplet among 4 rod electrodes and the main drawback was that the shape of the drop was not as uniform as the shape of the liquid in the tips presented here. The consequence of the uneven droplet shape was that not all the cells in the droplet were exposed to the homogeneous electric field. Therefore, the percentage of transfected cells was not consistent. This drawback was overcome by incorporation of the electrodes into the walls of the

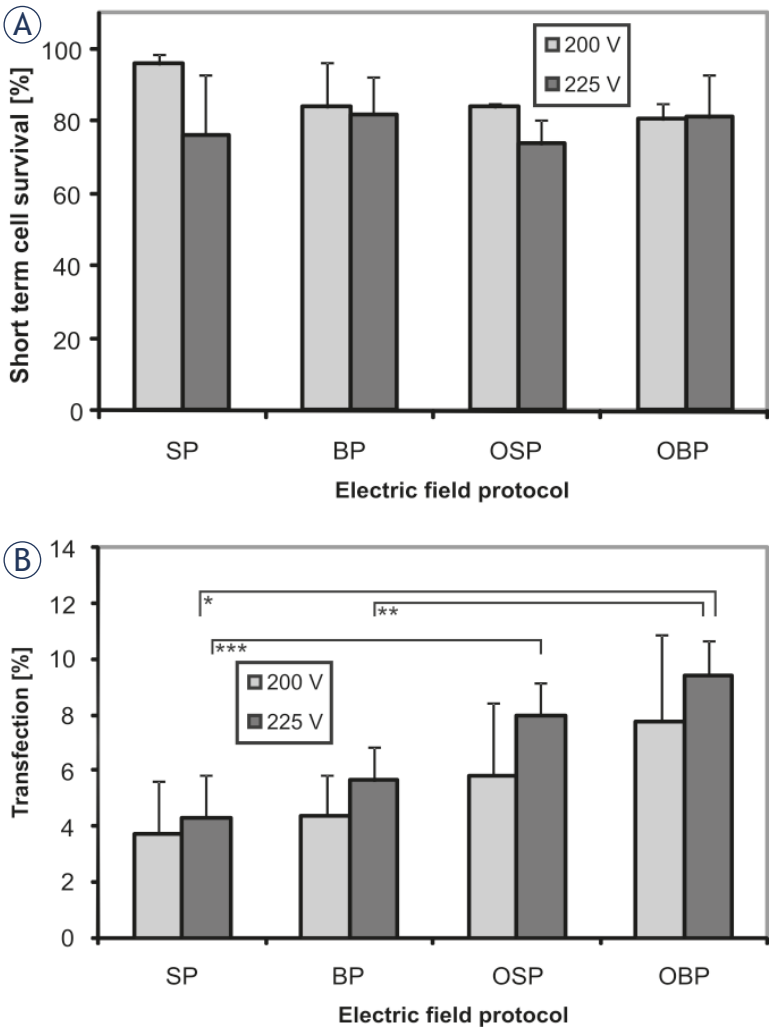

FIGURE 3. Influence of different electric field protocols on short term cell survival and transfection efficiency 24h after exposure to electric pulses. The cell survival (A) and the percentage of cells expressing GFP (B) for single polarity (SP), both polarities (BP), orthogonal single polarity (OSP) and orthogonal both polarities (OBP) electric field protocol. Cells were exposed to a train of eight pulses with amplitude 200 V and 225 V, duration 1 ms and repetition frequency of 1 Hz. Results were obtained by means of fluorescence microscopy. Each value in the graph represents mean of three independent experiments ± standard deviation. Statistical significance is marked by * (P = 0.008), ** (P = 0.042), and *** (P = 0.05). Changing the electric field orientation during the pulse application has increased the percentage of cells expressing GFP (B) whereas the cell viability remained the same (A).

pipette tip. In addition the tip allows working with small volume of cell suspension which may be particularly important in treating of valuable cells or plasmid. However, the aim of our work was to demonstrate proof of principle. Therefore, in our experiments cell suspension volumes of 100 µl were used to compare our data with the data used earlier. Nevertheless, the current tips allow working with smaller volumes down to 30 µl and the tips design could be scaled down to even smaller sizes.

In conclusion, the new pipette tip with integrated electrodes can be successfully used for gene electrotransfer, as obtained results are comparable with previously published results. The advantage of this new pipette with integrated electrodes is that it allows handling of small volumes/samples and requires less cell manipulation in comparison to established methods.

Acknowledgements

The work was supported by Slovenian Research Agency (ARRS) under grants Z2-2025, IP-0510, and P2-0249.

References

1. Neumann E, Kakorin S, Toensing K. Fundamentals of electroporative delivery of drugs and genes. *Bioelectrochem Bioenerg* 1999; **48:** 3-16.
2. Mir LM. Therapeutic perspectives of in vivo cell electropermeabilization. *Bioelectrochemistry* 2001; **53:** 1-10.
3. Teissie J, Golzio M, Rols MP. Mechanisms of cell membrane electropermeabilization: A minireview of our present (lack of ?) knowledge. *Biochim Biophys Acta-General Subjects* 2005; **1724:** 270-80.
4. Teissie J, Escoffre JM, Rols MP, Golzio M. Time dependence of electric field effects on cell membranes. A review for a critical selection of pulse duration for therapeutical applications. *Radiol Oncol* 2008; **42:** 196-206.
5. Cemazar M, Sersa G. Electrotransfer of therapeutic molecules into tissues. *Curr Opin Mol Ther* 2007; **9:** 554-62.
6. Mir LM. Nucleic acids electrotransfer-based gene therapy (electrogenetherapy): past, current, and future. *Mol Biotechnol* 2009; **43:** 167-76.
7. Kanduser M, Miklavcic D, Pavlin M. Mechanisms involved in gene electrotransfer using high- and low-voltage pulses - An in vitro study. *Bioelectrochemistry* 2009; **74:** 265-71.
8. Gresch O, Engel FB, Nesic D, Tran TT, England HM, Hickman ES, et al. New non-viral method for gene transfer into primary cells. *Methods* 2004; **33:** 151-63.
9. Thomas CE, Ehrhardt A, Kay MA. Progress and problems with the use of viral vectors for gene therapy. *Nature Rev Genet* 2003; **4:** 346-58.
10. Wells DJ. Electroporation and ultrasound enhanced non-viral gene delivery in vitro and in vivo. *Cell Biol Toxicol* 2010; **26:** 21-8.
11. Haberl S, Pavlin M. Use of collagen gel as a three-dimensional in vitro model to study electropermeabilization and gene electrotransfer. *J Membrane Biol* 2010; **236:** 87-95.
12. Ferber D. Gene therapy: Safer and virus-free? *Science* 2001; **294:** 1638-42.
13. Prud'homme GJ, Glinka Y, Khan AS, Draghia-Akli R. Electroporation-enhanced nonviral gene transfer for the prevention or treatment of immunological, endocrine and neoplastic diseases. *Curr Gene Ther* 2006; **6:** 243-73.
14. Daud AI, DeConti RC, Andrews S, Urbas P, Riker AI, Sondak VK, et al. Phase I trial of interleukin-12 plasmid electroporation in patients with metastatic melanoma. *J Clin Oncol* 2008; **26:** 5896-903.
15. Tevz G, Kranjc S, Cemazar M, Kamensek U, Coer A, Krzan M, et al. Controlled systemic release of interleukin-12 after gene electrotransfer to muscle for cancer gene therapy alone or in combination with ionizing radiation in murine sarcomas. *J Gene Med* 2009; **11:** 1125-37.16.
16. Pavlin D, Cemazar M, Coer A, Sersa G, Pogacnik A, Tozon N. Electrogene therapy with interleukin-12 in canine mast cell tumors. *Radiol Oncol* 2011; **45:** 30-9.
17. Cemazar M, Golzio M, Sersa G, Rols MP, Teissie J. Electrically-assisted nucleic acids delivery to tissues in vivo: Where do we stand? *Curr Pharm Des* 2006; **12:** 3817-25.
18. Cao F, Xie XY, Gollan T, Zhao L, Narsinh K, Lee RJ, Wu JC. Comparison of gene-transfer efficiency in human embryonic stem cells. *Mol Imaging Biol* 2010; **12:** 15-24.
19. Maurisse R, De Semir D, Emamekhoo H, Bedayat B, Abdolmohammadi A, Parsi H, et al. Comparative transfection of DNA into primary and transformed mammalian cells from different lineages. *BMC Biotechnol* 2010; **10:** 9.
20. Golzio M, Teissie J, Rols MP. Direct visualization at the single-cell level of electrically mediated gene delivery. *Proc Natl Acad Sci USA* 2002; **99:** 1292-7.
21. Faurie C, Phez E, Golzio M, Vossen C, Lesbordes JC, Delteil C, et al. Effect of electric field vectoriality on electrically mediated gene delivery in mammalian cells. *Biochim Biophys Acta-Biomembr* 2004; **1665:** 92-100.
22. Rebersek M, Faurie C, Kanduser M, Corovic S, Teissie J, Rols MP, et al. Electroporator with automatic change of electric field direction improves gene electrotransfer in-vitro. *Biomed Eng Online* 2007; **6:** 25.
23. Wasungu L, Escoffre J-M, Valette A, Teissie J, Rols M-P. A 3D in vitro spheroid model as a way to study the mechanisms of electroporation. *Int J Pharm* 2009; **379:** 278-84.
24. Wang J, Zhan Y, Ugaz VM, Lu C. Vortex-assisted DNA delivery. *Lab Chip* 2010; **10:** 2057-61.
25. Rebersek M, Corovic S, Sersa G, Miklavcic D. Electrode commutation sequence for honeycomb arrangement of electrodes in electrochemotherapy and corresponding electric field distribution. *Bioelectrochemistry* 2008; **74:** 26-31.
26. Faurie C, Rebersek M, Golzio M, Kanduser M, Escoffre JM, Pavlin M, et al. Electro-mediated gene transfer and expression are controlled by the lifetime of DNA/membrane complex formation. *J Gene Med* 2010; **12:** 117-25.

research article

Differences in plasma TIMP-1 levels between healthy people and patients with rectal cancer stage II or III

Irena Oblak[1], Franc Anderluh[1], Vaneja Velenik[1], Barbara Mozina[2], Janja Ocvirk[3], Eva Ciric[1], Natasa Hrovatic Podvrsnik[1]

[1] Department of Radiotherapy, [2] Department of Laboratory Diagnostics, [3] Department of Medical Oncology, Institute of Oncology Ljubljana, Ljubljana, Slovenia

Received 9 June 2011
Accepted 3 July 2011

Disclosure: No potential conflicts of interest were disclosed.

Correspondence to: Assist. Prof. Oblak Irena, MD, PhD, Department of Radiotherapy, Institute of Oncology Ljubljana, Zaloška 2, 1000 Ljubljana, Slovenia. Phone: +386 1 5879 290; Fax: +386 1 5879 304; E-mail: ioblak@onko-i.si

Background. The purpose of the study was to analyse whether the levels of the tissue inhibitor of matrix metalloproteinases-1 (TIMP-1) are higher in patients with rectal cancer as compared with healthy blood donors.

Patients and methods. Two hundred and seventeen patients (147 male, 70 female) with histologically confirmed non-metastatic rectal cancer (clinical stage II-III) and 45 healthy blood donors (15 male, 30 female) were included in analysis. Patient´s mean age was 66 years (range: 34-87 years) and healthy blood donor´s mean age was 35 years (range: 18-64 years). Plasma TIMP-1 concentrations were measured with an enzyme-linked immunosorbent assay (ELISA) using commercially available TIMP-1 ELISA kit. Mann-Whitney-test for independent groups was used to assess the differences of plasma TIMP-1 levels and clinicopathological parameters. Two-sided tests were used and the differences at $P<0.05$ were considered as statistically significant.

Results. Median patients TIMP-1 level was 180 ng/mL (range: 22-538 ng/mL); the mean (±SD) level was 193.7 (79.5) ng/mL. The median healthy blood donors TIMP-1 level was 112 ng/mL (range: 48-211 ng/mL); the mean (±SD) level was 115 (35.7) ng/mL. TIMP-1 levels in patients with rectal cancer were statistically significantly higher than TIMP-1 levels in healthy blood donors ($P<0.0001$). Significant differences in TIMP-1 levels were not found comparing gender ($P=0.43$), but in both groups TIMP-1 levels were increased with higher age ($P=0.007$).

Conclusions. Patients with rectal cancer had statistically significantly higher mean and median TIMP-1 level than healthy blood donors which is in accordance with the results published in other publications. These findings suggest possibility that plasma TIMP-1 levels could be used as new biological markers for early cancer detection.

Key words: TIMP-1; rectal cancer; healthy blood donors

Introduction

Tumour aggressiveness and metastatic potential, resulting in a poor prognosis, have been shown to be increased with the activation of matrix metalloproteinases (MMPs) and their tissue inhibitors (TIMPs). They play an important role in the process of degradation of the extracellular matrix and the basal membrane in relation to tumours invasiveness. The activity of the MMPs depends on the balance between the level of the active enzyme and its tissue inhibitor.[1-4] The TIMP family consists of four members: TIMP-1, TIMP-2, TIMP-3 and TIMP-4, which primary act as negative regulators of the degradation process of the extracellular matrix. Latest evidence suggests that they also participate in cell signalling by regulating cell growth, apoptosis, angiogenesis and genomic instability.[3,5,6]

Many researchers focused on clinical impact of TIMPs in cancer biology by rating tumour tissue TIMP expression or plasma circulating TIMP level. They found out that TIMPs can be useful diagnostic and prognostic markers like other new markers.[3,6-8] Most of these studies evaluated TIMP-1 and they recognized it as an important marker for patient management and prognosis in several ma-

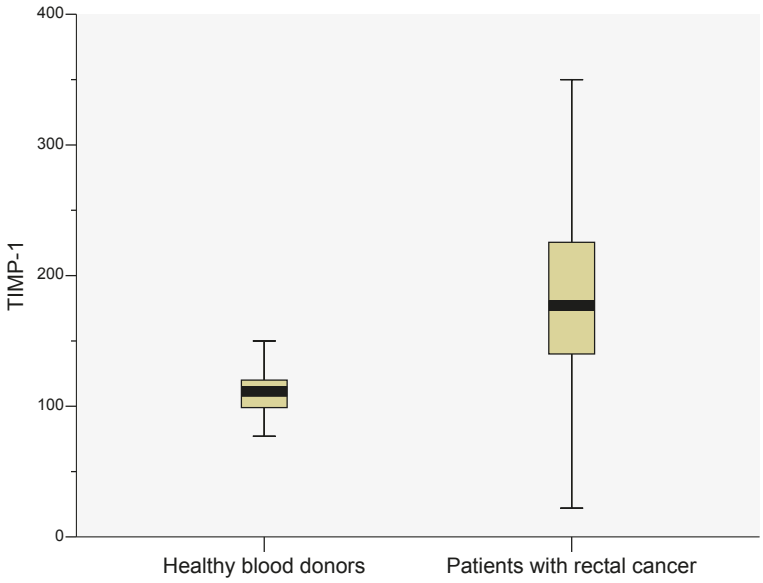

FIGURE 1. TIMP-1 levels (in ng/mL) in healthy blood donors and in patients.

lignancies such as colorectal, breast, lung, ovarian, bladder carcinoma[3,6] and in several nonmalignant diseases such as asthma, diabetes, cardiovascular and autoimmune diseases.[6]

Elevated plasma TIMP -1 levels were reported to be significantly increased in colon cancer patients compared with healthy population, and they were also associated with advanced disease stage and poor prognosis.[3,5,6,9-12] The aim of this study is to determine whether the TIMP-1 levels are higher in patients with rectal cancer as compared with healthy blood donors.

Patients and methods

Patients

Two hundred and seventeen patients (147 male, 70 female) with histologically confirmed non-metastatic rectal cancer (clinical stage II or III) and 45 healthy blood donors (15 male, 30 female) were included in analysis. Patient´s mean age was 66 years (range: 34-87 years) and healthy blood donor´s mean age was 35 years (range: 18-64 years).

Determination of plasma TIMP-1 level

All blood samples were taken in the same laboratory, and processed and stored with the same procedures. The blood samples were collected in vacutainer EDTA tubes. After centrifugation at 1500xg at 4°C for 10 minutes, plasma was separated and kept at -80°C until analysis. Plasma TIMP-1 concentrations were measured with an enzyme-linked immunosorbent assay (ELISA) using commercially available TIMP-1 ELISA kit, purchased from Oncogene Science, Cambridge (MA), USA. All procedures were performed according to the manufacturer´s protocol in duplicate using diluted samples. Measurements differed by less than 10% and the mean value was calculated and used for statistical analysis. The inter-assay precision coefficients of variation of TIMP-1 ranged between 3.9% and 8.8% at the different levels.

Statistical analysis

Statistical analysis was performed using personal computer and software statistical package SPSS, version 13 (SPSS Inc., USA). The main endpoint of the study was to determine if rectal cancer patients have higher TIMP-1 levels compared to healthy blood donors. Mann-Whitney-test for independent groups was used to assess the differences of plasma TIMP-1 levels and clinicopathological parameters. Two-sided tests were used and the differences at $P<0.05$ were considered as statistically significant.

Ethical consideration

Prior to analysis, all patients and healthy blood donors received detailed oral and written information about the research and procedures, and they signed an informed consent for their plasma analysis for the purposes of the research. The trial was approved by the ethic committees of the Institute of Oncology, Ljubljana, Slovenia and by the National Medical Ethics Committee of Republic of Slovenia and was in agreement with the Declaration of Helsinki.

Results

TIMP-1 levels

Median patients TIMP-1 level was 180 ng/mL (range: 22-538 ng/mL); the mean (±SD) level was 193.7 (79.5) ng/mL. The median healthy blood donors TIMP-1 level was 112 ng/mL (range: 48-211 ng/mL); the mean (±SD) level was 115 (35.7) ng/mL (Figure 1). TIMP-1 levels in patients with rectal cancer were statistically significantly higher than TIMP-1 levels in healthy blood donors ($P<0.0001$). Significant differences in TIMP-1 levels were not found comparing gender ($P=0.43$), but in both groups TIMP-1 levels were increased with higher age ($P=0.007$) (Figures 2 and 3).

Discussion

TIMP-1 plays an important role in regulation of extracellular matrix remodelling, which is one of the processes involved in cancer growth and spread. Several authors reported that patients with malignant disease had significantly higher TIMP-1 levels in comparison with healthy population.[5,9,11-14] In our study similar results were found. Patients with rectal cancer had statistically significant higher TIMP-1 levels in comparison with healthy blood donors (P<0.0001).

These findings also raise the idea that plasma TIMP-1 measurements could be useful in screening for malignant disease, such as rectal cancer in our case. Future randomised studies will demonstrate if the plasma TIMP-1 could be helpful for screening and detecting colorectal cancer beside digitorectal examination, faecal occult blood testing, recto-, sigmoido- and colonoscopy, DNA stool analysis and genetic testing.[8,15] Screening has in oncology special value as patients with lower stages have better prognosis.[16]

Like other researchers[3,12,14] we did not find significant differences in TIMP-1 levels and gender, but Holten-Andersen *et al.*[11] demonstrated that the mean TIMP-1 levels were approximately 10% higher in males than in females. The reason for this they attributed to the fact that the male population has higher incidence of tromboembolic diseases, which result in higher release rate of TIMP-1 in plasma from activated platelets.[11]

In many studies (in ours as well) TIMP-1 level was found to be increased with age,[3,9,11,14,17] although Tayebjee *et al.* in their study found an inverse relationship between TIMP-1 level and age.[18]

Conclusions

Patients with rectal cancer had statistically significantly higher mean and median TIMP-1 level than healthy blood donors which is in accordance with the results published in others publications. These findings suggest possibility that plasma TIMP-1 levels could be used as new biological markers for early cancer detection.

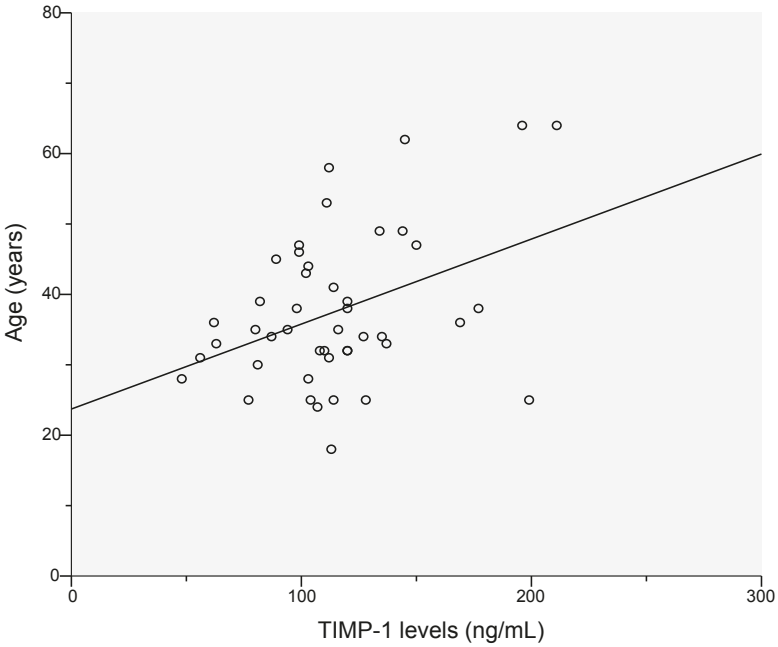

FIGURE 3. TIMP-1 levels and age in patients (p=0.007).

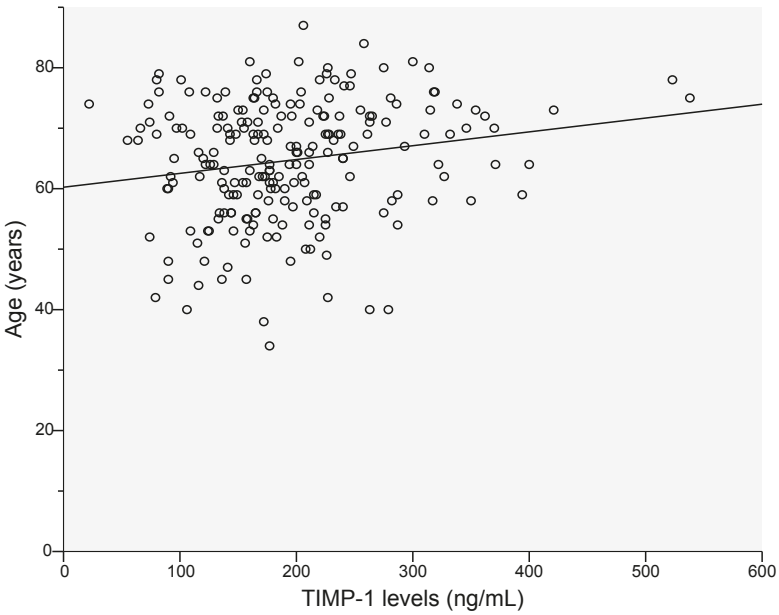

FIGURE 2. TIMP-1 levels and age in healthy blood donors (p=0.007).

References

1. Pesta M, Topolcan O, Holubec L, Rupert K, Cerna M, Holubec L, et al. Clinicopathological assesment and quantitative estimation of the matrix metalloproteinases MMP-2 and MMP-7 and the inhibitors TIMP-1 and TIMP-2 in colorectal carcinoma tissue samples. *Anticancer Res* 2007; **27:** 1863-8.

2. Li M, Yamamoto H, Adachi Y, Maruyama Y, Shinomura Y. Role of matrix metaloproteinase-7 (matrilysin) in human cancer invasion, apoptosis, growth and angiogenesis. *Exp Biol Med* 2006; **231:** 20-7.

3. Giaginis C, Nikiteas N, Margeli A, Tzanakis N, Rallis G, Kouraklis G, et al. Serum tissue inhibitor of metalloproteinase 1 and 2 (TIMP-1 and TIMP-2) levels in colorectal cancer patients: association with clinicopathological variables and patients survival. *Int J Biol Markers* 2009; **24:** 245-52.

4. Alo-Aho R, Kahari VM. Colagenases in cancer. *Biochemie* 2005; **87:** 273-86.

5. Sørensen NM, Sørensen IV, Wűrtz SØ, Schrohl AS, Dowell B, Davis G, et al. Biology and potential clinical implications of tissue inhibitor of metalloproteinases-1 in colorectal cancer treatment. *Scan J Gastroenterol* 2008; **43:** 774-86.

6. Frederiksen CB, Lomholt AF, Lottenburger T, Davis GJ, Dowell BL, Blankenstein MA, et al. Assesment of the biological variation of plasma tissue inhibitor of metalloproteinase-1. *Int J Biol Markers* 2008; **23:** 42-7.

7. Horvat M, Stabuc B. Microsatellite instability in colorectal cancer. *Radiol Oncol* 2011; **45:** 75-81.

8. Yaolin Zhou Y, Boardman LA, Miller RC. Genetic testing for young-onset colorectal cancer: case report and evidence-based clinical guidelines. *Radiol Oncol* 2010; **44:** 57-61.

9. Wass ET, Hendriks T, Lomme RM, Woblles T. Plasma levels of matrix metalloproteinase-2 and tissue inhibitor of metalloproteinase-1 correlate with disease stage and survival in colorectal cancer patients. *Dis Colon Rectum* 2005; **48:** 700-10.

10. Kahlert C, Bandapalli OR, Schirmacher P, Weitz J, Brand K. Invasion front-specific overexpression of tissue inhibitor of metalloproteinase-1 in liver metastases from colorectal cancer. *Anticancer Res* 2008; **28:** 1459-66.

11. Holten-Andersen MN, Murphy G, Nielsen HJ, Pedersen AN, Christensen IJ, Høyer-Hansen G, et al. Quantitation of TIMP-1 in plasma of healthy blood donors and patients with advanced cancer. *Br J Cancer* 1999; **80:** 495-503.

12. Hammer JH, Basse L, Svendsen MN, Werther K, Brüner N, Christensen IJ, et al. Impact of elective resection on plasma TIMP-1 in patients with colon cancer. *Colorectal Dis* 2006; **8:** 168-72.

13. Holten-Andersen MN, Christensen IJ, Nielsen HJ, Stephens RW, Jensen V, Nielsen OH, et al. Total levels of tissue inhibitor of metalloproteinases 1 in plasma yield high diagnostic sensitivity and specificity in patients with colon cancer. *Clin Cancer Res* 2002; **8:** 156-64.

14. Holten-Andersen MN, Stephens RW, Nielsen HJ, Murphy G, Christensen IJ, Stetler-Stevenson W, et al. High preoperative plasma tissue inhibitor of metalloproteinase-1 levels are associated with short survival of patients with colorectal cancer. *Clin Cancer Res* 2000; **6:** 4292-9.

15. Sofic A, Beslic S, Kocijancic I, Sehovic N. CT colonography in detection of colorectal carcinoma. *Radiol Oncol* 2010; **44:** 19-23.

16. Oblak I, Petric P, Anderluh F, Velenik V, Hudej R, Fras AP. Anal cancer chemoirradiation with curative intent - a single institution experience. *Neoplasma* 2009; **56:** 150-5.

17. Ishida H, Murata N, Hayashi Y, Tada M, Hashimoto D. Serum levels of tissue inhibitor of metalloproteinases-1 (TIMP- 1) in colorectal cancer patients. *Surg Today* 2003; **33:** 885-92.

18. Tayebjee MH, Lip GYH, Blann AD, MacFadyen RJ. Effects of age, gender, ethnicity, diurnal variations and exercise on circulating levels of matrix metalloproteinases (MMP)-2 and -9, and their inhibitors, tissue inhibitors of matrix metalloproteinases (TIMP)-1 and -2. *Thromb Res* 2005; **115:** 205-10.

research article

3-D conformal radiotherapy with concomitant and adjuvant temozolomide for patients with glioblastoma multiforme and evaluation of prognostic factors

Yilmaz Tezcan and Mehmet Koc

Department of Radiation Oncology, Meram Faculty of Medicine, Selcuk University, Konya, Turkey

Received 10 April 2011
Accepted 25 May 2011

Correspondence to: Yilmaz Tezcan, M.D. Department of Radiation Oncology, Meram Faculty of Medicine, Selcuk University, 42090-Konya, Turkey. Phone: +332 223 6942; Fax; +0332 223 6182; E-mail: yilmaztezcan@yahoo.com

Disclosure: No potential conflicts of interest were disclosed.

Background. The aim of the retrospective study was to evaluate the outcome and prognostic factors of newly diagnosed glioblastoma patients who received 3-D conformal radiotherapy (RT) combined with concomitant and/or adjuvant temozalamide (TMZ) postoperatively.

Patients and methods. Fifty patients with glioblastoma multiforme were treated with 3-D conformal RT combined with concomitant and/or adjuvant TMZ postoperatively. Median age was 57 years (range, 12-79) and median Karnofsky performance status (KPS) was 70 (range, 40-100). A multivariate Cox regression model was used to test the effect of age, sex, KPS, extent of surgery, tumour dimension (<5cm *vs.* ≥5cm), full dose RT (≥60 Gy *vs.* <60 Gy), concurrent TMZ and adjuvant TMZ treatment (adjuvant therapy plus 6 cycles of TMZ group versus <6 cycles of TMZ group) on the overall survival.

Results. The median follow up time was 10 months (range 3-42). One- and 2-year overall survival rates were 46% and 20%, respectively. The prognostic factors important for the overall survival were a full dose RT (≥60 Gy) (p=0.005) and the application of adjuvant TMZ for 6 cycles (p=0.009).

Conclusions. The results of our study confirm the efficiency of RT plus concomitant and adjuvant TMZ, with an acceptable toxicity in patients. We suggest that at least 6 cycles of adjuvant TMZ should be administered to obtain a benefit from the adjuvant treatment.

Key words: glioblastoma multiforme; conformal radiotherapy; temozolomide; prognostic factors

Introduction

Glioblastoma is the most common primary brain tumour in adults and accounts for approximately 60-70% of all gliomas.[1-3] The incidence of malignant glioma is increasing among elderly patients.[4] Malignant glioma may develop at all ages, it can also occur in children, but the peak incidence being in the fifth and sixth decades of life.[5] Malignant gliomas are 40% more common in men than in women and twice as common in whites as in blacks. The median age of patients at the time of diagnosis is 64 years in the case of glioblastomas. Median survival time is less than 1 year after diagnosis.[1,2]

A recent meta-analysis based on 12 randomized trials showed a small survival benefit (6% in the one year survival rate, from 40% to 46%) from the addition of alkylating agents.[7] Until recently, treatment options for patients with malignant glioma were limited and mainly the same for all subtypes of malignant glioma. The treatment included surgery to the extent feasible and radiotherapy (RT). Chemotherapy (CT) used as the adjuvant treatment or at recurrence had a marginal role.[8-10]

Concomitant and adjuvant temozolomide (TMZ) CT significantly improved median, 2- and 5-year survival in a large randomized trial, and is the current standard of care for patients with glioblastoma up to age 70.[3,11] No randomized data are available for elderly patients (>70 years) with a good performance status. The contribution of adjuvant TMZ and the optimal cycle schedule is also still not known.

Prognostic factors of glioblastoma multiforme (GBM) and anaplastic astrocytomas include age at diagnosis, Karnofsky performance status (KPS), histology, extent of resection, duration of symptoms, and neurologic functional/mental status.[12]

In the present study, we evaluated the outcome of newly diagnosed glioblastoma patients who received 3-D conformal RT combined with concomitant and/or adjuvant TMZ postoperatively. Additionally, prognostic factors and obtaining a benefit from 6 cycles of adjuvant TMZ for the survival were evaluated.

Patients and methods

Patient

Between December 2005 and August 2010, 50 patients with GBM were treated with 3-D conformal RT combined with concomitant and/or adjuvant TMZ postoperatively. The median age was 57 years (range, 12-79) and the male: female ratio was 2.1:1. All of the patients had computed tomography scan or magnetic resonance imaging preoperatively. Median KPS was 70 (range, 40-100) before RT.

Tumour characteristics

Median tumour diameter was 5 cm (range; 1-12 cm), patients with tumour dimensions less than 5 cm were 32% and ≥5 cm were 68%. The location of the tumour was temporal in 40%, parietal in 30%, frontal in 24%, occipital in 6% and others in 11%, respectively.

Treatment

The surgery was limited to stereotactic biopsy in 28% of the patients, the subtotal resection was performed in 18%, the gross total resection in 44%, and only the radiologic diagnosis was done in 10% of the patients. The median interval between surgery and radiotherapy was 38 days (range; 19-74 days).

3-D conformal RT, delivered by linear accelerators with a 6 mV or more energy, consisted of the fractionated focal irradiation, at a dose of 2 Gy per fraction, given once daily 5 days per week. The median total RT dose was 60 Gy (range; 30-68 Gy). The dose was defined according to the guidelines of the International Commission on Radiation Units and Measurements. The initial radiotherapy field for 44-46 Gy was planned according to preoperative and postoperative cranial magnetic resonance imaging data. We used CT planning with the use of contrast media. The clinical target volume was determined as gross tumour volume plus surrounding oedema on T2 weighted images with a margin of 2-2.5 cm. After 44-46 Gy, the treatment volume was reduced to encompass the contrast enhancing tumour on T1 weighted images plus 1.5-2 cm margins. The mean boost dose was 14-16 Gy.

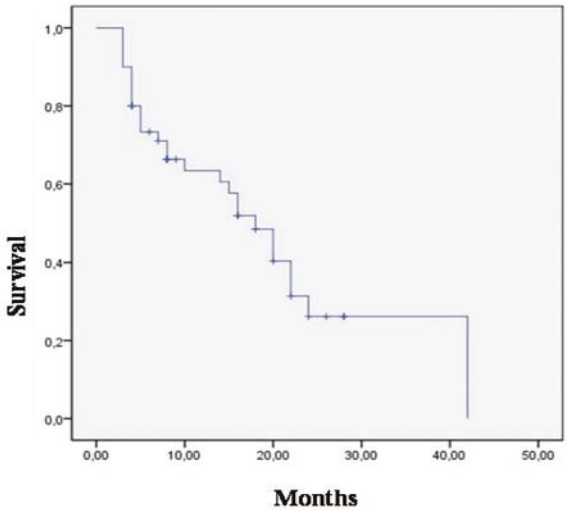

FIGURE 1. Oveall survival for 50 patients with glioblastoma multiforme.

TMZ was given to patients at a dose of 75 mg/m^2/day, 7 days per week, during the course of RT for approximately 6 weeks. After the completion of RT, patients were received an average of 6 cycles (range, 1-6) of adjuvant TMZ (150 -200 mg/m^2/day, 5 days during each 28-day).

Forty (80%) of 50 patients were given higher or equal than 60 Gy RT, thirty nine (78%) of 50 patients received concurrent TMZ, 75 mg/m^2 and 21 (42%) patients completed the six cycles of adjuvant TMZ. Ten (20%) of patients were given palliative RT (lower than 60 Gy), 11 patients (32%) were not given concurrent TMZ and 29 patients were not given adjuvant TMZ due to lower performance status, comorbidities, more symptoms etc. Characteristics of the patients are summarized in Table 1.

Age, sex, KPS, tumour diameter, type of surgery, dose of RT, concurrent and 6 cycles of adjuvant TMZ were analysed as a prognostic factors.

Statistical analysis

The statistical analysis was performed by SPSS 13. version. The primary end point was the overall

TABLE 1. Demographic characteristics of the patients

Characteristics	Number of patients	%	Median survival (Months)	12-month survival %	24-month survival %	Univariate analysis p	Multivatiate analysis p
Sex						0.279	0.759
Female	16	32	12	38.2	0		
Male	34	68	18	50.1	23.5	0.279	0.759
Age (yr)	**0.005**						0.601
< 70	14	28	17	41.7	21.1	**0.005**	0.601
≥ 70	36	72	13	35.7	0		
KPS	**0.0001**						0.151
< 70	24	48	7	0	0		
≥ 70	26	52	27	76.7	35.2	**0.0001**	0.151
Tumour diameter (cm)	0.849						0.928
< 5	15	30	17	61.5	38.5	0.849	0.929
≥ 5	35	70	15	40	30		
Extent of surgery						**0.0001**	**0.0001**
Total	22	44	24	95.5	57.3	**0.0001**	**0.0001**
Subtotal	9	18	6.7	11	0		
Biopsy	14	28	7.2	7	0		
Radiological	5	10	8.2	20	0		
≥60 Gy RT	**0.0001**						**0.005**
Yes	40	80	20	49.9	22.9	**0.0001**	**0.005**
No	10	20	5	0	0		
Concurrent CT-RT	**0.005**						
Yes	39	78	18.9	48.6	24.3	**0.005**	
No	11	22	7.5	9.1	0		
Adjuvant CT (6 cycles)	**0.0001**						**0.009**
Yes	21	42	28	80.7	37.8	**0.0001**	**0.009**
No	29	58	7	6.9	0		

KPS = Karnofsky performance status; RT = radiotherapy; CT = chemotherapy

survival and the progression free survival (PFS). The overall survival was estimated from the date of the histopathologic diagnosis (in 5 patients at radiological diagnosis) to the date of death or last follow-up. The overall survival was analyzed by the Kaplan-Meier method. The survival curves were compared by the log rank test. Patients were categorized in some variables including patient characteristics such as age (<70 or ≥70 years), sex, KPS (<70 or ≥70), tumour diameters (<5 cm or ≥ 5 cm) treatment parameters such as surgery (gross-total or subtotal resection), concurrent and 6 cycles of adjuvant TMZ. The effect of these variables on the survival was assessed by using a multivariate Cox-regression model.

Results

Median follow up time was 10 (months range; 3-42 months). One-and 2-year survival rates were 46% and 20%, respectively. While 36 (72%) of 50 patients died, 14 (28%) of them are alive (Figure 1).

The median overall survival was 20 months for patients who received ≥60 Gy RT and 5 months for the <60 Gy (p 0.0001) (Figure 2); 18.9 months for patients who received concurrent TMZ with RT and 7.5 months for patients who did not receive it (p=0.0001) (Figure 3); 28 months for patients who have been completing 6 cycles of adjuvant TMZ and 7 months for patients who have not been completing 6 cycles of therapy (p=0.0001). The me-

dian overall survival was 27 months for patients who had KPS≥70 and 7 months who had KPS<70 (p=0.0001) (Figure 4); 17 months for patients with age <70 and 13 months with ≥70 (p=0.005); 24 months for patients who had gross total resection, 6.7 months for patients who were diagnosed with biopsy and 8.2 months for patients who were diagnosed with radiology (p=0.0001).

One- and 2-year progression free survival (PFS) rates were 40% and 16%, respectively. Median PFS was 11 months for patients completing 6 cycles of adjuvant TMZ and 5.2 months for patients not completing 6 cycles of therapy. The difference between the two groups was significant (p=0.0001). The median PFS survival was 10.7 months for patients who had KPS≥70, 5.3 months for those who had KPS<70 (p=0.0001). Median PFS was 8.7 months for patients who were given ≥60 Gy and 4.5 months who were given <60 Gy (p=0.0001). However, the comparison of PFS between the patients of age ≥70 and those of age <70 (7.9 months *vs.* 7.0 months) showed no significant difference (p=0.358).

A multivariate Cox regression model was used to test the effect of age, sex, KPS, extent of surgery, tumour dimension (<5cm *vs.* ≥5cm), full dose radiotherapy (≥60Gy *vs.* <60Gy) concurrent TMZ and adjuvant TMZ treatment (adjuvant therapy with 6 cycles of TMZ group *vs.* <6 cycles of TMZ group) on the overall survival. The prognostic factors important for the overall survival were full dose RT (≥60 Gy) (p=0.005) and the application of adjuvant TMZ for 6 cycles (p=0.009) (Table 1).

Toxicity

The most common non-hematologic adverse effect was grade I nausea, which could be controlled by anti-emetics. It was seen in 34% of patients during the course of concurrent RT and TMZ and in 39% of patients during adjuvant TMZ. During the concomitant TMZ treatment, 2 patients (4%) experienced grade III or IV neutropenia and one patient (2%) had grade III or IV thrombocytopenia. Grade III or IV thrombocytopenia was seen in 3 patients (6%) during the adjuvant TMZ treatment. Only one patient discontinued the treatment due to hematologic toxicity. At the median follow up of 10 months we didn't see any late toxic effect.

Discussion

Patients with GBM, which is the most common primary brain tumour in adults, have a median overall survival rate of approximately 15 months, even with the aggressive resection, RT with concurrent and adjuvant CT.[11] Despite modern treatment techniques, tumours virtually always recur, usually arising within <2 cm of the prior resection margin. A long term overall survival is less than 5%.[13,14]

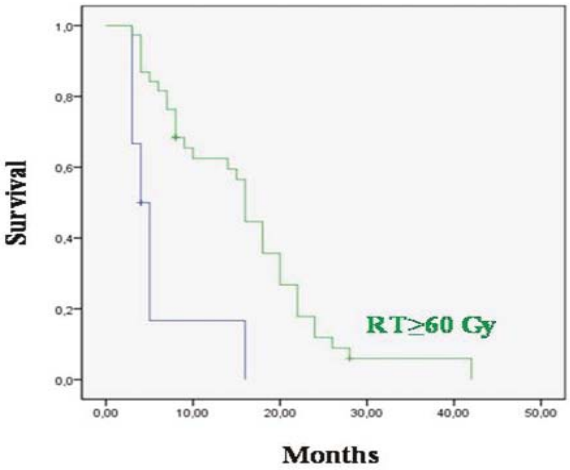

FIGURE 2. Overall survival for 40 patients who received ≥60 Gy RT and for 10 of them who received <60 Gy (p=0.0001).

A recent randomized trial by the European Organization for Research and Treatment of Cancer (EORTC) and the National Cancer Institute of Canada (NCIC) demonstrated that concomitant radiotherapy plus continuous daily TMZ followed by adjuvant TMZ significantly prolonged the survival in patients with glioblastoma. Five hundred seventy-three patients were randomly assigned to either standard RT alone or RT and concomitant and maintenance administration of TMZ (TMZ/RT). RT consisted of 30 fractions of 2 Gy each, administered Monday–Friday for 6-7 weeks. TMZ chemotherapy, at a low dose of 75 mg/m^2, was administered daily, including weekends, from the first to the last day of RT, for up 49 days. After a 4-week break, patients were to receive up to six cycles of maintenance TMZ (150–200 mg/m^2) daily for 5 days every 4 weeks. The median survival was 14.6 months for the radiotherapy plus TMZ group and 12.1 months for the radiotherapy alone group (P<0.001). PFS improved significantly in the radiotherapy plus TMZ group compared to the radiotherapy group (7.2 *vs.* 5 months, P<0.001). The 2-year survival rate was 26.5 for the combined treatment group.[11]

After the report of the EORTC-NCIC regimen of the maximal surgical resection followed by concurrent RT and TMZ followed by at least 6 monthly adjuvant TMZ cycles became the standard of care for newly diagnosed GBM. Patients in the EORTC-

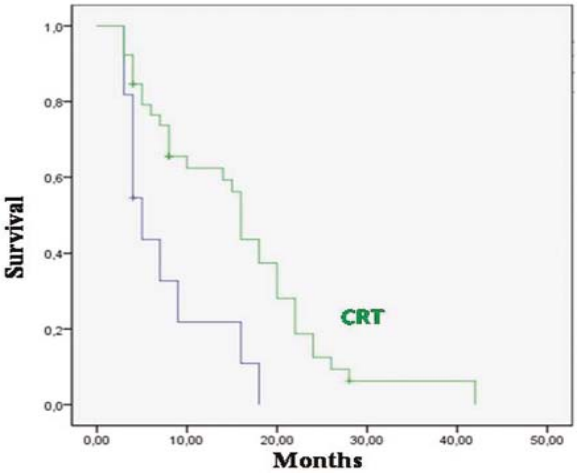

FIGURE 3. Overall survival for 39 patients who received concurrent chemo-radiotherapy.

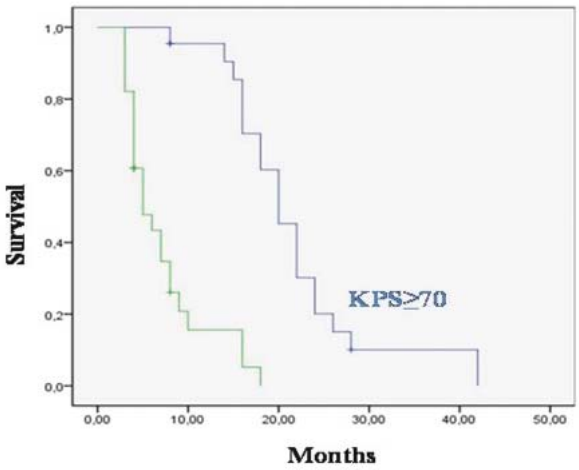

FIGURE 4. Overall survival 26 patients with Karnofsky performance status (KPS) ≥70 and 7and for 24 patients with KPS<70.

NCIC phase 3 study without disease progression discontinued adjuvant TMZ after six monthly cycles in part because of concerns regarding long-term toxicity such as myelodysplasia. Although no data are yet available demonstrating the improvement in the survival with the prolonged adjuvant therapy, reports of serious side effects from prolonged TMZ use are rare[15], and most neuro-oncologists in the United States advocate at least 12 post-RT adjuvant TMZ cycles for patients without disease progression. Ongoing clinical trials also typically incorporate 12 adjuvant TMZ cycles.[16]

In Erpolat *et al.* study, all patients received concomitant TMZ and radiotherapy at a daily dose of 75 mg/m^2, with or without adjuvant TMZ as recommended by the EORTC/NCIC trial. The overall survival and PFS were analyzed based on the comparison of the two groups whether or not they received adjuvant TMZ. Although the overall survival significantly increased in the adjuvant TMZ group (18.9 months *vs.* 9.8 months, P=0.015), the log rank test did not show significance for PFS (P=0.108). On both univariate and multivariate analysis, it was shown that the application of at least 4 cycles of adjuvant TMZ improved the overall survival and PFS. Their results suggest that at least 4 cycles of adjuvant TMZ should be added to the concomitant therapy to ensure the sufficient exposure to the drug.[17]

We have also shown that the treatment with concurrent and adjuvant TMZ is associated with a significant increase in the overall survival compared to without concurrent and/or adjuvant TMZ alone on univariate analyses. The median overall survival was 18.9 months for patients who received concurrent TMZ with RT and 7.5 months for patients not receiving concurrent TMZ (log-rank, p=0.0001) and 28 months for patients who completing 6 cycles of adjuvant TMZ and 7 months for patients not completing 6 cycles of therapy (log-rank, p=0.0001).

Hegi *et al.* investigated the relationship between promoter methylation of the MGMT DNA-repair gene and responsiveness to TMZ.[18] The authors demonstrated that the survival benefit of TMZ was limited to those patients with tumour containing methylated MGMT promoters. Among these patients, the median survival with radiotherapy and TMZ was 21.7 months (95% CI 17.4–30.4), compared to 15.3 months with radiotherapy alone (95% CI 13.0–20.9; p=0.007). An insignificant survival difference was demonstrated between treatment groups in patients with unmethylated MGMT promoters. This finding points to a genetic basis for the efficacy of TMZ and underscores the role of gene expression in optimal patient selection.[3,19] Although these articles represent a substantial step forward in the treatment of GBM, at this point it is too early in standard clinical practice to choose the TMZ treatment according to molecular criteria alone.[20]

Curran *et al.*[12] reported that the prognosis of malignant gliomas is relevant to the clinicopathologic variables such as treatment. Recursive partitioning analyses of the prognostic factors identified the five major variables including age, tumour type, performance status, mental status and treatment (extent of surgery and radiation dose). According to this classification, compared to young patients with good performance-mental status, the expectancy for those who have poor performance-mental status and/or advanced ages is dismal. For this rea-

son, the prediction of the treatment response is related to this classification.

In our study, multivariate and univariate analyses were performed based on these variables and demonstrated that the most important prognostic factors were: 6 cycles of adjuvant TMZ application, full dose radiotherapy (≥60Gy *vs.* <60Gy) and extent of surgery (gross total *vs.* others) for only the overall survival. However, younger age (<70), concurrent TMZ and good KPS (≥70) were significant for the overall survival on the univariate analysis but it did not reach a significant value on the multivariate analysis.

Advanced age has been associated not only with a poor prognosis but also with a reduced tolerance of the treatment and a decreased efficacy of the therapy.[12] The role of RT combined with concomitant and adjuvant TMZ, as established by the EORTC/NCIC trial as the standard treatment for patients with newly diagnosed GBM, remains unclear for the group of elderly patients. Gerstein *et al.* very recently reported that RT with concomitant TMZ is a feasible regimen with acceptable toxicity in elderly patients.[21] The promising outcome in patients with a good performance status and patients with gross total resections are notable. In our study, median overall survival was 17 months who age <70 and 13 months who age ≥70 (p=0.005).

The radiation therapy remains the most effective adjuvant modality in the management of GBM and the overall survival time appears to be correlated with the total dose delivered.[19,20] In our results on univariate and multivariate analysis ≥60 Gy RT was significantly improved for the overall survival (20 months *vs.* 5 months, p=0.0001 and p=0.005, respectively).

Mirimanoff *et al.* evaluated in EORTC/NCIC trial's patients whether the recursive partitioning analysis (RPA) retains its overall prognostic value and what the benefit of the combined modality is in each RPA class.[24] The overall survival was statistically different among RPA classes III, IV, and V, with median survival times of 17, 15, and 10 months, respectively, and 2-year survival rates of 32%, 19%, and 11%, respectively (p<0.0001). The survival with combined TMZ/RT was higher in RPA class III, with 21 months median survival time and a 43% 2-year survival rate, *vs.* 15 months and 20% for RT alone (p=0.006). In RPA class IV, the survival advantage remained significant, with median survival times of 16 *vs.* 13 months, respectively, and 2-year survival rates of 28% *vs.* 11%, respectively (p=0.0001). In RPA class V, however, the survival advantage of RT/TMZ was of borderline significance (p=0.054).

Our results demonstrated that a good performance status (KPS≥70) was significant for the overall survival on univariate analysis but it did not reach a significant value on the multivariate analysis.

Our study has several shortcomings. Firstly, it is retrospective in nature. Secondly, it has small sample size. However, the survival for patients who received TMZ according to the Stupp protocol was well, with a 1 and 2-year overall survival of 46% and 20% respectively. In addition, traditional prognostic factors were confirmed in our results, as age (<70), KPS (≥70), radiotherapy dose (≥60Gy), and gross total resection status were all favourable characteristics.

The results of our study confirm the efficiency of radiotherapy plus concomitant and adjuvant TMZ, with an acceptable toxicity in patients. We suggest that at least 6 cycles of adjuvant TMZ should be administered to obtain a benefit from the adjuvant treatment. Prospective randomized trials include the combination of TMZ with other drugs which need to be tested with large series of patients.

References

1. Buckner JC. Factors influencing survival in high-grade gliomas. *Semin Oncol* 2003; **30(6 Suppl 19):** 10-4.
2. Curran WJ Jr, Scott CB, Horton J, Nelson JS, Weinstein AS, Fischbach AJ, et al. Recursive partitioning analysis of prognostic factors in three Radiation Therapy Oncology Group malignant glioma trials. *J Natl Cancer Inst* 1993; **85:** 704-10.
3. Baur M, Preusser M, Piribauer M, Elandt K, Hassler M, Hudec M, et al. Frequent MGMT (06-methylguanine-DNA methyltransferase) hypermethylation in long-term survivors of glioblastoma: a single institution experience. *Radiol Oncol* 2010; **44:** 113-20.
4. Chakrabarti I, Cockburn M, Cozen W, Wang YP, Preston-Martin S. A population-based description of glioblastoma multiforme in Los Angeles County, 1974-1999. *Cancer* 2005; **104:** 2798- 806.
5. Kachanov DY, Dobrenkov KV, Shamanskaya TV, Abdullaev RT, Inushkina EV, Savkova RF, et al. Solid tumors in young children in Moscow Region of Russian Federation. *Radiol Oncol* 2008; **42:** 39-44.
6. Stupp R, Tonn JC, Brada M, Pentheroudakis G; ESMO Guidelines Working Group. High-grade malignant glioma: ESMO Clinical Practice Guidelines for diagnosis, treatment and follow-up. *Ann Oncol* 2010; **21(Suppl 5):** 190-3.
7. Stewart LA. Chemotherapy in adult high-grade glioma: a systematic review and meta-analysis of individual patient data from 12 randomised trials. *Lancet* 2002; **359:** 1011-8.
8. Stupp R, Gander M, Leyvraz S, Newlands E. Current and future developments in the use of the for the treatment of brain tumours. *Lancet Oncol* 2001; **2:** 552-60.
9. Stupp R, Hegi ME. Recent developments in the management of malignant glioma. In: Perry M, editor. *ASCO 2003 educational book*. Alexandria, VA: American Society of Clinical Oncology; 2003. p. 779-88.
10. DeAngelis LM. Brain tumors. *N Engl J Med* 2001; **344:** 114-23.

11. Stupp R, Mason WP, van den Bent MJ, Weller M, Fisher B, Taphoorn MJ, et al. Radiotherapy plus concomitant and adjuvant temozolomide for glioblastoma. *N Engl J Med* 2005; **352:** 987-96.

12. Curran WJ Jr, Scott CB, Horton J, Nelson JS, Weinstein AS, Fischbach AJ, et al. Recursive partitioning analysis of prognostic factors in three Radiation Therapy Oncology Group malignant glioma trials. *J Natl Cancer* Inst 1993; **85:** 704-10.

13. Mahaley MS Jr, Mettlin C, Natarajan N, Laws ER Jr, Peace BB. National survey of patterns of care for brain-tumor patients. *J Neurosurg* 1989; **71:** 826-36.

14. Stupp R, Hegi ME, van den Bent MJ, Mason WP, Weller M, Mirimanoff RO, et al. Changing paradigms – An update on the multidisciplinary management of malignant glioma. *Oncologist* 2006; **11:** 165-80.

15. Khasraw M, Bell D, Wheeler H. Long-term use of temozolomide: could you use temozolomide safely for life in gliomas? *J Clin Neurosci* 2009, **16:** 854-5.

16. Khasraw M, Lassman AB. Advances in the treatment of malignant gliomas. *Curr Oncol Rep* 2010; **12:** 26-33.

17. Erpolat OP, Akmansu M, Goksel F, Bora H, Yaman E, Büyükberber S. Outcome of newly diagnosed glioblastoma patients treated by radiotherapy plus concomitant and adjuvant temozolomide: a long-term analysis. *Tumori* 2009; **95:** 191-7.

18. Hegi ME, Diserens AC, Gorlia T, Hamou MF, de Tribolet N, Weller M, et al. MGMT gene silencing and benefit from temozolomide in glioblastoma. *N Engl J Med* 2005; **352:** 997-1003.

19. Velnar T, Smrdel U, Popovic M, Bunc G. Genetic markers in oligodendroglial tumours. *Radiol Oncol* 2010; **44:** 13-8.

20. Komotar RJ, Otten ML, Moise G, Connolly, Jr. ES. Radiotherapy plus concomitant and adjuvant temozolomide for glioblastoma – a critical review. *Clinical Medicine: Oncology* 2008: **2:** 421-2.

21. Gerstein J, Franz K, Steinbach JP, Seifert V, Fraunholz I, Weiss C, et al. Postoperative radiotherapy and concomitant temozolomide for elderly patients with glioblastoma. *Radiother Oncol* 2010; **97:** 382-6.

22. Walker MD, Strike TA, Sheline GE. An analysis of doseeffect relationship in the radiotherapy of malignant gliomas. *Int J Radiat Oncol Biol Phys* 1979; **5:** 1725-31.

23. Bleehen NM, Stenning SP. A Medical Research Council trial of two radiotherapy doses in the treatment of grades 3 and 4 astrocytoma. The Medical Research Council Brain Tumour Working Party. *Br J Cancer* 1991; **64:** 769-74.

24. Mirimanoff RO, Gorlia T, Mason W, Van den Bent MJ, Kortmann RD, Fisher B, et al. Radiotherapy and temozolomide for newly diagnosed glioblastoma: recursive partitioning analysis of the EORT C 26981/22981-NCIC CE3 phase - III randomized trial. *J Clin Oncol* 2006; **24:** 2563-9.

research article

Feasibility study on effect and stability of adaptive radiotherapy on kilovoltage cone beam CT

Poonam Yadav[1,2,3], Velayudham Ramasubramanian[3], Bhudatt R. Paliwal[1,2]

[1] Department of Human Oncology, University of Wisconsin, Madison, WI, USA
[2] Department of Medical Physics, University of Wisconsin, Madison, WI, USA
[3] Vellore Institute of Technology University, Vellore, Tamil Nadu, India

Received 7 February 2011
Accepted 24 March 2011

Correspondence to: Poonam Yadav, M.Sc., Department of Human Oncology, University of Wisconsin, 600 Highland Avenue, K4/347, Madison, WI 53705. E-mail: yadav@humonc.wisc.edu

Disclosure: No potential conflicts of interest were disclosed.

Background. We have analyzed the stability of CT to density curve of kilovoltage cone-beam computerized tomography (kV CBCT) imaging modality over the period of six months. We also, investigated the viability of using image value to density table (IVDT) generated at different time, for adaptive radiotherapy treatment planning. The consequences of target volume change and the efficacy of kV CBCT for adaptive planning issues is investigated.

Materials and methods. Standard electron density phantom was used to establish CT to electron density calibrations curve. The CT to density curve for the CBCT images were observed for the period of six months. The kV CBCT scans used for adaptive planning was acquired with an on-board imager system mounted on a "Trilogy" linear accelerator. kV CBCT images were acquired for daily setup registration. The effect of variations in CT to density curve was studied on two clinical cases: prostate and lung.

Results. The soft tissue contouring is superior in kV CBCT scans in comparison to mega voltage CT (MVCT) scans. The CT to density curve for the CBCT images was found steady over six months. Due to difficulty in attaining the reproducibility in daily setup for the prostate treatment, there is a day-to-day difference in dose to the rectum and bladder.

Conclusions. There is no need for generating a new CT to density curve for the adaptive planning on the kV CBCT images. Also, it is viable to perform the adaptive planning to check the dose to target and organ at risk (OAR) without performing a new kV CT scan, which will reduce the dose to the patient.

Key words: cone-beam computerized tomography, kV CBCT; CT to density table; electron density phantom; adaptive planning

Introduction

The ultimate goal of radiotherapy is to deliver a sufficient dose to the target (tumor) region while sparing the healthy tissues around target so that successful target cell killing can be achieved with minimum toxicity to the organ at risk (OAR). Limited patient motion also helps to assure that the dose delivered during the treatment is close to the dose computed on initial kVCT images used for the treatment planning. Modern irradiation techniques such as stereotactic radiation and intensity-modulated radiotherapy (IMRT) are capable of generating the complex dose distribution with high dose areas firmly conformed to the target volume.[1-3] The sparing of surrounding normal tissue is efficiently achieved if the patient is accurately positioned on the treatment table with respect to the imaging setup. To achieve this, imaging has become an important tool in radiotherapy treatment procedures specifically in the image guided radiation therapy (IGRT) and the adaptive radiation therapy. The development of body cast and head mask system has provided a non-invasive patient fixation. However, the interfractional and intrafractional anatomy change of the patient cannot be detected

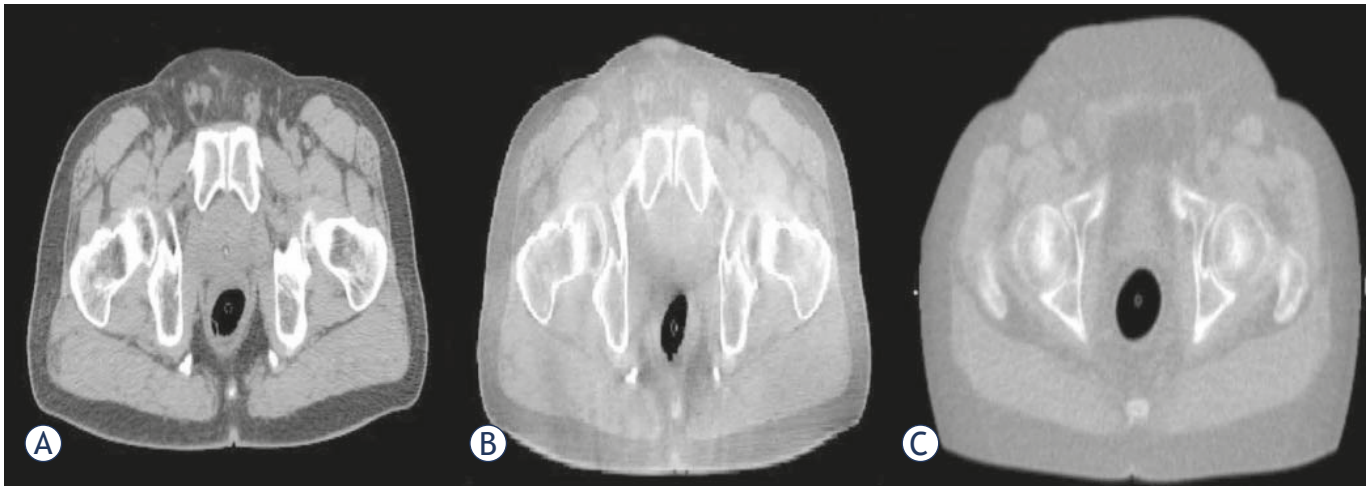

FIGURE 1. (A) kVCT, (B) kV CBCT and (C) MVCT images in transverse view are represented. As seen in figure the soft tissues contrast is better for kV CBCT images in comparison to MVCT image.

by any means of the non-invasive method.[4] Also; the daily changes in human body alter the soft tissue landscapes within a patient's anatomy, which further result in more gradual changes in target and other related structures during the course of the radiation therapy.

Mega voltage CT (MVCT) imaging on TomoTherapy Hi-ART (TomoTherapy Inc. Madison, WI) machine, mega voltage and kilovoltage cone beam computerized tomography (CBCT) on Varian linear accelerator with mobile C-arm kilovoltage imager are often used to keep track of the anatomical changes, taking place during the treatment. This raises the probability of dose conformation in the target region and decreases the severity of side effects. For some cases, acquiring electronic portal images frequently, prior to delivery of each fraction usually does the assessment of positional changes and registering these images with digitally reconstructed CT data.[5] Corrections are made on the basis of the significance of differences. But the simple translation cannot capture the full extent of anatomic changes, as organs are not rigid. The actual deformation depends on the changes in shape as well as location of the OAR or target and hence is 3-dimensional (3D) in nature. The changes are thus not fully accessible with the simple translation.

CBCT adequately provides the volumetric data of target and surrounding anatomical structures (bones and soft tissue).[6-8] The 3D kV CBCT systems are extensively used in IGRT for patient setup, visualization and localization. Multiple vendors have installed on board imagers using kV X-ray on linear accelerators. Onboard imager helps to resolve the critical aspects of IMRT such as patient setup and target localization.[9] A CBCT image of the patient can be acquired in about 60 seconds just before the delivery of each treatment fraction. The CBCT using a kilovoltage imaging system mounted on a linear accelerator has emerged as a significant technique for realising the soft tissue registration.[10] Presently, adaptive planning is frequently done on MVCT and kV-CBCT images to conform the dose distribution and dose coverage to the target and OAR due to significant weight loss during the treatment, shrinkage in tumor or re-growth of the tumor volume. For any sort of the adaptive planning, it is important to make use of correct parameters like image set and CT to density table.[11] Doing adaptive planning on the regular basis requires a routine check of the machine's CT to density curve. The changes in the CT to density curve are introduced due to the variation in the Hounsfield number (HU) or CT number. Richter *et al.* (2008) have studied that the mean difference of 564 HU ± 377 HU was observed in the CT values of the CBCT image and CT image. Thus, it becomes important to check for the stability of the CT to density curve and its effect on the planning. Also, for the adaptive planning, it is important to have a good images quality. Figure 1 shows that for soft tissues, the kV CBCT images are superior to the MVCT images, thus making re-contouring is easier on kVCT images. The adaptive radiotherapy treatment is practically helpful. Real time in-

trinsic anatomical imaging data, dose calculations using valid CBCT numbers and necessary amendment in plan on the basis of the revised target and OARs localization are primary requirements for it.[12-14]

Seco and Evans in 2006, observed that the use of electron density, rather than mass density, at the treatment planning system gives better precision in dose calculations.[15] Also, Morin *et al.* in 2006 investigated the feasibility of using MV CBCT for the dosimetric impact of changing anatomy and subsequently applying it for the adaptive radiotherapy.[16] Yang *et al.* (2007) investigated the effect of scatter on the reconstructed CBCT pixel values and found that CBCT image reconstruction of a transverse slice was dependent on the scatter through the entire volume.[17] So, adequate phantoms (earlier only 5 cm long phantom were used and so consequently had less scan volume) should be used for HU number to the electron density calibration for real patient imaging. At present, there is a lack of literature which can elucidate the details of the precisions and limitations of HU to the electron density calibration of kV CBCT over the longer duration of time and this limitation hampers the utilization of capabilities of this technology for the adaptive radiotherapy.

The overall purpose of this paper is to study the stability of the CT to density curve of kV CBCT imaging modality over the period of six months using electron density phantom and subsequently, analyzing the effect of CT to density curve in the clinical plans. We have investigated the feasibility and usefulness of kV CBCT for the adaptive radiotherapy and the dosimetric aspects with respect to volumetric changes and calibration curve are analyzed.

Materials and methods

"Trilogy" (Varian) offers a broad range of external beam energy for the treatment of palliative cases, 3D conformal radiation therapy (CRT), and IMRT with multiple dose rate options. It is a comprehensive delivery system built on the foundations of Clinac iX platform. Along with the capabilities of a Clinac 21EX, the Trilogy accelerator has an extensive list of new features like Stereotactic mode (6 MV beam, up to 1000 MU/min dose rate, up to 6000 MU/field total dose, 60 MU/deg dose rate for arc-based treatments and maximum field size of 15cm * 15cm), remote couch motion, 0.75 mm radius isocenter for all three rotational axes and 0.5 mm radius isocenter for gantry and collimator axes. Instant imaging is obtained with the help of the portal imager. On-Board Imager, kV imaging system is standard on Trilogy linear accelerator which makes dynamic targeting IGRT more efficient and convenient. During this work, we have used this machine. The stability of the CT to electron density calibration is an indicator of the CT number integrity and a prerequisite for the dose recalculation. To study the stability of CT to the electron density table, the electron density phantom was used.

The electron density phantom (Fluke model 76-462) is composed of an inner head and outer torso section and has a series of inserts of known physical densities. The phantom is manufactured from durable epoxy and the tissue equivalent plugs and can be positioned at 17 different locations within the scan field. The phantom has the inserts for the breast, lung (inhale and exhale), liver, dense bone, muscle, adipose and trabecular bone. A distance registration can be quickly accessed with special marker plugs. The CBCT scans were acquired with an on-board imager system mounted on a Trilogy linear accelerator (Varian Medical Systems). The scan duration was 60 seconds with 640 projections acquired over 360 degrees. The "Electron Density" phantom was scanned multiple times over a period of six months. The kV CBCT images acquired were then imported to the Pinnacle 8.1 treatment planning system (TPS) (Philips Medical Systems, Fitchburg, WI) to measure image values. Regions of interest were contoured at the centre of each of the phantom plugs and the mean HU values within the contours were recorded. The electron densities of each phantom plug were recorded from the manufacturer specifications and the physical density corresponding to the mean CT values was recorded and plotted as the CT to density curve. The CT to density curve was recorded for a period of six months by scanning the phantom twice a week.

The effect of variations in CT to density curve was studied on two clinical cases: prostate and lung. The lung was treated using 3D CRT and the prostate by using an IMRT treatment plan. The lung tumor was prescribed to 52 Gy in 2 Gy per fraction for the treatment and the prostate was prescribed to 70 Gy in 2.5 Gy per fraction. Each case had one kVCT image called reference image which was used as a planning CT. kV CBCT images were acquired for registration purposes. A treatment plan with the appropriate target coverage and minimum dose to sensitive structures was planned on kVCT. The dose distribution based

on the daily kV CBCT images was calculated using Pinnacle[3] 8.1 treatment planning system (TPS) (Philips Medical Systems, Fitchburg, WI). The kV CBCT images were exported to Pinnacle planning station and the images were aligned with the kVCT images using fusion tools. Dose re-computations for each case were recalculated for the acquired CT to density curves. Changes in the dose volume histograms (DVHs) and the dose distribution due to changes in CT to density were used to compare the plans. DVH points, such as D90 (dose to 90% of target volume), D95 (dose to 95% of target volume) for the planning target volume (PTV) and the D50 (dose to 50% of target volume) and D30 (dose to 30% of the target volume) for the critical structures were calculated and analysed for all the plans generated using different CT to density tables.

Results

The CT image used for the treatment planning and the kV CBCT image acquired on one of the treatment day are shown in Figure 1, an MVCT image is also shown for the image quality comparison. The kV CBCT images have good soft tissue visibility and can be used for the contouring if required. The CT to density curve is generated over a period of six months for the kV CBCT using the electron density phantom. The CT to density curve for the CBCT images is fairly consistent. As seen in Figure 2, a small percentage difference of 3% is observed in comparison to the original used kV CBCT, CT to density curve. This percentage difference was consistent in the consecutive months. In order to analyze the effect of this difference on the clinical plans, kV CBCT acquired for the patient set were exported to Pinnacle and images were registered to the primary planning kVCT scan using the Syntegra automatic registration software operating within Pinnacle. Figure 3 shows the difference in the DVH for lung case generated using the original CT to density curve and the CT to density curve generated for the month of November. Figure 4 shows the DVH results using the CT to density curve for last four months. It was noted that for the entire analysis period, there was no significant variation in calibration curve for all physical densities and also does not show a significant difference in the clinical DVHs.

For the prostate case, the dose to the prostate remains fairly alike for all treatments but the dose to the bladder and rectum shows a considerable variation between the first and last day of the treatment

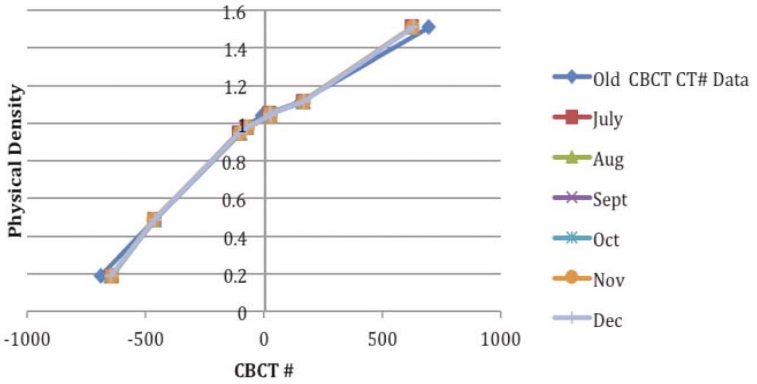

FIGURE 2. CT to density curve generated over a period of six months using electron density phantom.

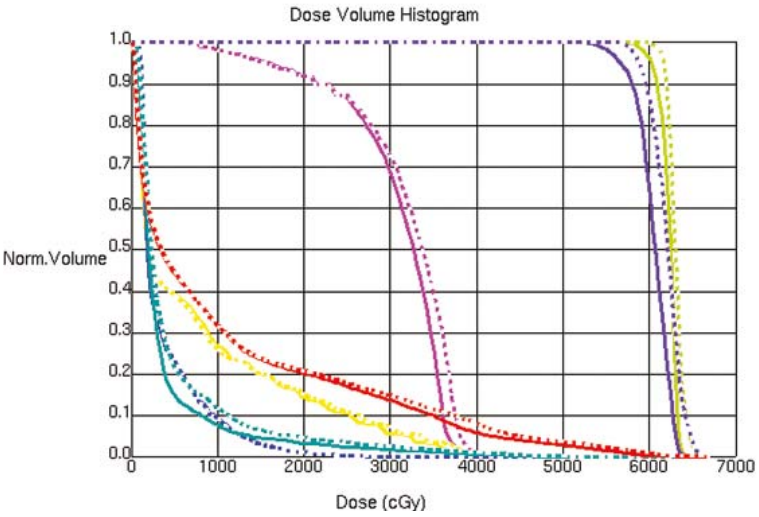

FIGURE 3. Dose volume histogram for the lung case using the original CT to density curve, for the month of October and November.

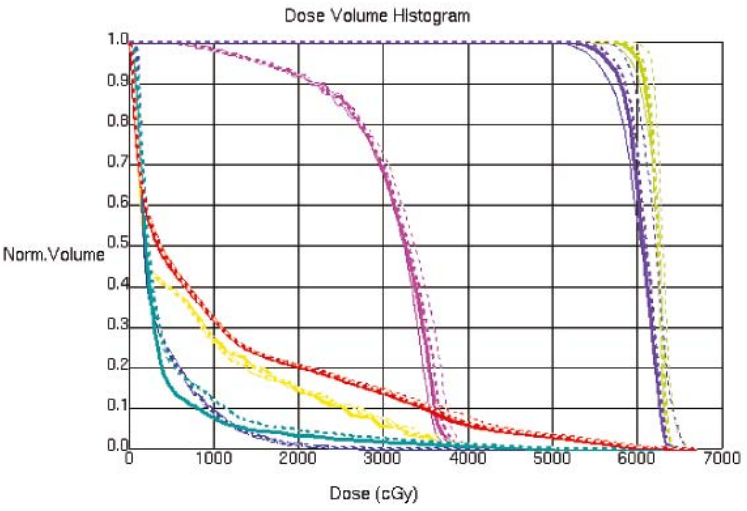

FIGURE 4. Dose volume histogram for the lung case using CT to density curves generated for last four months.

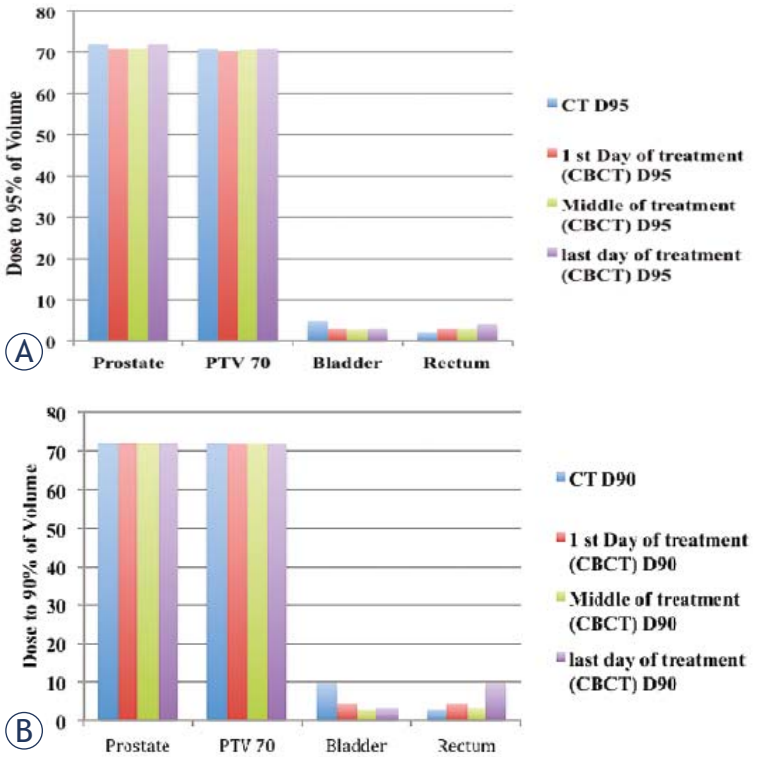

FIGURE 5. Histogram representing the dose received by the (A) 95% and (B) 90% of volume for prostate PTV70, bladder and rectum on the first, middle and last day of the treatment and for day of kVCT scan and original CT scan.

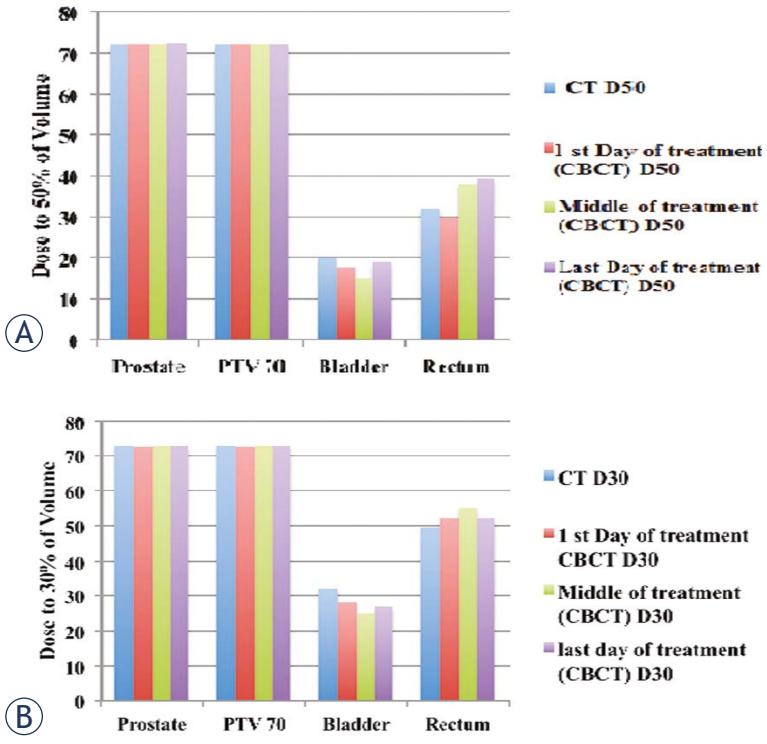

FIGURE 6. Histogram representing the dose received by the (A) 50% and (B) 30% of prostate, PTV70, bladder and rectum volume on the first, middle and last day of the treatment and for day of kVCT scan and original CT scan.

for D90 (dose received by 90% of the volume) and D95 (dose received by 95% of the volume) as shown in Figure 5 (a, b). Figure 6(a, b) summarizes the results for D30 and D50. For better comparison the results from the original plan (kV CT based plan) is also displayed. The PTV volume showed a slight variation on day-to-day basis. Similar trend is observed for the bladder but there is less variation in the rectum volume. The results for the variation in the volumes of PTV, bladder and rectum wall are represented in the histogram format in Figure 7. It is observed that the patient's bladder was systematically smaller on all CBCT scans compared with the planning CT scan. In order to investigate the deviation in dosimetry for the treatment period, we also analyzed the standard deviation for the entire treatment period. It has been observed that there is a negligible standard deviation in the daily prostate mean dose in kV CBCT plan as well as in case of kVCT plan. The relative standard deviation of 0.5 is observed for PTV (PTV70) in kV CBCT plan and kV CT plans. On the other hand, the relative standard deviation of 4.5 in case of bladder and approximately 2 for rectum are noticed. The relative standard deviation in daily dose to 50%, 30% and 20% of bladder is around 4 to 4.3 for CBCT plan and likewise, for a daily dose to 50%, 30% and 20% of rectum wall is 2.3, 2 and 3.9, respectively. The difference in the dose received by the 90%, 95%, 50% and 30% volume of the PTV, bladder and rectum was not due to the CT to the density table but was mainly due to the displacement of the prostate due to the variation in the bladder and rectum filling on each day.

Discussion

Adaptive radiotherapy is an evolving area of much interest, aimed at developing techniques by which a course of radiation therapy could continually be monitored and modified to reflect the anatomic changes known to occur. So, acquiring dose information at radiation treatment course time serves as feedback necessary for the re-evaluation and subsequently adjusting the plan if necessary to account for discrepancies, anatomical changes and variation in the tumor size is a critical part of the adaptive radiotherapy. The CT to density curve for the kV CBCT shows very slight changes over the period of six months. Thus, the adaptive planning on the kV CBCT images can be performed without generating a new CT to density curve as required for the adaptive planning on MVCT images.

Studies show that the dose difference of 5% can be observed if an incorrect image value to density table is used for the adaptive planning for MVCT. CBCT helps in attaining a prudent and efficient plan, as over the entire treatment period no system related dosimetric discrepancies are observed and also the same CT to density curve is functional over the entire length of the treatment. The difference in the dose to the rectum and bladder are due to the lack of reproducibility of the daily set up for the prostate treatment. Hence, it is important to perform the adaptive planning to check the dose to the target and OAR, if possible without performing a new CT scan, which will reduce the dose to the patient. Also, the image quality of the kV CBCT images are superior for the soft tissues for contouring. Usually, using the large margin for the PTV can help to compensate for setup errors but this may not be of great help for the prostate cases since the rectum and bladder volume shows the variation on each day of the treatment. Also, by increasing the PTV, the dose to bladder and rectum may increase. The presented study confirms consistently the variations in tumor (both shape and size), and bulk of soft tissue information for daily image guidance. Significance of dose difference of 5% to 6 % or more on the single day of the treatment is beyond the scope of this study.

Conclusions

CBCT based imaging is a preferable option for the anatomical delineation of soft tissues due to its superiority in comparison to MVCT based imaging. From the perspective of the adaptive planning, this system improves the overall workflow with a quick review and analysis of the dynamic requirements. The acceptability of the same CT to the density curve is ascertained by the stability of the curve for the adequate treatment period. Though there might be variations to be accommodated in the treatment plan, the main reason behind such variations is due to differences in anatomy over time. Thus, kV CBCT has potential to act as a valuable tool for adaptive radiotherapy and significantly helps in avoiding the excessive patient scanning which may lead to cumulative high doses in patients.

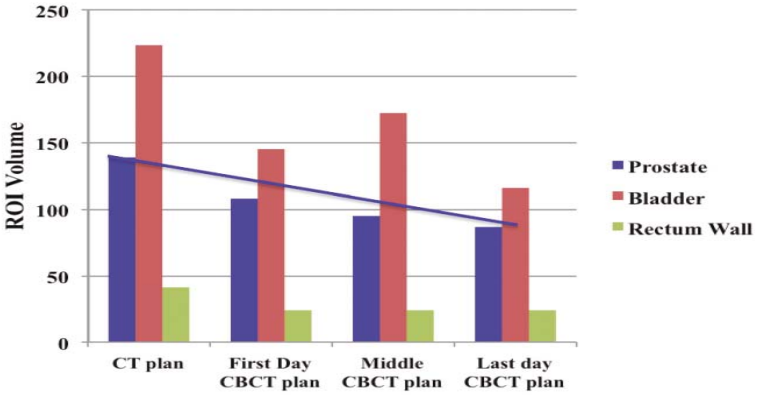

FIGURE 7. Histogram shows the variation in the volumes of prostate, bladder and rectum wall on, first, middle and last day of the treatment and for day of kVCT scan. The units of ROI volumes are represented in cc.

References

1. Kuban D, Pollack A, Huang E, Levy L, Dong L, Starkschall G, et al. Hazards of dose escalation in prostate cancer radiotherapy. *Int J Radiat Oncol Biol Phys* 2003; **57:** 1260-8.
2. Hurkmans CW, Cho BC, Damen E, Zijp L, Mijnheer BJ. Reduction of cardiac and lung complication probabilities after breast irradiation using conformal radiotherapy with or without intensity modulation. *Radiother Oncol* 2002; **62:** 163-71.
3. Tubiana M, Eschwege F. Conformal radiotherapy and intensity modulated radiotherapy: clinical data. *Acta Oncol* 2000; **39:** 555-67.
4. Thieke C, Malsch U, Schlegel W, Debus J, Huber P, Bendl R, et al. Kilovoltage CT using a linac-CT scanner combination. *Br J Radiol* 2006; **79(Spec No 1):** S79-S86.
5. Künzler T, Grezdo J, Bogner J, Birkfellner W, Georg D. Registration of DRRs and portal images for verification of stereotactic body radiotherapy: a feasibility study in lung cancer treatment. *Phys Med Biol* 2007; **52:** 2157-70.
6. Oldham M, Letourneau D, Watt L, Hugo G, Yan D, Lockman D, et al. Cone-beam CT guided radiotherapy: a model for on-line applications. *Radiother Oncol* 2005; **75:** 271–278.
7. Smitsmans MH, de Bois J, Sonke JJ, Betgen A, Zijp LJ, Jaffray DA, et al. Automatic prostate localization on cone-beam CT scans for high precision image guided radiotherapy. *Int J Radiat Oncol Biol Phys* 2005; **63:** 975-84.
8. Purdie TG, Bissonnette JP, Franks K, Bezjak A, Payne D, Sie F, et al. Cone-beam computed tomography for on-line image guidance of lung stereotactic radiotherapy:lLocalization, verification, and intrafraction tumor position. *Int J Radiat Oncol Biol Phys* 2007; **68:** 243-52.
9. Ding GX, Duggan DM, Coffey CW, Deeley M, Hallahan DE, Cmelak A, et al. A study on adaptive IMRT treatment planning using kV cone-beam CT. *Radiother Oncol* 2007; **85:** 116-25.
10. Lawson JD, Schreibmann E, Jani AB, Fox T. Quantitative evaluation of a cone-beam computed tomography–planning computed tomography deformable image registration method for adaptive radiation therapy. *J Appl Clin Med Phys* 2007; **8(4):** 2432.
11. Yadav P, Tolakanahalli R, Rong Y, Paliwal BR. The effect and stability of MVCT images on adaptive TomoTherapy. *J Appl Clin Med Phys* 2010; **11(4):** 3229.
12. Korreman S, Rasch C, McNair H, Verellen D, Oelfke U, Maingon P, et al. The European Society of Therapeutic Radiology and Oncology–European Institute of Radiotherapy (ESTRO–EIR) report on 3D CT-based in-room image guidance systems: A practical and technical review and guide. *Radiother Oncol* 2010; **94:** 129-44.
13. Galerani AP, Grills I, Hugo G, Kestin L, Mohammed N, Chao KK, et al. Dosimetric Impact of Online Correction via Cone-Beam CT-Based Image Guidance for Stereotactic Lung Radiotherapy. *Int J Radiat Oncol Biol Phys* 2010; **78:** 1571-8.

14. Duma MN, Kampfer S, Wilkens JJ, Schuster T, Molls M, Geinitz H. Comparative Analysis of an Image-Guided Versus a Non–Image-Guided Setup Approach in Terms of Delivered Dose to the Parotid Glands in Head-and-Neck Cancer IMRT. *Int J Radiat Oncol Biol Phys* 2010; **77:** 1266-73.

15. Seco J, Evans PM. Assessing the effect of electron density in photon dose calculations. *Med Phys* 2006; **33:** 540-52.

16. Morin O, Gillis A, Chen J, Aubin M, Bucci MK, Roach M 3rd, et al. Megavoltage cone-beam CT: system description and clinical applications. *Med Dosim* 2006; **31:** 51-61.

17. Yang Y, Schreibmann E, Li T, Wang C, Xing L. Evaluation of on-board kV cone beam CT (CBCT)-based dose calculation. *Phys Med Biol* 2007; **52:** 685-705.

Radiol Oncol 2011; 45(3): 159-165.
doi:10.2478/v10019-011-0018-3

Sodoben razvoj kirurškega zdravljenja malignih gliomov

Vranič A

Izhodišča. Maligni gliomi obsegajo velik del možganskih tumorjev. Z napredkom nevroonkologije se je dolžina preživetja brez ponovitve tumorja pri bolnikih z malignimi gliomi bistveno podaljšala. Celokupno preživetje bolnikov z malignimi gliomi pa je še vedno v veliki meri odvisno od popolnosti kirurške resekcije tumorja. Da bi zmanjšali pooperativne nevrološke izpade, so razvili številne pred- in medoperativne tehnike, ki nam pomagajo pri varni resekciji malignih gliomov.

Zaključki. V kirurgiji malignih gliomov uporabljamo številne kirurške tehnike, kot so mikrokirurgija, nevroendoskopija, stereotaktična biopsija ali brahiterapija. Posebno vrednost imajo slikovne in funkcijske tehnike. Slikovne tehnike nam pomagajo pri boljšem predoperativnem prikazu tumorja in pri izbiri pristopa do tumorja. Funkcijske tehnike pa nam omogočijo določiti elokventna področja možganov.

Radiol Oncol 2011; 45(3): 166-173.
doi:10.2478/v10019-011-0009-4

Polidimetilsiloksan: novi kontrastni material za lokalizacijo okultnih lezij v dojki

Vitral GSF, Raposo NRB

Izhodišča. Za radiološko vodeno lokalizacijo okultnih lezij v dojki (ROLL) pogosto uporabljamo radiološko kontrastno sredstvo z jodom. Z njim želimo potrditi, da je predhodno injiciran ^{99m}Tc-MAA v tarčnem tkivu. Tako kontrastno sredstvo ima nekaj pomanjkljivosti. Namen raziskave je bil ovrednotiti varnost, učinkovitost in tehnično primernost uporabe polidimetilsiloksana (PDMS) kot radiološkega kontrasta pri ROLL-u.

Materiali in metode. Varnosti uporabe PDMS smo preverjali na laboratorijskih podganah Wistar (n=50). Radiološka uporaba kontrasta pa smo ocenjevali s klinično raziskavo bolnic, pri katerih smo naredili reduktivno mamoplastiko (n=32). Tehnično izvedljivost smo ovrednotili s pomočjo scintigrafije in histološke analize.

Rezultati. PDMS ni imel toksičnih stranskih učinkov. V klinični raziskavi smo ugotovili, da je PDMS označil manjši volumen tkiva dojke kot standardno kontrastno sredstvo ($p < 0.001$). Poleg tega PMDS ni interferiral s scintigrafijo ($p = 0.528$) in ni bilo zaznati histoloških sprememb v tkivu.

Zaključek. Rezultati študije kažejo prednost PDMS kot kontrastnega sredstva v primerjavi s kontrastom na osnovi joda. Raziskava dokazuje tudi tehnično izvedljivost uporabe PDMS pri ROLL-u.

Radiol Oncol 2011; 45(3): 174-179.
doi:10.2478/v10019-011-0023-6

Urografija z magnetno resonanco pri otrocih – kdaj in zakaj?

Vegar-Zubović S, Kristić S, Lincender L

Izhodišča. Namen raziskave je bil določiti pomen urografije z magnetno resonanco (MRU) v diagnostiki bolezenskih sprememb urinarnega trakta pri otrocih.

Bolniki in metode. 21 pediatričnih uroloških bolnikov smo preiskovali s T1 obteženimi slikami pred in po aplikaciji kontrasta ter s T2 obteženimi slikami in 3D gradient eho sekvencami po aplikaciji kontrasta. Rezultate preiskav smo primerjali z izsledki pridobljenimi z ultrazvočno preiskavo, ki smo jo naredili pri vseh bolnikih, z intravenozno urografijo, ki smo jo naredili pri 14 bolnikih z diagnosticirano hidronefrozo in z mikcijskimi cistogrami, ki smo jih naredili pri 6 bolnikih, kjer smo sumili na hidronefrozo zaradi vesikoureteralnega refluksa (VUR).

Rezultati. Z MRU smo ugotovili vzrok hidronefroze pri vseh 14 bolnikih: 5 bolnikov je imelo stenozo v predelu ureteropelvičnega spoja (UPJ), 1 bolnik je imel funkcionalno stenozo, 3 rezidualno hidronefrozo, 1 bolnik kombinacijo stenoze UPJ in stenoze v predelu vezikoureteralnega spoja (VUJ) s hidromegaureterjem, 2 fetalni ureter in 3 bolniki insuficientne široke ureteralne ostije. V primerjavi s prejšnjimi preiskavami smo pri vseh bolnikih, ki smo jim naredili MRU, dodatno razjasnili naravo urološke bolezni: pri 1 bolniku kalicealno litiazo, pri 4 stenozo UPJ, pri 1 stenozo VUJ, pri 1 nevrogeni mehur, pri 1 hipotonični ureter, pri 1 urinarno infekcijo, pri 1 pelvično in uretersko duplikaturo, pri 1 urinarni zastoj in pri 1 bolniku fetalni ureter. Z MRU smo prav tako odkrili: pri 3 bolnikih policistično ledvico, pri 1 kalicealno cisto, pri 2 enostavno ledveno cisto, pri 1 dolga hipotonična zavita ureterja in pri 1 bolniku hipertrofično kolumno Bertini.

Zaključki. Z MRU lahko pridobimo slike z visoko kontrastno in prostorsko resolucijo celotnega urinarnega trakta v katerikoli ravnini. Prav tako MRU omogoča natančno ugotovitev in razločevanje patoloških sprememb. Predvidevamo, da bo MRU lahko velikokrat nadomestil dosedanje slikovne metode ugotavljanja bolezenskih sprememb urinarnega trakta.

Radiol Oncol 2011; 45(3): 180-183.
doi:10.2478/v10019-011-0021-8

Z računalniško tomografijo potrjena pseudoanevrizma levega prekata pri bolniku z dilatativno alkoholno kardiomiopatijo

Letonja M, Šantl Letonja M

Izhodišča. Pseudoanevrizme so redki zapleti miokardnega infarkta in se pogosto pojavljajo z rupturo. Še vedno je izziv, s katero slikovno diagnostiko naj opredelimo končno diagnozo pseudoanevrizme in jo ločimo od prave anevrizme, kar je klinično pomembno zaradi različnega zdravljenja.

Prikaz primera. Opisujemo nenavaden primer 56-letnega bolnika z znaki srčnega popuščanja, ki so se stopnjevali nekaj mesecev pred hospitalizacijo. Menimo, da je bolnik med poslabšanjem simptomov utrpel klinično nem miokardni infarkt, ki se je zapletel z rupturo proste stene, kjer je nastala pseudoanevrizma brez tamponade srca. Z ehokardiografijo smo prikazali dilatativno kardiomiopatijo, ki je bila prisotna že leta pred poslabšanjem simptomov, in pseudoanevrizmo na anterolateralni steni levega prekata, kjer so redko opisane. Pseudoanevrizma je bila potrjena s preiskavo CT. Zaradi močno zmanjšanega srčnega iztisa in neodzivnosti simptomov na terapijo srčnega popuščanja se nismo odločili za resekcijo anevrizme in bolnik je umrl zaradi slabšanja srčnega popuščanja in embolije.

Zaključki. Primer prikazuje pomen neinvazivne diagnostike akutnega poslabšanja kroničnega srčnega popuščanja, kjer s slikovno diagnostiko najprej naredimo ehokardiografsko preiskavo in radiogram pljuč in srca. Na podlagi izsledkov obeh preiskav se odločamo za nadaljnjo slikovno diagnostiko. V prikazanem primeru smo opravili preiskavo CT, s katero smo dokončno potrdili pseudoanevrizmo levega prekata, ki je nastala pri bolniku z dilatativno kardiomiopatijo.

Radiol Oncol 2011; 45(3): 184-188.
doi:10.2478/v10019-011-0010-y

Scintigrafija v zamaknjenem energijskem oknu: metoda za oris telesnih kontur pri limfoscintigrafiji brez uporabe zunanjega ploščatega vira

Momennezhad M, Zakavi SR, Kakhki VRD, Jangjoo A, Ghavamnasiri MR, Sadeghi R

Izhodišča. Ocenjevali smo uporabnost metode zamaknjenega energetskega okna za oris bolnikovih telesnih kontur po intradermalni injekciji majhnega odmerka radiofarmaka pri limfoscintigrafiji.

Bolniki in metode. V raziskavo smo vključili 60 bolnic z rakom dojke, pri katerih smo naredili limfoscintigrafijo. Statične scintigrafske posnetke v sprednji in stranski projekciji smo naredili 30 minut po injekciji radiofarmaka s pomočjo kamere gama in kolimatorja visoke ločljivosti za nizke energije sevanja. Po dvodnevnem protokolu smo dodatne statične posnetke naredili 20 ur po aplikaciji radiofarmaka. Pri scintigrafiji smo uporabljali dva energijska okna: (1) okno Tc-99m (130-150 keV) in (2) okno sipanih fotonov (60-120 keV). Posnetke narejene v vsakem od oken smo med seboj združili s pomočjo računalniškega programa za fuzijo slik. Pri 20 preiskovankah smo za oris telesa po standardnem postopku (brez premikanja preiskovanke po končani limfoscintigrafiji) uporabili še zunanji ploščati vir.

Rezultati. Zgodnji posnetki (po 30 minutah) v zamaknjenem energijskem oknu so jasno pokazali telesno konturo. V primerjavi z zgodnjimi so bili pozni posnetki po 20 urah nekoliko slabše kakovosti. S scintigrafijo v zamaknjenem energijskem oknu smo s fuzijo slik dosegli jasen prikaz in lokalizacijo varovalnih bezgavk in oris kontur telesa na zgodnjih posnetkih, tega nismo dosegli na poznih posnetkih po 20 urah. Dodatna obdelava (rekonstrukcija slik v zamaknjenem energijskem oknu in fuzija slik) je povprečno trajala 10±5 sekund.

Zaključki. Scintigrafija v zamaknjenem energijskem oknu je koristna za oris bolnikovih telesnih kontur po injekciji majhnega odmerka radiofarmaka. Preiskovanke sevalno dodatno ne obremenjuje in bistveno ne podaljša scinigrafske preiskave.

Radiol Oncol 2011; 45(3): 189-195.
doi:10.2478/v10019-011-0017-4

Uporabnost prehrane z nizko vsebnostjo joda pri vodenju bolnikov z diferenciranim karcinomom ščitnice – prvi rezultati

Dobrenić M, Huić D, Zuvić M, Grošev D, Petrović R, Samardžić T

Izhodišča. Pred aplikacijo radioaktivnega joda priporočamo bolnikom z diferenciranim karcinomom ščitnice prehrano z nizko vsebnostjo joda. Bolniki s povišanim nivojem tiroglobulina (Tg) ter negativnim izvidom skeniranja celotnega telesa z ^{131}I predstavljajo diagnostični in terapevtski problem. Namen raziskave je bil oceniti koristnost dvotedenske prehrane z nizko vsebnostjo joda pri bolnikih s povišanim nivojem serumskega Tg in negativnim izvidom skeniranja celotnega telesa z ^{131}I.

Bolniki in metode. Vpliv dvotedenske prehrane z nizko vsebnostjo joda na privzem radioaktivnega joda v tkivih smo ocenjevali s primerjanjem izvidov skeniranja z radioaktivnim jodom pred in po prehrani z nizko vsebnostjo joda. Šestnajst bolnikov s serumskim Tg > 2 µg/L, negativnimi protitelesi proti Tg in negativnim izvidom skeniranja z radioaktivnim jodom je dobivalo dva tedna pred aplikacijo ^{131}I prehrano z nizko vsebnostjo joda. Štirinajstih bolnikih je prejelo radioaktivni jod zaradi diagnostičnega postopka, dva bolnika pa zaradi zdravljenja. Pri vsakem bolniku smo izmerili jutranjo koncentracijo joda v urinu dan pred in petnajsti dan po začetku prehrane z nizko vsebnostjo joda.

Rezultati. S prehrano z nizko vsebnostjo joda so bolniki zmanjšali nivo joda v telesu za 50% (od 28% do 65%, p<0,001). Trinajst bolnikov (82%) je doseglo blago zmanjšanje joda (50-99 µg/L), en bolnik (6%) je dosegel ciljno zmerno znižanje nivoja joda (<50 µg/L). Vsa diagnostična skeniranja po prehrani z nizko vsebnostjo joda so bila negativna. Obe poste-rapijski skeniranji pa sta pokazali kopičenje radioaktivnega joda izven običajne distribucije (v vratni regiji in difuzno jetrno kopičenje). Rezultati so pokazali, da dvo tedenska prehrana z nizko vsebnostjo joda učinkovito zmanjša nivo joda v telesu, pri tem pa nima učinka na diagnostično skeniranje z ^{131}I.

Zaključki. S strožjim prehranskim protokolom in z daljšim obdobjem zmanjšanega vnosa joda bi lahko dosegli želeno zmerno zmanjšanje joda pri bolnikih, ki se pripravljajo na skeniranje z ^{131}I. Na ta način bi lahko povečali kopičenje radioaktivnega joda v preostanku ščitničnega tkiva oz. v metastazah.

Radiol Oncol 2011; 45(3): 196-203.
doi:10.2478/v10019-011-0013-8

Utišanje izražanja *stat3* z RNAi zavira rast celic humanega raka jajčnikov *in vitro*

Zhao SH, Zhao F, Zheng JY, Gao LF, Zhao XJ, Cui MH

Izhodišča. Namen raziskave je bil analizirati učinek rekombinantnih plazmidov pSilencer2.1-U6-siRNA-*stat3* na rast rakavih celic jajčnikov *in vitro*.

Materiali in metode. Sintetizirali smo tri različna zaporedja DNA (*stat3*-1, *stat3*-2, *stat3*-3), ki se po transkripciji specifično vežejo na različna mesta na *stat3* mRNA molekuli. Vstavili smo jih v plazmide pSilencer2.1-U6-siRNA-*stat3*, s katerimi smo nato transfecirali celice SKOV3. Izražanje STAT3, BcL-2, ciklina D1 in C-myc v celicah smo določili s prenosom *western* in *northern*. Celični cikel smo določili s pretočno citometrijo, rast celic s testom MTT in apoptozo z metodo TUNEL.

Rezultati. Izmed vseh treh molekul siRNA, je le molekula siRNA, ki se veže na *stat3*-3, učinkovito znižala izražanje *stat3* v celicah SKOV3. S testom MTT, pretočno citometrijo in metodo TUNEL smo pokazali, da lahko transfekcija SKOV3 celic s *stat3*-3 siRNA močno zmanjša rast celic. Prav tako pride do ustavitve celičnega cikla in povečanja apoptoze.

Zaključki. Plazmid pSilencer2.1-U6-siRNA-*stat3*-3 lahko močno zniža izražanje STAT3 v humanih celicah raka jajčnikov, kar privede do zaviranja rasti in povečane apoptoze rakavih celic.

Radiol Oncol 2011; 45(3): 204-208.
doi:10.2478/v10019-011-0025-4

Koničasta komora z vgrajenimi elektrodami za gensko elektrotransfekcijo celic v suspenziji: raziskava izvedljivosti v CHO celicah

Reberšek M, Kandušer M, Miklavčič D

Izhodišča. Genska elektrotransfekcija je nevirusna metoda vnosa genov v celico, ki temelji na elektroporaciji celic. Spreminjanje smeri električnega polja med dovajanjem električnih pulzov izboljša učinkovitost genske elektrotransfekcije. V raziskavi smo z gensko elektrotransfekcijo testirali koničasto komoro z vgrajenimi elektrodami za elektroporacijo celic v suspenziji.

Materiali in metode. Nova koničasta komora je sestavljena iz štirih valjastih elektrod, ki omogočajo generiranje električnega polja v različnih smereh. Poskuse smo izvedli na CHO celicah v fosfatnem pufru. Uporabljen je bil plazmid DNA, ki kodira zeleni fluorescentni protein (GFP). Učinkovitost genske elektrotransfekcije smo določili s štetjem celic, ki izražajo GFP 24 ur po poskusu.

Rezultati. Eksperimentalni rezultati kažejo, da se odstotek celic, ki izražajo GFP, poveča, če smer električnega polja med dovajanjem električnih pulzov spremenimo. Izražanje GFP-ja je skoraj dvakrat višje, kadar električne pulze dovajamo pravokotno v primerjavi z istosmernim dovajanjem; takšno spreminjanje smeri električnega polja pa ne vpliva bistveno na preživetje celic.

Zaključki. Rezultati testa opisane koničaste komore so primerljivi z že objavljenimi rezultati na genski elektrotransfekciji, kjer so uporabili podobne električne parametre in geometrijo elektrod. Poleg tega pa opisana koničasta komora omogoča delo z majhnimi volumni/vzorci in zahteva manj manipulacije s celicami.

Radiol Oncol 2011; 45(3): 209-212.
doi:10.2478/v10019-011-0027-2

Razlike v vrednostih TIMP-1 v plazmi med zdravimi darovalci krvi in bolniki z rakom danke stadija II ali III

Oblak I, Anderluh F, Velenik V, Možina B, Ocvirk J, Ćirić E, Hrovatič Podvršnik N

Izhodišča. Namen klinične raziskave je bil ugotoviti, ali so vrednosti tkivnega zaviralca metaloproteinaz tipa 1 (TIMP-1) v plazmi bolnikov z rakom danke višje kot pri zdravih darovalcih krvi.

Bolniki in metode. V analizo smo vključili 217 bolnikov (147 moških, 70 žensk) s histološko potrjenim nemetastatskim rakom danke (klinični stadij II-III) in 45 zdravih darovalcev krvi (15 moških, 30 žensk). Povprečna starost bolnikov je bila 66 let (razpon: 34-87 let), povprečna starost zdravih darovalcev krvi pa 35 let (razpon: 18-64 let). Koncentracije TIMP-1 v plazmi so bile izmerjene s komercialnim encimskim imunskim testom (ELISA). Za oceno razlik med vrednostmi TIMP-1 in kliničnopatološkimi parametri smo uporabili Mann-Whitneyev-test Uporabljali smo dvosmerne statistične teste in razlike pri $P<0.05$ označili kot statistično pomembne.

Rezultati. Srednja vrednost TIMP-1 pri bolnikih z rakom danke je bila 180 ng/ml (razpon: 22-538 ng/ml), povprečna vrednost (± SD) je znašala 193,7 (79,5) ng/ml. Srednja vrednost TIMP-1 zdravih darovalcev krvi je bila 112 ng/ml (razpon: 48-211 ng/ml), povprečna vrednost (± SD) pa je znašala 115 (35,7) ng/ml. Vrednosti TIMP-1 pri bolnikih z rakom danke so bile statistično značilno višje kot vrednosti TIMP-1 zdravih darovalcev krvi ($P<0,0001$). Med spoloma pomembnejših razlik v vrednostih TIMP-1 nismo našli ($P=0,43$), v obeh skupinah pa so bile vrednosti TIMP-1 višje pri starejših bolnikih ($P=0,007$).

Zaključki. Bolniki z rakom danke so imeli statistično pomembno višje povprečne in srednje vrednosti TIMP-1 kot zdravi darovalci krvi, kar je v skladu z že objavljenimi rezultati. Naša odkritja nakazujejo možnost, da bi se lahko vrednosti TIMP-1 v plazmi uporabljale kot novi biološki označevalec za zgodnje odkrivanje raka.

Radiol Oncol 2011; 45(3): 213-219.
doi:10.2478/v10019-011-0019-2

3-D konformno obsevanje s hkratnim in dodatnim zdravljenjem s temozolomidom pri bolnikih z multiformnim glioblastomom in določitev napovednih dejavnikov

Tezcan Y, Koc M

Izhodišča. Namen retrospektivne raziskave je bil ovrednotiti potek bolezni in določiti napovedne dejavnike pri bolnikih z multiformnim glioblastomom, ki smo jih pooperativno zdravili s 3-D konformnim obsevanjem ter hkrati in/ali dodatno s temozolomidom (TMZ).

Bolniki in metode. Na ta način smo zdravili 50 bolnikov. Njihova srednja starost je bila 57 let (12-79), srednja vrednost stanja splošne zmogljivosti po Karnofskyjem (KPS) je bila 70 (40-100). Z multivariatno Coxsovo regresijsko analizo smo ugotavljali vpliv starosti, spola, KPS, obsežnosti kirurgije, velikosti tumorja (<5cm vs. ≥5cm), obsevalne doze (60 Gy vs. <60 Gy), hkratnega zdravljenja s TMZ in dodatnega zdravljenja s TMZ (6 krogov TMZ vs. <6 krogov) na celokupno preživetje bolnikov.

Rezultati. Srednji čas sledenja bolnikov je bil 10 mesecev (3-42). Eno- in 2-letno celokupno preživetje je bilo 46% in 20%. Pozitivni napovedni dejavniki za celokupno preživetje so bili obsevanje z visoko obsevalno dozo (60 Gy) (p=0,005) in dodatno zdravljenje z TMZ z najmanj 6 krogi (p=0,l009).

Zaključki. Rezultati naše raziskave potrjujejo učinkovitost zdravljenja s pooperativnim obsevanjem ter hkratnim in dodatnim s TMZ. Stranski učinki so bili mili in sprejemljivi. Da bi dosegli dobrobit, priporočamo najmanj 6 krogov dodatnega zdravljenja s TMZ.

Radiol Oncol 2011; 45(3): 220-226.
doi:10.2478/v10019-011-0024-5

Učinek in stabilnost adaptivne radioterapije s kilovoltnim CT s koničnim žarkovnim snopom: študija izvedljivosti

Yadav P, Ramasubramanian V, Paliwal BR

Izhodišča. V obdobju šestih mesecev smo analizirali stabilnost krivulje med CT in gostoto računalniško tomografskega slikovnega sistema s koničnim žarkovnim snopom (kV CBCT). Raziskali smo uporabnost tabele povezav med slikovno vrednostjo in gostoto (IVDT). Tabele smo ustvarili v obdobju 6 mesecev za adaptivno načrtovanje v radioterapiji in raziskali tudi vpliv sprememb tarčnega volumna ter učinkovitost kV CBCT pri adaptivnem planiranju.

Materiali in metode. Za določitev kalibracijskih krivulj zveze med CT in elektronsko gostoto smo uporabili standardni fantom z različnimi elektronskimi gostotami. Krivuljo povezave med CT in gostoto slik CBCT smo spremljali 6 mesecev. Slike kV CBCT, ki smo jih uporabili za adaptivno planiranje, smo zajeli z vgrajenim slikovnim sistemom linearnega pospeševalnika "Trilogy". Slike kV CBCT so bile narejene za dnevno kontrolo nastavitev. Vpliv variacij kalibracijskih krivulj smo proučevali na dveh kliničnih primerih: prostati in pljučih.

Rezultati. Vrisovanje mehkih tkiv z uporabo kV CBCT je boljše kot z uporabo MVCT. V obdobju šestih mesecev je bila kalibracijska krivulja med CT in gostoto CBCT stabilna. Ugotavljali pa smo različne odmerke sevanja, ki ga zaradi težav z doseganjem ponovljivosti pri dnevnih nastavitvah pri obsevanje prostate prejmeta danka in mehur.

Zaključki. Ustvarjanje nove kalibracijske krivulje za adaptivno planiranje na kV CBCT slikah ni potrebno. Adaptivno planiranje brez novega kVCT slikanja se je izkazalo uporabno pri preverjanje odmerka sevanja na tarčo ter kritične organe, ta metoda bo tudi zmanjšala odmerek sevanja, ki ga prejme bolnik.

Fundacija "Docent dr. J. Cholewa"
je neprofitno, neinstitucionalno in nestrankarsko
združenje posameznikov, ustanov in organizacij, ki želijo
materialno spodbujati in poglabljati raziskovalno
dejavnost v onkologiji.

Dunajska 106
1000 Ljubljana

ŽR: 02033-0017879431

Activity of "Dr. J. Cholewa" Foundation for Cancer Research and Education – a report for the first half of 2011

The Dr. Josip Cholewa Foundation for Cancer Research and Education is a non-profit, non-government and non-political association of individuals, institutions and organisations with the aim to support various initiatives in cancer research, prevention and education. Its aim is to inform and serve medical and other professionals and many individuals from general population with interest in various fields of clinical oncology and in cancer education and cancer research. Among other things, the Foundation seeks to distribute research grants and other forms of assistance to qualified applicants who wishes to start or continue with their research in various specialties of oncology. It also helps professional and other associations in Slovenia to organise scientific and other meetings of specific interest in different fields of advanced cancer research, clinical oncology and cancer education. It is involved in the organisation of specific oncology meetings for medical professionals, especially those in primary medical service. It also supports Slovenian Cancer Association to publish various cancer information and cancer awareness brochures and booklets for general population. The Foundation continues to support the publication of "Radiology and Oncology" international medical scientific journal with an important SCI impact factor that is edited, published and printed in Ljubljana, Slovenia. Besides that, "Radiology and Oncology" is an open access journal, with a free internet access on its website.

The Foundation also supports the implementation of all advances in cancer therapy and education into normal hospital, ambulatory and health promotion practice. With changes in cancer epidemiology in Slovenia in recent decades, with a number of changes in incidence and prevalence rates of various types of cancer. Thus several new activities will probably have to be added to its scope of interest in the not so distant future, as the need for up to date cancer prevention and early detection measures available to Slovenian population and patients has grown substantially in the last few years.

The Dr. Josip Cholewa Foundation for Cancer Research and Education will continue to support various activities in cancer research and education in the remaining months of 2011. As of necessity, greater emphasis will probably be given to cancer education and information about cancer for the general public. This may include education and information about cancer prevention, early detection and treatment of cancer. These activities may lead to greater application of the latest methods in cancer diagnostics and therapy, as well as in cancer education in clinical and public environment in Slovenia.

Prof. Borut Štabuc, MD, PhD
Andrej Plesničar, MD, MSc
Tomaž Benulič, MD

Kakovost • Izbira • Zadovoljstvo

THE

Natrelle™

COLLECTION

Prsni vsadki in ekspanderji tkiv

Individualne ženske
Individualen izbor

ALLERGAN

DISTRIBUCIJA IN PRODAJA:
SANOLABOR, d.d.,
Leskoškova 4, 1000 Ljubljana, Slovenija
Tel:+386 (0)1 585-42-11
Fax:+386 (0)1 585-42-98
www.sanolabor.si

Sanolabor

PROMOCIJA, MARKETING IN STROKOVNA PODPORA:
EWOPHARMA d.o.o., Cesta 24.junija 23, 1000 Ljubljana, Slovenija
Jurij Pivka, vodja poslovne enote -Medicinska estetika
Tel: +386 (0) 59 084 845, mobilnik: +386 (0) 51 326 058
Fax: +386 (0) 59 084 849

Merck Serono Onkologija | ključ je v kombinaciji

Erbitux 5 mg/ml raztopina za infundiranje (Skrajšan povzetek glavnih značilnosti zdravila)

Sestava: En ml raztopine za infundiranje vsebuje 5 mg cetuximaba in pomožne snovi. Cetuksimab je himerno monoklonsko IgG1 protitelo. **Terapevtske indikacije:** Zdravilo Erbitux je indicirano za zdravljenje bolnikov z metastatskim kolorektalnim rakom z ekspresijo receptorjev EGFR in nemutiranim tipom KRAS v kombinaciji s kemoterapijo in kot samostojno zdravilo pri bolnikih, pri katerih zdravljenje z oksaliplatinom in irinotekanom ni bilo uspešno. Zdravilo Erbitux je indicirano za zdravljenje bolnikov z rakom skvamoznih celic glave in vratu v kombinaciji z radioterapijo za lokalno napredovalo bolezen in v kombinaciji s kemoterapijo na osnovi platine za ponavljajočo se in/ali metastatsko bolezen. **Odmerjanje in način uporabe:** Zdravilo Erbitux pri vseh indikacijah infundirajte enkrat na teden. Pred prvo infuzijo mora bolnik prejeti premedikacijo z antihistaminikom in kortikosteroidom. Začetni odmerek je 400 mg cetuksimaba na m2 telesne površine. Vsi naslednji tedenski odmerki so vsak po 250 mg/m2. **Kontraindikacije:** Zdravilo Erbitux je kontraindicirano pri bolnikih z znano hudo preobčutljivostno reakcijo (3. ali 4. stopnje) na cetuksimab. **Posebna opozorila in previdnostni ukrepi:** Če pri bolniku nastopi blaga ali zmerna reakcija, povezana z infundiranjem, lahko zmanjšate hitrost infundiranja. Priporočljivo je, da ostane hitrost infundiranja na nižji vrednosti tudi pri vseh naslednjih infuzijah. Če se pri bolniku pojavi huda kožna reakcija (≥ 3. stopnje po kriterijih US NCI-CTC), morate prekiniti terapijo s cetuksimabom. Z zdravljenjem smete nadaljevati le, če se je reakcija izboljšala do 2. stopnje. Zaradi možnosti pojava znižanja nivoja magnezija v serumu se pred in periodično med zdravljenjem priporoča določanje koncentracije elektrolitov. Če se pojavi sum na nevtropenijo, je potrebno bolnika skrbno nadzorovati. Potrebno je upoštevati kardiovaskularno stanje bolnika in sočasno dajanje kardiotoksičnih učinkovin kot so fluoropirimidini. **Interakcije:** farmakokinetične značilnosti cetuksimaba ostanejo nespremenjene po sočasni uporabi enkratnega odmerka irinotekana, tudi farmakokinetika irinotekana je nespremenjena pri sočasni uporabi cetuksimaba. Pri kombinaciji s fluoropirimidini se je povečala pogostnost srčne ishemije, vključno z miokardnim infarktom in kongestivno srčno odpovedjo ter pogostnost sindroma dlani in stopal. V kombinaciji s kemoterapijo na osnovi platine se lahko poveča pogostnost hude levkopenije ali hude nevtropenije. **Neželeni učinki:** Zelo pogosti (≥ 1/10): hipomagneziemija, povečanje ravni jetrnih encimov, kožne reakcije, blage ali zmerne reakcije povezane z infundiranjem, blag do zmeren mukozitis. Pogosti (≥ 1/100, < 1/10): dehidracija, hipokalciemija, anoreksija, glavobol, konjunktivitis, driska, navzeja, bruhanje, hude reakcije povezane z infundiranjem, utrujenost. **Posebna navodila za shranjevanje:** Shranjujte v hladilniku (2 °C - 8 °C). **Pakiranje:** 1 viala z 20 ml ali 100 ml raztopine. **Način in režim izdaje:** H. **Imetnik dovoljenja za promet:** Merck KGaA, 64271 Darmstadt, Nemčija. **Datum zadnje revizije besedila:** november 2010.

Pred predpisovanjem zdravila natančno preberite celoten Povzetek glavnih značilnosti zdravila. Podrobne informacije o zdravilu so objavljene na spletni strani Evropske agencije za zdravila (EMEA) http://www.emea.europa.eu.

Dodatne informacije so na voljo pri: Merck d.o.o., Dunajska cesta 119, 1000 Ljubljana, tel.: 01 560 3810, faks: 01 560 3831, el. pošta: info@merck.si

www.merckserono.net

www.Erbitux-international.com

Merck Serono

Merck Serono is a division of Merck.

MERCK

Samo za strokovno javnost PM-ONC-12/10/25.11.2010

POVZETEK GLAVNIH ZNAČILNOSTI ZDRAVILA

Ime zdravila: Temodal 20 mg, 100 mg, 140mg, 180 mg, 250 mg, Temodal 2,5 mg/ml prašek za raztopino za infundiranje **Kakovostna in količinska sestava:** Vsaka kapsula zdravila Temodal vsebuje 20 mg, 100 mg, 140 mg, 180 mg ali 250 mg temozolomida. Ena viala vsebuje 100 mg temozolomida Po rekonstituciji 1 ml raztopine za infundiranje vsebuje 2,5 mg temozolomida. Pomožna snov: Ena viala vsebuje 2,4 mmol natrija. **Terapevtske indikacije:** Zdravilo Temodal 2,5 mg/ml je indicirano za zdravljenje: odraslih bolnikov z novo diagnosticiranim multiformnim glioblastomom, sočasno z radioterapijo (RT) in pozneje kot monoterapija in otrok, starih 3 leta in več, mladostnikov in odraslih bolnikov z malignimi gliomi, npr. multiformnimi glioblastomi ali anaplastičnimi astrocitomi, ki se po standardnem zdravljenju ponovijo ali napredujejo. **Odmerjanje in način uporabe:** Zdravilo Temodal 2,5 mg/ml smejo predpisati le zdravniki, ki imajo izkušnje z zdravljenjem možganskih tumorjev. *Odrasli bolniki z novo diagnosticiranim multiformnim glioblastomom* Zdravilo Temodal 2,5 mg/ml se uporablja v kombinaciji z žariščno radioterapijo (faza sočasne terapije), temu pa sledi do 6 ciklov monoterapije (monoterapijska faza) z temozolomidom (TMZ). *Faza sočasne terapije* TMZ naj bolnik jemlje v odmerku 75 mg/m2 na dan 42 dni, sočasno z žariščno radioterapijo (60 Gy, danih v 30 delnih odmerkih). Zmanjševanje odmerka ni priporočeno, vendar se boste vsak teden odločili o morebitni odložitvi jemanja TMZ ali njegovi ukinitvi na podlagi kriterijev hematološke in nehematološke toksičnosti. TMZ lahko bolnik jemlje ves čas 42-dnevnega obdobja sočasne terapije (do 49 dni), če so izpolnjeni vsi od naslednjih pogojev:

- absolutno število nevtrofilcev (ANC – Absolute Neutrophil Count) ≥ 1,5 x 109/l;
- število trombocitov ≥ 100 x 109/l;
- skupna merila toksičnosti (SMT) za nehematološko toksičnost ≤ 1. stopnje (z izjemo alopecije, navzee in bruhanja).

Med zdravljenjem morate pri bolniku enkrat na teden pregledati celotno krvno sliko.

Faza monoterapije Štiri tedne po zaključku faze sočasnega zdravljenja s TMZ in RT naj bolnik jemlje TMZ do 6 ciklov monoterapije. V 1. ciklu (monoterapije) je odmerek zdravila 150 mg/m2 enkrat na dan 5 dni, temu pa naj sledi 23 dni brez terapije. Na začetku 2. cikla odmerek povečajte na 200 mg/m2, če je SMT za nehematološko toksičnost za 1. cikel stopnje ≤ 2 (z izjemo alopecije, slabosti in bruhanja), absolutno število nevtrofilcev (ANC) ≥ 1,5 x 109/l in število trombocitov ≥ 100 x 109/l. Če odmerka niste povečali v 2. ciklu, ga v naslednjih ciklih ne smete povečevati. Ko pa odmerek enkrat povečate, naj ostane na ravni 200 mg/m2 na dan v prvih 5 dneh vsakega naslednjega cikla, razen če nastopi toksičnost. Zmanjšanje odmerka in ukinitev zdravila med fazo monoterapije opravite, kot je opisano v preglednicah 2 in 3. Med zdravljenjem morate 22. dan pregledati celotno krvno sliko (21 dni po prvem odmerku TMZ). *Odrasli in pediatrični bolniki, stari 3 leta ali več, s ponavljajočim se ali napredujočim malignim gliomom:* Posamezen cikel zdravljenja traja 28 dni. Bolniki, ki še niso bili zdravljeni s kemoterapijo, naj jemljejo TMZ v odmerku 200 mg/m2 enkrat na dan prvih 5 dni, temu pa naj sledi 23-dnevni premor (skupaj 28 dni). Pri bolnikih, ki so že bili zdravljeni s kemoterapijo, je začetni odmerek 150 mg/m2 enkrat na dan, v drugem ciklu pa se poveča na 200 mg/m2 enkrat na dan 5 dni, če ni bilo hematoloških toksičnih učinkov. **Kontraindikacije:** Preobčutljivost za zdravilno učinkovino ali katerokoli pomožno snov. Preobčutljivost za dakarbazin (DTIC). **Posebna opozorila in previdnostni ukrepi:** *Pljučnica, ki jo povzroča Pneumocystis carinii* Pilotno preskušanje podaljšane 42-dnevne sheme zdravljenja je pokazalo, da pri bolnikih, ki so sočasno prejemali TMZ in RT, obstaja še posebej veliko tveganje za nastanek pljučnice zaradi okužbe s Pneumocystis carinii (PCP). *Malignosti* Zelo redko so poročali tudi o primerih mielodisplastičnega sindroma in sekundarnih malignostih, vključno z mieloidno levkemijo. Antiemetično zdravljenje Navzea in bruhanje sta pogosto povezana z zdravljenjem s TMZ. *Antiemetično zdravljenje* se lahko da pred uporabo TMZ ali po njej. *Odrasli bolniki z novo diagnosticiranim multiformnim glioblastomom* Antiemetična profilaksa je priporočljiva pred začetnim odmerkom sočasne faze in je močno priporočljiva med fazo monoterapije. *Ponavljajoči se ali napredujoči maligni gliom* Pri bolnikih, ki so močno bruhali (stopnja 3 ali 4) v prejšnjih ciklih zdravljenja, je potrebno antiemetično zdravljenje. *Laboratorijske vrednosti* Pred jemanjem zdravila morata biti izpolnjena naslednja pogoja za laboratorijske izvide: ANC ≥ 1,5 x 109/l in število trombocitov ≥ 100 x 109/l. Na 22. dan (21 dni po prvem odmerku) ali v roku 48 ur od navedenega dne, morate pregledati celotno krvno sliko in jo nato spremljati vsak teden, dokler ni ANC > 1,5 x 109/l in število trombocitov > 100 x 109/l. Če med katerimkoli ciklom ANC pade na < 1,0 x 109/l ali število trombocitov na < 50 x 109/l, morate odmerek zdravila v naslednjem ciklu zmanjšati za eno stopnjo (glejte poglavje 4.2). Stopnje odmerka so 100 mg/m2, 150 mg/m2 in 200 mg/m2. Najmanjši priporočeni odmerek je 100 mg/m2. *Pediatrična uporaba* Kliničnih izkušenj z uporabo TMZ pri otrocih, mlajših od 3 let, ni. Izkušnje z uporabo tega zdravila pri starejših otrocih in mladostnikih so zelo omejene. *Starejši bolniki* (stari > 70 let) Videti je, da je pri starejših bolnikih tveganje za nevtropenijo ali trombocitopenijo večje, kot pri mlajših. Zato je pri uporabi zdravila TMZ pri starejših bolnikih potrebna posebna previdnost.

Moški bolniki Moškim, ki se zdravijo s TMZ je treba svetovati, naj ne zaplodijo otroka še šest mesecev po prejetem zadnjem odmerku in naj se pred zdravljenjem posvetujejo o možnostih za shranitev zmrznjene sperme. *Natrij* To zdravilo vsebuje 2,4 mmol natrija na vialo. To je treba upoštevati pri bolnikih na nadzorovani dieti z malo natrija. **Medsebojno delovanje z drugimi zdravili in druge oblike interakcij:** Študije medsebojnega delovanja so izvedli le pri odraslih. V ločeni študiji 1. faze, sočasna uporaba TMZ in ranitidina ni povzročila spremembe obsega absorpcije temozolomida ali izpostavljenosti njegovem aktivnem presnovku monometiltriazenoimidazol karboksamidu (MTIK). Analiza populacijske farmakokinetike v preskušanjih 2. faze je pokazala, da sočasna uporaba deksametazona, proklorperazina, fenitoina, karbamazepina, ondansetrona, antagonistov receptorjev H2 ali fenobarbitala ne spremeni očistka TMZ. Sočasno jemanje z valprojsko kislino je bilo povezano z majhnim, a statistično pomembnim zmanjšanjem očistka TMZ. Študij za določitev učinka TMZ na presnovo ali izločanje drugih zdravil niso izvedli. Ker pa se TMZ ne presnavlja v jetrih in se na beljakovine veže le v majhni meri, je malo verjetno, da bi vplival na farmakokinetiko drugih zdravil.

Uporaba TMZ v kombinaciji z drugimi mielosupresivnimi učinkovinami lahko poveča verjetnost mielosupresije. **Neželeni učinki:** Pri bolnikih, ki se zdravijo s TMZ v kombinaciji z RT ali monoterapijo po RT zaradi novo diagnosticiranega multiformnega glioblastoma ali z monoterapijo pri bolnikih s ponavljajočim se ali napredujočim gliomom, so bili zelo pogosti neželeni učinki podobni; slabost, bruhanje, zaprtje, neješčnost, glavobol in utrujenost. Pri bolnikih z novo diagnosticiranim glioblastomom multiforme na monoterapiji so zelo pogosto poročali o konvulzijah, medtem ko je bil izpuščaj opisan zelo pogosto pri bolnikih z novo diagnosticiranim multiformnim glioblastomom, ki so prejemali TMZ sočasno z RT, ter pri tistih, ki so zdravilo prejemali v obliki monoterapije, pogosto pa pri tistih s ponavljajočim se gliomom. Pri obeh indikacijah so o večini hematoloških neželenih reakcij poročali pogosto ali zelo pogosto. **Imetnik dovoljenja za promet:** Schering-Plough Europe, Rue de Stalle 73, Bruselj Belgija **Način in režim izdaje zdravila:** Zdravilo Temodal 20 mg, 100 mg, 140mg, 180 mg, 250 mg se izdaja na recept (Rp/Spec), Temodal 2,5 mg/ml prašek za raztopino za infundiranje pa je namenjeno uporabi samo v bolnišnicah (H). **Datum priprave informacije:** februar 2010

1. Stupp R, et.al. Effects of radiotherapy with concomitant and adjuvant temozolomide versus radiotherapy alone on survival in glioblastoma in a randomised III study: 5-year analysis of the EORTC-NCIC trial
2. Povzetek temeljnih značilnosti zdravila Temodal

5 jakosti v 5 barvah za lažje in natančnejše dnevno odmerjanje[2]

250 mg	180 mg	140 mg	100 mg	20 mg

Schering-Plough CE AG
Dunajska cesta 22, 1000 Ljubljana
tel: 01 300 10 70
fax: 01 300 10 80

Schering-Plough

Resnični napredek

Pomembno izboljšanje preživetja potrjeno tudi ob daljšem spremljanju bolnikov[1]

Temodal® temozolomide capsules

SKRAJŠAN POVZETEK GLAVNIH ZNAČILNOSTI ZDRAVILA

Samo za strokovno javnost.

Ime zdravila: Tarceva 25 mg/100 mg/150 mg filmsko obložene tablete
Kakovostna in količinska sestava: Ena filmsko obložena tableta vsebuje 25 mg, 100 mg ali 150 mg erlotiniba (v obliki erlotinibijevega klorida).
Terapevtske indikacije: Nedrobnocelični rak pljuč: Zdravilo Tarceva je indicirano za samostojno vzdrževalno zdravljenje bolnikov z lokalno napredovalim ali metastatskim nedrobnoceličnim rakom pljuč s stabilno boleznijo po 4 ciklih standardne kemoterapije na osnovi platine v prvi liniji zdravljenja. Zdravilo Tarceva je indicirano tudi za zdravljenje bolnikov z lokalno napredovalim ali metastatskim nedrobnoceličnim rakom pljuč po neuspehu vsaj ene predhodne kemoterapije. Pri predpisovanju zdravila Tarceva je treba upoštevati dejavnike, povezane s podaljšanim preživetjem. Koristnega vpliva na podaljšanje preživetja ali drugih klinično pomembnih učinkov zdravljenja niso dokazali pri bolnikih z EGFR-negativnimi tumorji. Rak trebušne slinavke: Zdravilo Tarceva je v kombinaciji z gemcitabinom indicirano za zdravljenje bolnikov z metastatskim rakom trebušne slinavke. Pri predpisovanju zdravila Tarceva je treba upoštevati dejavnike, povezane s podaljšanim preživetjem. Koristnega vpliva na podaljšanje preživetja niso dokazali za bolnike z lokalno napredovalo boleznijo.
Odmerjanje in način uporabe: Zdravljenje z zdravilom Tarceva mora nadzorovati zdravnik z izkušnjami pri zdravljenju raka. Zdravilo Tarceva vzamemo najmanj eno uro pred zaužitjem hrane ali dve uri po tem. Kadar je potrebno odmerek prilagoditi, ga je treba zmanjševati v korakih po 50 mg. Pri sočasnem jemanju substratov in modulatorjev CYP3A4 bo morda potrebna prilagoditev odmerka. Pri dajanju zdravila Tarceva bolnikom z jetrno okvaro je potrebna previdnost. Če se pojavijo hudi neželeni učinki, pride v poštev zmanjšanje odmerka ali prekinitev zdravljenja z zdravilom Tarceva. Uporaba zdravila Tarceva pri bolnikih s hudo jetrno ali ledvično okvaro ter pri otrocih ni priporočljiva. Bolnikom kadilcem je treba svetovati, naj prenehajo kaditi, saj so plazemske koncentracije erlotiniba pri kadilcih manjše kot pri nekadilcih. Nedrobnocelični rak pljuč: Priporočeni dnevni odmerek zdravila Tarceva je 150 mg. Rak trebušne slinavke: Priporočeni dnevni odmerek zdravila Tarceva je 100 mg, v kombinaciji z gemcitabinom. Pri bolnikih, pri katerih se kožni izpuščaj v prvih 4 do 8 tednih zdravljenja ne pojavi, je treba ponovno pretehtati nadaljnje zdravljenje z zdravilom Tarceva.
Kontraindikacije: Preobčutljivost za erlotinib ali katero koli pomožno snov.
Posebna opozorila in previdnostni ukrepi: Močni induktorji CYP3A4 lahko zmanjšajo učinkovitost erlotiniba, močni zaviralci CYP3A4 pa lahko povečajo toksičnost. Sočasnemu zdravljenju s temi zdravili se je treba izogibati. Bolnikom, ki kadijo, je treba svetovati, naj prenehajo kaditi, saj so plazemske koncentracije erlotiniba pri kadilcih zmanjšane v primerjavi s plazemskimi koncentracijami pri nekadilcih. Verjetno je, da je velikost zmanjšanja klinično pomembna. Pri bolnikih, pri katerih se akutno pojavijo novi in/ali poslabšajo nepojasnjeni pljučni simptomi, kot so dispneja, kašelj in vročina, je treba zdravljenje z zdravilom Tarceva prekiniti, dokler ni znana diagnoza. Bolnike, ki se sočasno zdravijo z erlotinibom in gemcitabinom, je treba skrbno spremljati zaradi možnosti pojava toksičnosti, podobni intersticijski bolezni pljuč. Če je ugotovljena intersticijska bolezen pljuč, zdravilo Tarceva ukinemo in uvedemo ustrezno zdravljenje. Pri približno polovici bolnikov, ki so se zdravili z zdravilom Tarceva, se je pojavila driska (vključno z zelo redkimi primeri, ki so se končali s smrtnim izidom). Zmerno do hudo drisko zdravimo z loperamidom. V nekaterih primerih bo morda potrebno zmanjšanje odmerka. V primeru hude ali dolgotrajne driske, navzeje, anoreksije ali bruhanja, povezanih z dehidracijo, je treba zdravljenje z zdravilom Tarceva prekiniti in dehidracijo ustrezno zdraviti. O hipokaliemiji in ledvični odpovedi so poročali redko. Posebno pri bolnikih z dejavniki tveganja (sočasno jemanje drugih zdravil, simptomi, bolezni ali drugi dejavniki, vključno z visoko starostjo) moramo, če je driska huda ali dolgotrajna oziroma vodi v dehidracijo, zdravljenje z zdravilom Tarceva prekiniti in bolnikom zagotoviti intenzivno intravensko rehidracijo. Dodatno je treba pri bolnikih s prisotnim tveganjem za razvoj dehidracije spremljati ledvično delovanje in serumske elektrolite, vključno s kalijem. Pri uporabi zdravila Tarceva so poročali o redkih primerih jetrne odpovedi. K njenemu nastanku je lahko pripomogla predhodno obstoječa jetrna bolezen ali sočasno jemanje hepatotoksičnih zdravil. Pri teh bolnikih je treba zato premisliti o rednem spremljanju jetrnega delovanja. Dajanje zdravila Tarceva je treba prekiniti, če so spremembe jetrnega delovanja hude. Bolniki, ki prejemajo zdravilo Tarceva, imajo večje tveganje za razvoj perforacij v prebavilih, ki so jih opazili občasno (vključno z nekaterimi primeri, ki so se končali s smrtnim izidom). Pri bolnikih, ki sočasno prejemajo zdravila, ki zavirajo angiogenezo, kortikosteroide, nesteroidna protivnetna zdravila (NSAID) in/ali kemoterapijo na osnovi taksanov, ali so v preteklosti imeli peptični ulkus ali divertikularno bolezen, je tveganje večje. Če pride do tega, je treba zdravljenje z zdravilom Tarceva dokončno ukiniti. Poročali so o primerih kožnih bolezni z mehurji in luščenjem kože, vključno z zelo redkimi primeri, ki so nakazovali na Stevens-Johnsonov sindrom/toksično epidermalno nekrolizo in so bili v nekaterih primerih smrtni. Zdravljenje z zdravilom Tarceva je treba prekiniti ali ukiniti, če se pri bolniku pojavijo hude oblike mehurjev ali luščenja kože. Zelo redko so poročali o primerih perforacije ali ulceracije roženice; opazili so tudi druge očesne bolezni. Zdravljenje z zdravilom Tarceva je treba prekiniti ali ukiniti, če se pri bolnikih pojavijo akutne očesne bolezni, kot je bolečina v očeh, ali se le-te poslabšajo. Tablete vsebujejo laktozo in jih ne smemo dajati bolnikom z redkimi dednimi stanji: intoleranco za galaktozo, laponsko obliko zmanjšane aktivnosti laktaze ali malabsorpcijo glukoze/galaktoze.
Medsebojno delovanje z drugimi zdravili in druge oblike interakcij: Erlotinib se pri ljudeh presnavlja v jetrih z jetrnimi citokromi, primarno s CYP3A4 in v manjši meri s CYP1A2. Presnova erlotiniba zunaj jeter poteka s CYP3A4 v črevesju, CYP1A1 v pljučih in CYP1B1 v tumorskih tkivih. Z zdravilnimi učinkovinami, ki se presnavljajo s temi encimi, jih zavirajo ali pa so njihovi induktorji, lahko pride do interakcij. Erlotinib je srednje močan zaviralec CYP3A4 in CYP2C8, kot tudi močan zaviralec glukuronidacije z UGT1A1 *in vitro*. Pri kombinaciji ciprofloksacina ali močnega *zaviralca CYP1A2* (npr. fluvoksamina) z erlotinibom je potrebna previdnost. V primeru pojava neželenih učinkov, povezanih z erlotinibom, lahko odmerek erlotiniba zmanjšamo. Predhodno ali sočasno zdravljenje z zdravilom Tarceva ni spremenilo očistka prototipov *substratov CYP3A4*, midazolama in eritromicina. Inhibicija glukoronidacije lahko povzroči interakcije z zdravili, ki so *substrati UGT1A1* in se izločajo samo po tej poti. Močni *zaviralci aktivnosti CYP3A4* zmanjšajo presnovo erlotiniba in zvečajo koncentracije erlotiniba v plazmi. Pri sočasnem jemanju erlotiniba in močnih zaviralcev CYP3A4 je zato potrebna previdnost. Če je treba, odmerek erlotiniba zmanjšamo, še posebno pri pojavu toksičnosti. Močni *spodbujevalci aktivnosti CYP3A4* zvečajo presnovo erlotiniba in pomembno zmanjšajo plazemske koncentracije erlotiniba. Sočasnemu dajanju zdravila Tarceva in induktorjev CYP3A4 se je treba izogibati. Pri bolnikih, ki potrebujejo sočasno zdravljenje z zdravilom Tarceva in močnim induktorjem CYP3A4, je treba premisliti o povečanju odmerka do 300 mg ob skrbnem spremljanju njihove varnosti. Zmanjšana izpostavljenost se lahko pojavi tudi z drugimi induktorji, kot so fenitoin, karbamazepin, barbiturati ali šentjanževka. Če te zdravilne učinkovine kombiniramo z erlotinibom, je potrebna previdnost. Kadar je mogoče, je treba razmisliti o drugih načinih zdravljenja, ki ne vključujejo močnega spodbujanja aktivnosti CYP3A4. Bolnikom, ki jemljejo *kumarinske antikoagulante*, je treba redno kontrolirati protrombinski čas ali INR. Sočasno zdravljenje z zdravilom Tarceva in *statinom* lahko poveča tveganje za miopatijo, povzročeno s statini, vključno z rabdomiolizo; to so opazili redko. Sočasna uporaba *zaviralcev P-glikoproteina*, kot sta ciklosporin in verapamil, lahko vodi v spremenjeno porazdelitev in/ali spremenjeno izločanje erlotiniba. Za erlotinib je značilno zmanjšanje topnosti pri pH nad 5. *Zdravila, ki spremenijo pH v zgornjem delu prebavil*, lahko spremenijo topnost erlotiniba in posledično njegovo biološko uporabnost. Učinka antacidov na absorpcijo erlotiniba niso proučevali, vendar je ta lahko zmanjšana, kar vodi v nižje plazemske koncentracije. Kombinaciji erlotiniba in zaviralca protonske črpalke se je treba izogibati. Če menimo, da je uporaba antacidov med zdravljenjem z zdravilom Tarceva potrebna, jih je treba jemati najmanj 4 ure pred ali 2 uri po dnevnem odmerku zdravila Tarceva. Če razmišljamo o uporabi ranitidina, moramo zdravili jemati ločeno: zdravilo Tarceva je treba vzeti najmanj 2 uri pred ali 10 ur po odmerku ranitidina. V študiji faze Ib ni bilo pomembnih učinkov *gemcitabina* na farmakokinetiko erlotiniba, prav tako ni bilo pomembnih učinkov erlotiniba na farmakokinetiko gemcitabina. Erlotinib poveča koncentracijo platine. Pomembnih učinkov *karboplatina* ali paklitaksela na farmakokinetiko erlotiniba ni bilo. *Kapecitabin* lahko poveča koncentracijo erlotiniba. Pomembnih učinkov erlotiniba na farmakokinetiko kapecitabina ni bilo.
Neželeni učinki: *Zelo pogosti neželeni učinki* so kožni izpuščaj in driska, kot tudi utrujenost, anoreksija, dispneja, kašelj, okužba, navzea, bruhanje, stomatitis, bolečina v trebuhu, pruritus, suha koža, suhi keratokonjunktivitis, konjunktivitis, zmanjšanje telesne mase, depresija, glavobol, nevropatija, dispepsija, flatulenca, alopecija, okorelost, pireksija, nenormalnosti testov jetrne funkcije. *Pogosti neželeni učinki* so krvavitve v prebavilih, epistaksa, keratitis, paronihija, fisure na koži. *Občasno* so poročali o perforacijah v prebavilih, hirzutizmu, spremembah obrvi, krhkih nohtih, odstopanju nohtov od kože, blagih reakcijah na koži (npr. hiperpigmentacija), spremembah trepalnic, hudi intersticijski bolezni pljuč (vključno s smrtnimi primeri). *Redko* pa so poročali o jetrni odpovedi. *Zelo redko* so poročali o Stevens-Johnsonovem sindromu/toksični epidermalni nekrolizi ter o ulceracijah in perforacijah roženice.
Režim izdaje zdravila: H/Rp. **Imetnik dovoljenja za promet:** Roche Registration Limited, 6 Falcon Way, Shire Park, Welwyn Garden City, AL7 1TW, Velika Britanija. **Verzija:** 2.0/10. **Informacija pripravljena:** avgust 2011.

021-11-TAR

DODATNE INFORMACIJE SO NA VOLJO PRI:
Roche farmacevtska družba d.o.o.
Vodovodna cesta 109, 1000 Ljubljana.
Povzetek glavnih značilnosti zdravila je dosegljiv na www.roche.si ali www.onkologija.si.

Roche

Tarceva®
erlotinib

ČAS ZA ŽIVLJENJE.

DOKAZANO PODALJŠA PREŽIVETJE PRI BOLNIKIH:

- z lokalno napredovalim ali metastatskim nedrobnoceličnim rakom pljuč[1]
- z metastatskim rakom trebušne slinavke[1]

[1] Povzetek glavnih značilnosti zdravila TARCEVA, www.ema.europa.eu

odprto

Novartis Oncology prinaša spekter inovativnih zdravil, s katerimi poskuša spremeniti življenje bolnikov z rakavimi in hematološkimi obolenji.

Ta vključuje zdravila kot so Glivec® (imatinib), Tasigna® (nilotinib), Afinitor® (everolimus), Zometa® (zoledronska kislina), Femara® (letrozol), Sandostatin® LAR® (oktreotid/i.m. injekcije) in Exjade® (deferasiroks).

Novartis Oncology ima tudi obširen razvojni program, ki izkorišča najnovejša spoznanja molekularne genomike, razumskega načrtovanja in tehnologij za odkrivanje novih učinkovin.

glivec imatinib

Tasigna nilotinib

AFINITOR (everolimus) tablete

ZOMETA zoledronska kislina

Femara letrozol

Sandostatin LAR oktreotid/i.m. injekcije

EXJADE deferasiroks

NOVARTIS ONCOLOGY

Novartis Pharma Services Inc. • Podružnica v Sloveniji • Verovškova 57 • 1000 Ljubljana

Samo za strokovno javnost.

NV-JA-08/11-SI

DORIBAX®* – novi karbapenem

*Zdravilo Doribax® je indicirano za zdravljenje:

- bolnišničnih pljučnic,
- intraabdominalnih okužb z zapleti,
- okužb sečil z zapleti pri odraslih.

DORIBAX®
doripenem za injiciranje

SKRAJŠANO NAVODILO ZA PREDPISOVANJE

Doribax 500 mg prašek za raztopino za infundiranje

SESTAVA: 500 mg doripenema **INDIKACIJE:** zdravljenje bolnišnične pljučnice (vključno s pljučnico zaradi uporabe respiratorja), intraabdominalnih okužb z zapleti in okužb sečil z zapleti pri odraslih. **ODMERJANJE IN NAČIN UPORABE:** 500 mg v obliki 1 urne infuzije/8 ur. Pri bolnišnični pljučnici 500 mg v obliki 1 urne ali 4 urne infuzije/8 ur. Običajno zdravljenje z doripenemom traja 5 –14 dni. **Bolniki z okvarjenim delovanjem ledvic z zmerno ledvično okvaro:** 250 mg Doribaxa na 8 ur, bolniki s hudo ledvično okvaro: 250 mg na 12 ur. Uporaba zdravila Doribax pri bolnikih na kateri koli vrsti dialize ni priporočljiva. Pri starejših bolnikih in bolnikih z motnjami delovanja jeter prilagoditev odmerka ni potrebna. Pred uporabo je treba zdravilo Doribax rekonstituirati in nato še dodatno redčiti. **KONTRAINDIKACIJE:** Preobčutljivost za zdravilno učinkovino ali katerikoli drug karbapenemski antibiotik, huda preobčutljivost za katerikoli drug betalaktamski antibiotik. **POSEBNA OPOZORILA IN PREVIDNOSTNI UKREPI:** Preden začnete zdravljenje z zdravilom Doribax, morate bolnika temeljito izprašati o morebitnih preteklih preobčutljivostnih reakcijah. Pri bolnikih s takšnimi reakcijami v anamnezi morate zdravilo uporabljati previdno. Če nastopi preobčutljivostna reakcija na zdravilo Doribax, takoj prenehajte z dajanjem zdravila in uvedite ustrezne ukrepe. Pri resnih akutnih preobčutljivostnih reakcijah je potrebno takojšnje urgentno zdravljenje. Med zdravljenjem z drugimi karbapenemi so redko poročali o epileptičnih napadih. Uporaba doripenema je povezana s pojavom odpornosti in selekcijo sevov z manjšo občutljivostjo. Če pride med zdravljenjem do superinfekcije, uvedite ustrezne ukrepe. Izogibati se je treba daljši uporabi zdravila Doribax. Pri raziskovalni uporabi zdravila Doribax z inhalacijo se je pojavil pnevmonitis, zato zdravila ne smete uporabljati na ta način. Izkušnje pri bolnikih z zelo oslabljenim imunskim sistemom, bolnikih, ki prejemajo imunosupresivno zdravljenje in bolnikih s hudo nevtropenijo so omejene. **INTERAKCIJE:** Presnova doripenema preko encimov citokroma P450 je zelo omejena. Sočasna uporaba z valprojsko kislino in/ali probenecidom ni priporočljiva. **NOSEČNOST IN DOJENJE:** Zdravilo Doribax se v času nosečnosti lahko uporablja le, če je nujno potrebno. Odločitev o tem, ali naj ženska nadaljuje/preneha z dojenjem oziroma ali naj nadaljuje/prekine zdravljenje z zdravilom Doribax, je treba sprejeti z upoštevanjem koristi dojenja za otroka in koristi zdravljenja z zdravilom Doribax za mater. **NEŽELENI UČINKI:** Kandidiaza u ustih, glivična okužba vulve, preobčutljivostne reakcije, glavobol, flebitis, navzea, driska, kolitis zaradi C. difficile, zvišane vrednosti jetrnih encimov, pruritus, izpuščaj, nevtropenija, trombocitopenija, anafilaksija, toksična epidermalna nekroliza, Stevens-Johnsonov sindrom. **REŽIM IZDAJE ZDRAVILA:** H **IMETNIK DOVOLJENJA ZA PROMET** Janssen-Cilag International NV (predstavnik v Sloveniji: Johnson & Johnson d.o.o., Šmartinska 53, 1000 Ljubljana) **DATUM ZADNJE REVIZIJE BESEDILA:** 3.11.2010

janssen
PHARMACEUTICAL COMPANIES OF Johnson&Johnson

DOR-SLO-A-013-210311

Samo za strkovno javnost

Megace®

megestrolacetat 40mg/ml
peroralna suspenzija

učinkovita in preizkušena možnost zdravljenja anoreksije-kaheksije

Megace®

... še vedno EDINO ZDRAVILO, ki je v Sloveniji registrirano za zdravljenje anoreksije-kaheksije pri bolnikih z napredovalim rakom [1,2] - predpisovanje na zeleni recept v breme ZZZS [6]

Megace®

- izboljša apetit [1,5]
- pomaga ohraniti in pridobiti telesno težo [3,4,5]
- izboljša splošno počutje bolnikov [3,4]

SKRAJŠAN POVZETEK GLAVNIH ZNAČILNOSTI ZDRAVILA: MEGACE 40 mg/ml peroralna suspenzija

Sestava: 1 ml peroralne suspenzije vsebuje 40 mg megestrolacetata. **TERAPEVTSKE INDIKACIJE:** Zdravljenje anoreksije-kaheksije ali nepojasnjene, pomembne izgube telesne mase pri bolnikih z AIDS-om. Zdravljenje anorektično-kahektičnega sindroma pri napredovalem raku. **ODMERJANJE IN NAČIN UPORABE:** Pri aidsu je priporočeni začetni odmerek Megace za odrasle 800 mg (20 ml peroralne suspenzije) enkrat na dan eno uro pred jedjo ali dve uri po jedi in se lahko med zdravljenjem prilagodi glede na bolnikov odziv. V raziskavah bolnikov z aidsom so bili klinično učinkoviti dnevni odmerki od 400 do 800 mg/dan (10 do 20 ml), uporabljani štiri mesece. Pri anorektično-kahektičnem sindromu zaradi napredovalega raka je priporočljiv začetni odmerek 200 mg (5 ml) na dan; glede na bolnikov odziv ga je mogoče povečati do 800 mg na dan (20 ml). Običajni odmerek je med 400 in 800 mg na dan (10–20 ml). V raziskavah bolnikov z napredovalim rakom so bili klinično učinkoviti dnevni odmerki od 200 do 800 mg/dan (5 do 20 ml), uporabljani najmanj osem tednov. Pred uporabo je potrebno plastenko s suspenzijo dobro pretresti. Uporaba pri otrocih: Varnosti in učinkovitosti pri otrocih niso dokazali. Uporaba pri starostnikih: Zaradi pogostejših okvar jeter, ledvic in srčne funkcije, pogostejših sočasnih obolenj ali sočasnega zdravljenja z drugimi zdravili je odmerek za starejšega bolnika treba določiti previdno in običajno začeti z najnižjim odmerkom znotraj odmernega intervala. **KONTRAINDIKACIJE:** Preobčutljivost za megestrolacetat ali katerokoli pomožno snov. **POSEBNA OPOZORILA IN PREVIDNOSTNI UKREPI:** Uporaba gestagenov med prvimi štirimi meseci nosečnosti ni priporočljiva. Pri bolnikih s tromboflebitisom v anamnezi je treba zdravilo Megace uporabljati previdno. Zdravljenje z zdravilom Megace se lahko začne šele, ko so bili vzroki hujšanja, ki jih je mogoče zdraviti, ugotovljeni in obravnavani. Megestrolacetat ni namenjen za profilaktično uporabo za preprečitev hujšanja. Učinki na razmnoževanje virusa HIV niso ugotovljeni. Med zdravljenjem z megestrolacetatom in po prekinitvi kroničnega zdravljenja je treba upoštevati možnost pojava zavore nadledvične žleze. Morda bo potrebno nadomestno zdravljenje s stresnimi odmerki glukokortikoidov. Megestrolacetat se v veliki meri izloči prek ledvic. Ker je verjetnost zmanjšanega delovanja ledvic pri starostnikih večja, je pri določitvi odmerka potrebna previdnost, prav tako je koristno spremljanje ledvične funkcije. Peroralna suspenzija vsebuje saharozo. Bolniki z redko dedno intoleranco za fruktozo, malabsorpcijo glukoze/galaktoze ali pomanjkanjem saharoza-izomaltaze ne smejo jemati tega zdravila. Peroralna suspenzija vsebuje tudi majhne količine etanola (alkohola), in sicer manj kot 100 mg na odmerek. **INTERAKCIJE:** Aminoglutetimid: poročali so o zmanjšanju koncentracije progestogena v plazmi z možno izgubo terapevtskega delovanja zaradi inducirane presnove. Sočasno jemanje megestrolacetata (v obliki peroralne suspenzije) in zidovudina ali rifabutina ne povzroča sprememb farmakokinetičnih parametrov. **NEŽELENI UČINKI:** Pogosti (≥ 1/100, < 1/10): navzea, bruhanje, driska, flatulenca, izpuščaj, metroragija, impotenca, astenija, bolečina, edem. Neznana pogostnost (pogostnosti ni mogoče oceniti iz razpoložljivih podatkov): poslabšanje osnovne bolezni (širjenje tumorja), adrenalna insuficienca, kušingoidni izgled, Cushingov sindrom, diabetes mellitus, motena toleranca za glukozo, hiperglikemija, spremembe razpoloženja, sindrom karpalnega kanala, letargija, srčno popuščanje, tromboflebitis, pljučna embolija (v nekaterih primerih usodna), hipertenzija, navali vročine, dispneja, zaprtje, alopecija, pogosto uriniranje. **Vrsta ovojnine in vsebina:** Plastenka z 240 ml suspenzije. **Režim izdaje:** Rp/Spec. **Imetnik dovoljenja za promet:** Bristol-Myers Squibb spol. s r.o., Olivova 4, Praga 1, Češka; **Odgovoren za trženje v Sloveniji:** PharmaSwiss d.o.o., Ljubljana, tel: 01 236 4 700, faks: 01 236 4 705; MGS-120609. **Pred predpisovanjem preberite celoten povzetek glavnih značilnosti zdravila!**

Reference: 1. Povzetek glavnih značilnosti zdravila Megace – 12. junij 2009; **2.** Register zdravil Republike Slovenije XII – leto 2010; **3.** Beller, E., 1997. Ann Oncol 8: 277-283; **4.** Čufer, T, 2002. Onkologija 9(2): 73-75; **5.** Yavuzsen, T., 2005. J Clin Oncol 23(33): 8500-8511; **6.** Bilten Recept 8(2), 8.12.2010

MEG0211-01; februar 2011

Bristol-Myers Squibb

PharmaSwiss
Choose More Life

TANTUM® VERDE

Lajšanje bolečine in oteklin pri vnetju v ustni votlini in žrelu, ki nastanejo zaradi okužb in stanj po operaciji in kot posledica radioterapije (t.i. radiomukozitis).

Tantum Verde 1,5 mg/ml oralno pršilo, raztopina

Kakovostna in količinska sestava
1 ml raztopine vsebuje 1,5 mg benzidaminijevega klorida, kar ustreza 1,34 mg benzidamina. V enem razpršku je 0,17 ml raztopine. En razpršek vsebuje 0,255 mg benzidaminijevega klorida, kar ustreza 0,2278 mg benzidamina. En razpršek vsebuje 13,6 mg 96 odstotnega etanola, kar ustreza 12,728 mg 100 odstotnega etanola, in 0,17 mg metilparahidroksibenzoata (E218).

Terapevtske indikacije
Samozdravljenje: lajšanje bolečine in oteklin pri vnetju v ustni votlini in žrelu, ki so lahko posledica okužb in stanj po operaciji. Po nasvetu in navodilu zdravnika: lajšanje bolečine in oteklin v ustni votlini in žrelu, ki so posledica radiomukozitisa.

Odmerjanje in način uporabe
Uporaba 2- do 6-krat na dan (vsake 1,5 do 3 ure). Odrasli: 4 do 8 razprškov 2- do 6-krat na dan. Otroci od 6 do 12 let: 4 razprški 2- do 6-krat na dan. Otroci, mlajši od 6 let: 1 razpršek na 4 kg telesne mase; do največ 4 razprške 2 do 6-krat na dan.

Kontraindikacije
Znana preobčutljivost za zdravilno učinkovino ali katerokoli pomožno snov.

Posebna opozorila in previdnostni ukrepi
Pri manjšini bolnikov lahko resne bolezni povzročijo ustne/žrelne ulceracije. Če se simptomi v treh dneh ne izboljšajo, se mora bolnik posvetovati z zdravnikom ali zobozdravnikom, kot je primerno. Zdravilo vsebuje aspartam (E951) (vir fenilalanina), ki je lahko škodljiv za bolnike s fenilketonurijo. Zdravilo vsebuje izomalt (E953) (sinonim: izomaltitol (E953)). Bolniki z redko dedno intoleranco za fruktozo ne smejo jemati tega zdravila. Uporaba benzidamina ni priporočljiva za bolnike s preobčutljivostjo za salicilno kislino ali druga nesteroidna protivnetna zdravila. Pri bolnikih, ki imajo ali so imeli bronhialno astmo, lahko pride do bronhospazma. Pri takih bolnikih je potrebna previdnost.

Medsebojno delovanje z drugimi zdravili in druge oblike interakcij
Pri ljudeh raziskav o interakcijah niso opravljali.

Nosečnost in dojenje
Tantum Verde z okusom mentola 3 mg pastile se med nosečnostjo in dojenjem ne smejo uporabljati.

Vpliv na sposobnost vožnje in upravljanja s stroji
Uporaba benzidamina lokalno v priporočenem odmerku ne vpliva na sposobnost vožnje in upravljanja s stroji.

Neželeni učinki
Bolezni prebavil Redki: pekoč občutek v ustih, suha usta.
Bolezni imunskega sistema Redki: preobčutljivostna reakcija.
Bolezni dihal, prsnega koša in mediastinalnega prostora Zelo redki: laringospazem.
Bolezni kože in podkožja Občasni: fotosenzitivnost. Zelo redki: angioedem.

Rok uporabnosti
4 leta. Zdravila ne smete uporabljati po datumu izteka roka uporabnosti, ki je naveden na ovojnini. Posebna navodila za shranjevanje Za shranjevanje pastil niso potrebna posebna navodila. Plastenko z raztopino shranjujte v zunanji ovojnini za zagotovitev zaščite pred svetlobo. Shranjujte pri temperaturi do 25°C. Shranjujte v originalni ovojnini in nedosegljivo otrokom.

www.tantum-verde.si

CSC Pharma, d.o.o., Jana Husa 1a, 1000 Ljubljana, www.csc-pharma.si

Imetnik dovoljenja za promet
CSC Pharma d.o.o.
Jana Husa 1a
1000 Ljubljana

CSC ANGELINI

NA **VMESNI LISTI**[1]!

S klinično dokazano učinkovitostjo

EDINI Prosure®

2 TETRAPAKA NA DAN VSAJ 8 TEDNOV

Klinične raziskave pri bolnikih z rakom so pokazale, da Prosure®:

- **Izboljša apetit in poveča količino zaužite hrane.**[2,3,10,11]
- **Pripomore k pridobivanju telesne teže.**[2,3,7-9]
- **Poveča mišično maso.**[2,3,7,8]
- **Poveča fizično moč.**[6]
- **Omogoča večjo fizično dejavnost.**[3,4,5]
- **Izboljša kakovost življenja.**[2,5,6,8,10]
- **Ublaži vnetni odziv bolnikovega imunskega sistema na onkološko bolezen.**[8,10,12]

POMEMBEN JE **VSAK** KORAK!

1. Le na osnovi predpisa pooblaščenega zdravnika, za določeno skupino bolnikov in določen produkt. Za podrobnosti si oglejte spletno stran **www.zzzs.si**. **2.** Fearon K C H et al. Gut. 2003;52:1479-1486. **3.** Barber MD. et al. Brit J Can. 1999; 81:80-86. **4.** Moses AWG. et. al. Br J Can. 2004;90:996-1002. **5.** Bauer JD et al. Support Care Cancer. 2005;13:270-274. **6.** Von Meyenfeldt M. et.al. Proc Am Soc Clin Oncol. 2002;21:385A. **7.** Weed HG. et.al. Proc Am Soc Clin Oncol. 2005; 8112A. **8.** Read JA. et al. Support Care Cancer. 2007;15:301-307. **9.** Bayram I. et al. Pediatr Blood Cancer. 2009;52:571-574. **10.** Guarcello M. et. al. Nutr Ther & Metab. 2006;24:168-175. **11.** Jatoi A. et. al. Journal of Cl Oncology. 2004;22:2469-2476. **12.** Ryan A et al. Ann Surg. 2009;249:355-363.

Prosure®
Živeti življenje

NJUT0422011

Abbott
A Promise for Life

Preprečuje CINV* od samega začetka

z zdravilom EMEND v kombinaciji z drugimi antiemetiki

* - s kemoterapijo povzročena navzea in bruhanje

06-12-EMD-11-SLO-022-J

EMEND 80 mg trde kapsule EMEND 125 mg trde kapsule **SKRAJŠAN POVZETEK GLAVNIH ZNAČILNOSTI ZDRAVILA Pred predpisovanjem, prosimo, preberite celoten Povzetek glavnih značilnosti zdravila, ki ga dobite pri naših strokovnih sodelavcih! Sestava:** Ena EMEND 125 mg trda kapsula vsebuje 125 mg aprepitanta in 125 mg saharoze. Ena EMEND 80 mg trda kapsula vsebuje 80 mg aprepitanta in 80 mg saharoze. **Terapevtske indikacije:** Preprečevanje akutne in zapoznele navzee in bruhanja povezanih z zelo emetogeno kemoterapijo raka s cisplatinom pri odraslih. Preprečevanje navzee in bruhanja, povezanih z zmerno emetogeno kemoterapijo raka pri odraslih. Zdravilo EMEND 125 mg/80 mg se daje v sklopu kombiniranega zdravljenja. **Odmerjanje in način uporabe:** Zdravilo EMEND se daje 3 dni po shemi zdravljenja, ki vključuje kortikosteroid in antagonist 5-HT3. Priporočeno odmerjanje zdravila EMEND je 125 mg peroralno (p.o.) enkrat dnevno eno uro pred pričetkom kemoterapije prvi dan ter 80 mg (p.o.) enkrat na dan drugi in tretji dan. Fosaprepitant 115 mg, liofilizirano predzdravilo aprepitanta v obliki 15-minutne infuzije, lahko prvi dan, 30 minut pred kemoterapijo nadomesti uporabo zdravila EMEND (125 mg). Zdravilo EMEND se lahko jemlje s hrano ali brez. Trdo kapsulo je treba pogoltniti celo. Pri starostnikih, bolnikih z okvaro ledvic in pri bolnikih s končno ledvično odpovedjo, ki se zdravijo s hemodializo, bolnikih z blago okvaro jeter ter glede na spol odmerka ni treba prilagajati. Pri bolnikih z zmerno okvaro jeter je število podatkov omejeno, pri bolnikih s hudo okvaro jeter pa podatkov ni. Pri teh bolnikih je treba aprepitant uporabljati previdno. Uporabe pri bolnikih, ki so mlajši od 18 let, zaradi nezadostnih podatkov o varnosti in učinkovitosti ne priporočamo. **Kontraindikacije:** Preobčutljivost za zdravilno učinkovino ali katerokoli pomožno snov. Sočasno jemanje s pimozidom, terfenadinom, z astemizolom ali s cisapridom. **Posebna opozorila in previdnostni ukrepi:** Zdravilo EMEND je treba uporabljati previdno pri bolnikih, ki sočasno jemljejo peroralne zdravilne učinkovine, ki se primarno presnavljajo s CYP3A4 in z ozkim terapevtskim območjem, kot so ciklosporin, takrolimus, sirolimus, everolimus, alfentanil, diergotamin, ergotamin, fentanil in kinidin. Previdnost je še posebej potrebna pri sočasnem dajanju irinotekana, saj lahko kombinacija poveča toksični učinek. Pri sočasni uporabi zdravila EMEND z alkaloidi rženega rožička (ergot alkaloid) svetujemo previdnost zaradi morebitnega tveganja za pojav z ergot alkaloidi povezanih toksičnih učinkov. Sočasna uporaba zdravila EMEND z varfarinom zmanjša protrombinski čas, izražen kot INR. Pri bolnikih, ki se kontinuirano zdravijo z varfarinom, je treba INR skrbno spremljati med zdravljenjem z zdravilom EMEND in še 2 tedna po vsakem 3-dnevnem ciklusu zdravljenja navzee in bruhanja zaradi kemoterapije z zdravilom EMEND. Med jemanjem zdravila EMEND in še 28 dni po koncu jemanja se lahko zmanjša učinkovitost hormonskih kontraceptivov. Med zdravljenjem z zdravilom EMEND in 2 meseca po zadnjem odmerku zdravila EMEND je treba uporabljati alternativno ali dodatno kontracepcijsko metodo. Sočasnemu jemanju zdravila EMEND in zdravilnih učinkovin, ki močno inducirajo aktivnost CYP3A4 (npr. rifampicin, fenitoin, karbamazepin, fenobarbital), se je treba izogibati, ker kombinacija povzroči zmanjšanje plazemskih koncentracij aprepitanta. Sočasna uporaba zdravila EMEND in zeliščnih pripravkov, ki vsebujejo šentjanževko, ni priporočljiva. Potrebna je previdnost pri sočasni uporabi zdravila EMEND in zdravilnih učinkovin, ki zavirajo aktivnost CYP3A4 (npr. ketokonazol, itrakonazol, vorikonazol, posakonazol, klaritromicin, telitromicin, nefazodon in zaviralci proteaz), ker se zaradi kombinacije pričakuje zvišanje plazemskih koncentracij aprepitanta. Zdravilo EMEND vsebuje saharozo. Bolniki z redkimi dednimi motnjami – fruktozno intoleranco, malabsorpcijo glukoze in galaktoze ali insuficienco saharaze-izomaltaze – ne smejo jemati tega zdravila. **Medsebojno delovanje z drugimi zdravili in druge oblike interakcij:** Aprepitant (125 mg/80 mg) je substrat, zmerni zaviralec in induktor CYP3A4. Aprepitant je tudi induktor CYP2C9. Med zdravljenjem se CYP3A4 inhibira. Po koncu zdravljenja pa zdravilo EMEND povzroči blago indukcijo CYP2C9, CYP3A4 in glukuronidacije. Aprepitant nima medsebojnega vpliva z digoksinom, zato verjetno ne intereagira s P-glikoproteinskim prenašalcem. Kot blag induktor CYP2C9, induktor CYP3A4 in glukuronidacije lahko aprepitant zniža plazemske koncentracije substratov, ki se izločajo po teh poteh. Ta učinek se lahko pokaže šele po koncu zdravljenja z zdravilom EMEND. Za substrate CYP2C9 in CYP3A4 je indukcija prehodna, največji učinek pa je dosežen v 3-5 dneh po koncu 3 dnevnega zdravljenja z zdravilom EMEND. Učinek traja nekaj dni, potem pa počasa upada in je klinično nepomemben v dveh tednih po koncu zdravljenja. V tem obdobju svetujemo previdnost pri dajanju peroralnih zdravilnih učinkovin, ki se presnavljajo s CYP2C9. *Kortikosteroidi:* Pri sočasnem jemanju je treba običajni peroralni odmerek deksametazona zmanjšati za približno 50 %, običajni intravenski odmerek metilprednizolona zmanjšati za približno 25 % in običajni peroralni odmerek metilprednizolona zmanjšati za približno 50 %. *Kemoterapevtiki:* Pri bolnikih, ki poleg zdravila EMEND peroralno prejemajo kemoterapevtike, ki se primarno ali delno presnavljajo s CYP3A4 (npr. etopozid, vinorelbin), svetujemo previdnost.. Pri takih bolnikih bo morda potreben dodatni nadzor. *Imunosupresivi:* Zmanjšanja odmerka imunosupresivov, ki se presnavljajo s CYP3A4 (npr. ciklosporin, takrolimus, everolimus in sirolimus), ne priporočamo. *Midazolam:* Pri sočasni uporabi z zdravilom EMEND (125mg / 80 mg) je treba upoštevati možne učinke zvišanih plazemskih koncentracij midazolama in drugih benzodiazepinov, ki se presnavljajo predvsem s CYP3A4 (alprazolam, triazolam). *Tolbutamid:* Zdravilo EMEND je pri jemanju po shemi 125 mg prvi dan ter 80 mg/dan drugi in tretji dan zmanjšal AUC tolbutamida (ki je substrat za CYP2C9), ki so ga bolniki prejemali v enkratnem odmerku 500 mg per os pred začetkom 3 dnevne sheme odmerjanja zdravila EMEND ter 4., 8. in 15. dan. *Antagonisti 5 HT_3:* V kliničnih raziskavah medsebojnega delovanja aprepitant ni imel klinično pomembnih učinkov na farmakokinetiko ondansetrona, granisetrona in hidrodolasetrona. *Ketokonazol:* Pri enkratnem odmerku 125 mg aprepitanta 5. dan 10 dnevnega zdravljenja s ketokonazolom (ki je močan zaviralec CYP3A4) 400 mg na dan, se je AUC aprepitanta povečal za približno 5 krat, srednji končni razpolovni čas aprepitanta pa se je podaljšal za približno za 3 krat. *Rifampicin:* Pri enkratnem odmerku 375 mg aprepitanta 9. dan 14 dnevnega zdravljenja z rifampicinom (ki je močan induktor CYP3A4) 600 mg na dan, se je AUC aprepitanta zmanjšal za 91 %, srednji končni razpolovni čas aprepitanta pa se je skrajšal za 68 %. **Neželeni učinki:** Pri bolnikih, zdravljenih z aprepitantom, so opazili naslednje neželene učinke, ki so se pojavljali pogosteje kot pri standardni terapiji: Pogosti (>1/100, <1/10): anoreksija, glavobol, omotica, kolcanje, konstipacija, driska, dispepsija, spahovanje, astenija/utrujenost, zvišanje ALT, zvišanjeAST. Občasni (>1/1.000, <1/100): kandidoza, okužbe s stafilokoki, anemija, febrilna nevtropenija, povečanje telesne mase, polidipsija, dezorientacija, evforija, anksioznost, neobičajne sanje, motnje mišljenja, letargija, zaspanost, konjunktivitis, tinitus, bradikardija, palpitacije, bolezen srca in ožilja, zardevanje/navali vročine, faringitis, kihanje, kašelj, zatekanje izcedka iz nosu v žrelo, draženje žrela, perforirajoč duodenalen ulkus, navzea, bruhanje, refluks kisline, motnje okusa, neugodje v epigastriju, obstipacija, gastroezofagalna refluksna bolezen, bolečine v trebuhu, suha usta, enterokolitis, vetrovi, stomatitis, napihnjen trebuh, trdo blato, nevtropenični kolitis, izpuščaji, akne, fotosenzitivnost, prekomerno znojenje, mastna koža, srbenje, lezije kože, srbeči izpuščaj, mišični krči, bolečine v mišicah, mišična oslabelost, poliurija, disurija, polakisurija, edem, nelagodje v prsnem košu, splošno slabo počutje, žeja, mrzlica, motnja hoje, zvišanje alkalne fosfataze, hiperglikemija, mikrohematurja, hiponatriemija, zmanjšanje telesne mase, zmanjšano število nevtrofilcev. Poročali so o enem primeru angioedema in urtikarije. Pri enem bolniku, ki je dobival aprepitant ob kemoterapiji zaradi raka, so poročali o pojavu Stevens-Johnsonovega sindroma. V obdobju trženja zdravila so poročali še o (pogostnost je neznana): pruritus, izpuščaj, urtikarija, preobčutljivostne reakcije, vključno z anafilaktičnimi reakcijami. EMEND 80mg trde kapsule EMEND 125 mg trde kapsule **Imetnik dovoljenja za promet:** Merck Sharp & Dohme Ltd., Hertford Road, Hoddesdon, Hertfordshire EN 11 9BU, Velika Britanija **Način in režim izdaje zdravila:** Predpisovanje in izdaja zdravila je le na zdravniški recept. **Datum zadnje revizije besedila:** 01/2010

Samo za strokovno javnost.

EMEND® (aprepitant, MSD)

IVEMEND® (fosaprepitant dimeglumin, MSD)

Preventivno od začetka

MSD

Merck Sharp & Dohme, inovativna zdravila d.o.o.
Šmartinska cesta 140, 1000 Ljubljana; telefon: 01/ 5204 201, faks: 01/ 5204 349

Tiskano v Sloveniji, junij 2011.

Antraciklinska ekstravazacija lahko nastopi kadarkoli.

savene™
deksrazoksan

Edini dokazani antidot pri ekstravazaciji antraciklinov v okolno tkivo, ki ga je odobrila EMEA.

Bodite pripravljeni!

Savene™ – Povzetek informacij o predpisovanju zdravila (izdelan na podlagi Povzetka glavnih značilnosti zdravila - SPC). Za celotne informacije o predpisovanju zdravila glejte SPC.
Vsaka škatlica zdravila Savene™ vsebuje 10 vial Savene™ praška (deksrazoksan) (10 x 500 mg) in 3 vrečke Savene™ puferske raztopine za redčanje (3 x 500 ml) za infuzijo. Indikacije: Zdravljenje ekstravazacije antraciklinov. Odmerjanje in način uporabe: Z aplikacijo zdravila Savene™ je treba začeti čim prej in najpozneje v šestih urah po opaženi ekstravazaciji. Zdravilo Savene™ se daje kot intravenska infuzija enkrat na dan 3 zaporedne dni, glede na telesno površino: 1. dan 1000 mg/m^2; 2. dan 1000 mg/m^2; 3. dan 500 mg/m^2. Pri bolnikih s telesno površino, ki presega 2 m^2, enkratni odmerek ne sme preseči 2000 mg. Ledene obloge ali druge pripomočke za hlajenje je treba odstraniti s prizadetega predela najmanj 15 min pred aplikacijo. Pred infuzijo je treba Savene™ prašek še pred nadaljnjim redčenjem, s pufersko raztopino za redčenje, rekonstituirati s sterilno vodo. Uporaba zdravila Savene™ ni priporočljiva pri otrocih in bolnikih z okvarjenim delovanjem ledvic in jeter. Varnost in učinkovitost zdravila nista bili ovrednoteni pri starejših bolnikih. Kontraindikacije: Preobčutljivost za aktivno učinkovino ali katerokoli sestavino zdravila, ženske v rodni dobi, ki ne uporabljajo kontracepcije, dojenje in sočasno cepljenje s cepivom proti rumeni mrzlici. Opozorila in previdnostni ukrepi: Po končanem zdravljenju je treba prizadeti predel redno nadzorovati, dokler se stanje ne izboljša. Redno je treba izvajati tudi hematološke preiskave. Zdravilo Savene™ se sme aplicirati samo pod nadzorom zdravnika, ki ima izkušnje z uporabo kemoterapevtikov za zdravljenje raka. Pri bolnikih z znanimi motnjami v delovanju jeter je pred vsako aplikacijo zdravila Savene™ priporočljivo izvajati rutinske teste jetrne funkcije. Pri bolnikih z okvarjenim delovanjem ledvic je treba opazovati znake hematološke toksičnosti. Za moške je priporočljivo, da med zdravljenjem in do 3 mesece po njem ne zaplodijo otroka. Ženske v rodni dobi morajo med zdravljenjem uporabljati kontracepcijsko zaščito. To zdravilo običajno ni priporočljivo v kombinaciji z živimi oslabljenimi cepivi ali s fenitoinom. Bolniki, ki prejmejo Savene™, ne smejo sočasno prejemati dimetil sulfoksida (DMSO). Ker vsebuje Savene™ redčilo kalij, (98 mg/500 ml), je treba pri bolnikih s tveganjem za pojav hiperkaliemije skrbno nadzorovati plazemske vrednosti kalija. Ker vsebuje tudi natrij (1,61 g/500 ml), lahko škoduje bolnikom, ki so na dieti z nizko vsebnostjo natrija. Interakcije: Interakcije, značilne za vse citotoksike, ki lahko medsebojno učinkujejo tudi s peroralnimi antikoagulanti. Pri sočasni uporabi imunosupresivov kot sta ciklosporin in takrolimus je potrebna posebna pozornost zaradi obsežne imunosupresije. Nosečnost in dojenje: Nosečnice ne smejo prejemati zdravila Savene™, razen če to ni nujno potrebno. Ženske v rodni dobi morajo med zdravljenjem uporabljati kontracepcijska sredstva. Doječe matere morajo med zdravljenjem z zdravilom Savene™ prenehati dojiti. Stranski učinki: Zelo pogosti: navzea, bolečina na mestu vboda, pooperativna okužba. Pogosti: bruhanje, driska, stomatitis, suha usta, pireksija, flebitis na mestu vboda, eritem na mestu vboda, utrujenost, induracija na mestu vboda, oteklina na mestu vboda, periferni edem, somnolenca, okužba, nevtropenična okužba, zaplet rane, zmanjšanje telesne teže, izguba teka, mialgija, omotičnost, izguba senzibilitete, sinkopa, tremor, nožnična krvavitev, dispneja, pljučnica, izpadanje las, srbečica, flebitis, površinski tromboflebitis, venska tromboza udov, tromboza. Vsi neželeni učinki so opisani kot hitro reverzibilni. Redko so poročali o povečanih koncentracijah jetrnih encimov (ALT/AST). Imetnik dovoljenja za promet: SpePharm Holding B.V., Kingsfordweg 151, NL – 1043 GR Amsterdam, Nizozemska. Številka dovoljenja za promet: EU/1/06/350/001.

SpePharm

www.medis.si

MEDIS

Zadeli smo pravo tarčo

Izredno učinkovito zdravljenje prvega reda pri nedrobnoceličnem pljučnem raku z mutacijo EGFR

Iressa je prva in edina tarčna monoterapija, ki dokazano podaljša preživetje brez napredovanja bolezni v primerjavi z dvojno kemoterapijo kot zdravljenje prvega reda pri bolnikih z napredovalim nedrobnoceličnim pljučnim rakom z mutacijo EGFR. [1]

IRESSA® (GEFITINIB)
SKRAJŠAN POVZETEK GLAVNIH ZNAČILNOSTI ZDRAVILA

1. Povzetek glavih značilnosti zdravila Iressa (gefitinib). Junij 2009.

Sestava: Filmsko obložene tablete vsebujejo 250 mg gefitiniba. **Indikacije:** zdravljenje odraslih bolnikov z lokalno napredovalim ali metastatskim nedrobnoceličnim pljučnim rakom z aktivacijskimi mutacijami EGFR-TK **Odmerjanje in način uporabe:** Zdravljenje z gefitinibom mora uvesti in nadzorovati zdravnik, ki ima izkušnje z uporabo zdravil proti raku. Priporočeno odmerjanje zdravila IRESSA je ena 250-mg tableta enkrat na dan. Tableto je mogoče vzeti s hrano ali brez nje, vsak dan ob približno istem času. **Kontraindikacije:** preobčutljivost za zdravilno učinkovino ali katerokoli pomožno snov, dojenje **Opozorila in previdnostni ukrepi:** Pri 1,3 % bolnikov, ki so dobivali gefitinib, so opažali intersticijsko bolezen pljuč (IBP). Ta se lahko pojavi akutno in je bila v nekaterih primerih smrtna. Če se bolniku poslabšajo dihalni simptomi, npr. dispneja, kašelj in zvišana telesna temperatura, morate zdravljenje z zdravilom IRESSA prekiniti in bolnika takoj preiskati. če je potrjena IBP, morate terapijo z zdravilom IRESSA končati in bolnika ustrezno zdraviti. čeprav so bile nepravilnosti testov jetrnih funkcij pogoste, so jih redko zabeležili kot hepatitis. Zato so priporočljive redne kontrole delovanja jeter. V primeru blagih do zmernih sprememb v delovanju jeter je treba zdravilo IRESSA uporabljati previdno. Če so spremembe hude, pride v poštev prekinitev zdravljenja. Zdravilo IRESSA vsebuje laktozo. Bolniki z redko dedno intoleranco za galaktozo, laponsko obliko zmanjšane aktivnosti laktaze ali malabsorpcijo glukozežgalaktoze ne smejo jemati tega zdravila. Bolnikom naročite, da morajo takoj poiskati zdravniško pomoč, če se jim pojavijo kakršnikoli očesni simptomi, huda ali dolgotrajna driska, navzea, bruhanje ali anoreksija, ker lahko vse te posredno povzročijo dehidracijo. **Medsebojno delovanje zdravile:** Induktorji CYP3A4 lahko povečajo presnovo gefitiniba in zmanjšajo njegovo koncentracijo v plazmi. Zato lahko sočasna uporaba induktorjev CYP3A4 (npr. fenitoina, karbamazepina, rifampicina, barbituratov ali zeliščnih pripravkov, ki vsebujejo šentjanževko/Hypericum perforatum) zmanjša učinkovitost zdravljenja in se ji je treba izogniti. Pri posameznih bolnikih, ki imajo genotip slabih metabolizatorjev s CYP2D6, lahko zdravljenje z močnim zaviralcem CYP3A4 poveča koncentracijo gefitiniba v plazmi. Na začetku zdravljenja z zaviralcem CYP3A4 je treba bolnike natančno kontrolirati glede neželenih učinkov gefitiniba. Pri nekaterih bolnikih, ki so jemali varfarin skupaj z gefitinibom, so se pojavili zvišanje internacionalnega normaliziranega razmerja (INR) in/ali krvavitve. Bolnike, ki sočasno jemljejo varfarin in gefitinib, morate redno kontrolirati glede sprememb protrombinskega časa (PČ) ali INR. Zdravila, ki občutno in dolgotrajno zvišajo pH v želodcu npr. zaviralci protonske črpalke in antagonisti H2, lahko zmanjšajo biološko uporabnost gefitiniba in njegovo koncentracijo v plazmi in tako zmanjšajo učinkovitost. Redno jemanje antacidov, uporabljenih blizu časa jemanja zdravila IRESSA, ima lahko podoben učinek. **Neželeni učinki:** V kumulativnem naboru podatkov kliničnih preskušanj III. faze so bili najpogosteje opisani neželeni učinki, ki so se pojavili pri več kot 20 % bolnikov, driska in kožne reakcije (vključno z izpuščajem, aknami, suho kožo in srbenjem). Neželeni učinki se ponavadi pojavijo prvi mesec zdravljenja in so praviloma reverzibilni. Ostali pogostejši neželeni učinki so: anoreksija, konjunktivitis, blefaritis in suho oko, krvavitev, npr. epistaksa in hematurija, intersticijska bolezen pljuč (1,3 %), navzea, bruhanje, stomatitis, dehidracija, suha usta, nepravilnosti testov jetrnih funkcij, bolezni nohtov, alopecija, asimptomatično laboratorijsko zvišanje kreatinina v krvi, proteinurija, astenija, pireksija. **Vrsta in vsebina ovojnine:** škatla s 30 tabletami po 250 mg gefitiniba **Način izdajanja zdravila:** samo na recept **Datum priprave besedila:** junij 2009 **Imetnik dovoljenja za promet:** AstraZeneca AB, S-151 85, Sodertalje, Švedska Pred predpisovanjem, prosimo, preberite celoten povzetek glavnih značilnosti zdravila. **Dodatne informacije so na voljo pri:** AstraZeneca UK Limited, Podružnica v Sloveniji, Verovškova 55, 1000 Ljubljana, telefon: 01/51 35 600.

AstraZeneca
ONKOLOGIJA

IRESSA®
gefitinib

Instructions for authors

The editorial policy

Radiology and Oncology is a multidisciplinary journal devoted to the publishing original and high quality scientific papers, professional papers, review articles, case reports and varia (editorials, short communications, professional information, book reviews, letters, etc.) pertinent to diagnostic and interventional radiology, computerized tomography, magnetic resonance, ultrasound, nuclear medicine, radiotherapy, clinical and experimental oncology, radiobiology, radiophysics and radiation protection. Therefore, the scope of the journal is to cover beside radiology the diagnostic and therapeutic aspects in oncology, which distinguishes it from other journals in the field.

The Editorial Board requires that the paper has not been published or submitted for publication elsewhere; the authors are responsible for all statements in their papers. Accepted articles become the property of the journal and, therefore cannot be published elsewhere without the written permission of the editors.

Submission of the manuscript

The manuscript written in English should be submitted electronically to: gsersa@onko-i.si. In the case the figures are too big to be submitted electronically, authors are asked to send along the printed copy of the manuscript, together with all the files on CD, to the editorial office. The type of computer and word-processing package should be specified (Word for Windows is preferred).

Editorial Office Radiology and Oncology
Zaloska cesta 2
P.O. Box 2217
SI-1000 Ljubljana
Slovenia
Phone: +386 (0)1 5879 434,
Tel./Fax: +386 (0)1 5879 434,
E-mail: gsersa@onko-i.si

All articles are subjected to the editorial review and the review by independent referees. Manuscripts which do not comply with the technical requirements stated herein will be returned to the authors for the correction before peer-review. The editorial board reserves the right to ask authors to make appropriate changes of the contents as well as grammatical and stylistic corrections when necessary. Page charges will be charged for manuscripts exceeding the recommended page number, as well as additional editorial work and requests for printed reprints. All articles are published printed and on-line as the open access. To support the open access policy of the journal, the authors are encouraged to pay the open access charge of 500 EUR.

Preparation of manuscripts

Radiology and Oncology will consider manuscripts prepared according to the Uniform Requirements for Manuscripts Submitted to Biomedical Journals by International Committee of Medical Journal Editors (http://www.icmje.org/). The manuscript should be typed double-spaced with a 3-cm margin at the top and left-hand side of the sheet. The manuscript should be written in grammatically and stylistically correct language. Abbreviations should be avoided. If their use is neccessary, they should be explained at the first time mentioned. The technical data should conform to the SI system. The manuscript, including the references, must not exceed 15 typewritten pages, and the number of figures and tables is limited to 8. If appropriate, organize the text so that it includes: Introduction, Materials and methods, Results and Discussion. Exceptionally, the results and discussion can be combined in a single section. Start each section on a new page, and number each page consecutively with Arabic numerals.

The Title page should include a concise and informative title, followed by the full name(s) of the author(s); the institutional affiliation of each author; the name and address of the corresponding author (including telephone, fax and E-mail), and an abbreviated title. This should be followed by the abstract page, summarizing in less than 250 words the reasons for the study, experimental approach, the major findings (with specific data if possible), and the principal conclusions, and providing 3-6 key words for indexing purposes. Structured abstracts are preferred. Slovene authors are requested to provide title and the abstract in Slovene language in a separate file. The text of the research article should then proceed as follows:

Introduction should summarize the rationale for the study or observation, citing only the essential references and stating the aim of the study.

Materials and methods should provide enough information to enable experiments to be repeated. New methods should be described in detail.

Results should be presented clearly and concisely without repeating the data in the figures and tables. Emphasis should be on clear and precise presentation of results and their significance in relation to the aim of the investigation.

Discussion should explain the results rather than simply repeating them and interpret their significance and draw conclusions. It should discuss the results of the study in the light of previously published work.

Illustrations and tables must be numbered and referred to in the text, with the appropriate location indicated. Graphs and photographs, provided electronically, should be of appropriate quality for good reproduction. Color graphs and photographs are encouraged. Picture size must be 2.000 pixels on the longer side. In photographs, mask the identities of the patients. Tables should be typed double-spaced, with a descriptive title and, if appropriate, units of numerical measurements included in the column heading.

References must be numbered in the order in which they appear in the text and their corresponding numbers quoted in the text. Authors are responsible for the accuracy of their references. References to the Abstracts and Letters to the Editor must be identified as such. Citation of papers in preparation or submitted for publication, unpublished observations, and personal communications should not be included in the reference list. If essential, such material may be incorporated in the appropriate place in the text. References follow the style of Index Medicus. All authors should be listed when their number does not exceed six; when there are seven or more authors, the first six listed are followed by "et al.". The following are some examples of references from articles, books and book chapters:

Dent RAG, Cole P. *In vitro* maturation of monocytes in squamous carcinoma of the lung. *Br J Cancer* 1981; **43**: 486-95.

Chapman S, Nakielny R. *A guide to radiological procedures*. London: Bailliere Tindall; 1986.

Evans R, Alexander P. Mechanisms of extracellular killing of nucleated mammalian cells by macrophages. In: Nelson DS, editor. *Immunobiology of macrophage*. New York: Academic Press; 1976. p. 45-74.

Authorization for the use of human subjects or experimental animals

Manuscripts containing information related to human or animal use should clearly state that the research has complied with all relevant national regulations and institutional policies and has been approved by the authors' institutional review board or equivalent committee. These statements should appear in the Materials and methods section (or for contributions without this section, within the main text or in the captions of relevant figures or tables).

When reporting experiments on human subjects, authors should indicate whether the procedures followed were in accordance with the Helsinki Declaration. Patients have the right to privacy; therefore the identifying information (patient's names, hospital unit numbers) should not be published unless it is essential. In such cases the patient's informed consent for publication is needed, and should appear as an appropriate statement in the article.

The research using animal subjects should be conducted according to the EU Directive 2010/63/EU and following the Guidelines for the welfare and use of animals in cancer research (*Br J Cancer 2010; 102: 1555 – 77*). Authors must identify the committee approving the experiments, and must confirm that all experiments were performed in accordance with relevant regulations.

Transfer of copyright agreement

For the publication of accepted articles, authors are required to send the Transfer of Copyright Agreement to the publisher on the address of the editorial office. A properly completed Transfer of Copyright Agreement, signed by the Corresponding Author on behalf of all the authors, must be provided for each submitted manuscript. A form can be found on the journal's webpage.

Conflict of interest

When the manuscript is submitted for publication, the authors are expected to disclose any relationship that might pose real, apparent or potential conflict of interest with respect to the results reported in that manuscript. Potential conflicts of interest include not only financial relationships but also other, non-financial relationships. In the Acknowledgement section the source of funding support should be mentioned. The Editors will make effort to ensure that conflicts of interest will not compromise the evaluation process of the submitted manuscripts; potential editors and reviewers will exempt themselves from review process when such conflict of interest exists. The statement of disclosure must be in the Cover letter accompanying the manuscript or submitted on the form available on http://www.icmje.org/coi_disclosure.pdf

Page proofs will be sent by E-mail or faxed to the corresponding author. It is their responsibility to check the proofs carefully and return a list of essential corrections to the editorial office within three days of receipt. Only grammatical corrections are acceptable at this time.

Reprints: The electronic version of the published papers will be available on www.versitaopen.com free of charge.

Lilly Onkologija

Vsaka odprta vrata lahko pomenijo novo odkritje.

Z več kot 60 tarčnimi zdravili v razvoju, se naša prizadevanja v iskanju pristopov zdravljenja po meri bolnika, šele pričenjajo.

Lilly Onkologija

Niti dva bolnika z rakom nista enaka. Zato si Lilly Onkologija prizadeva, da razvije tako edinstvene pristope zdravljenja, kot so edinstveni ljudje, ki zdravljenje potrebujejo. Veliko smo prispevali k izboljšanju izidov zdravljenja in – z vsakimi vrati, ki jih odpremo – naredimo še en korak naprej. Naša prizadevanja v zagotavljanju zdravljenja po meri bolnika se nadaljujejo.

Znanost približujemo posamezniku.

SIALM00022

Lilly

Odgovori, ki štejejo.

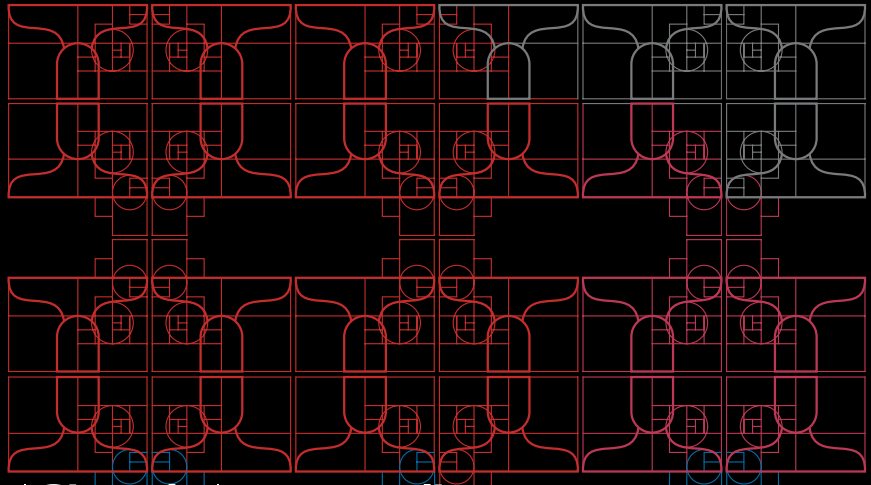

Radiology and Oncology | Ljubljana | Slovenia | www.versitaopen.com

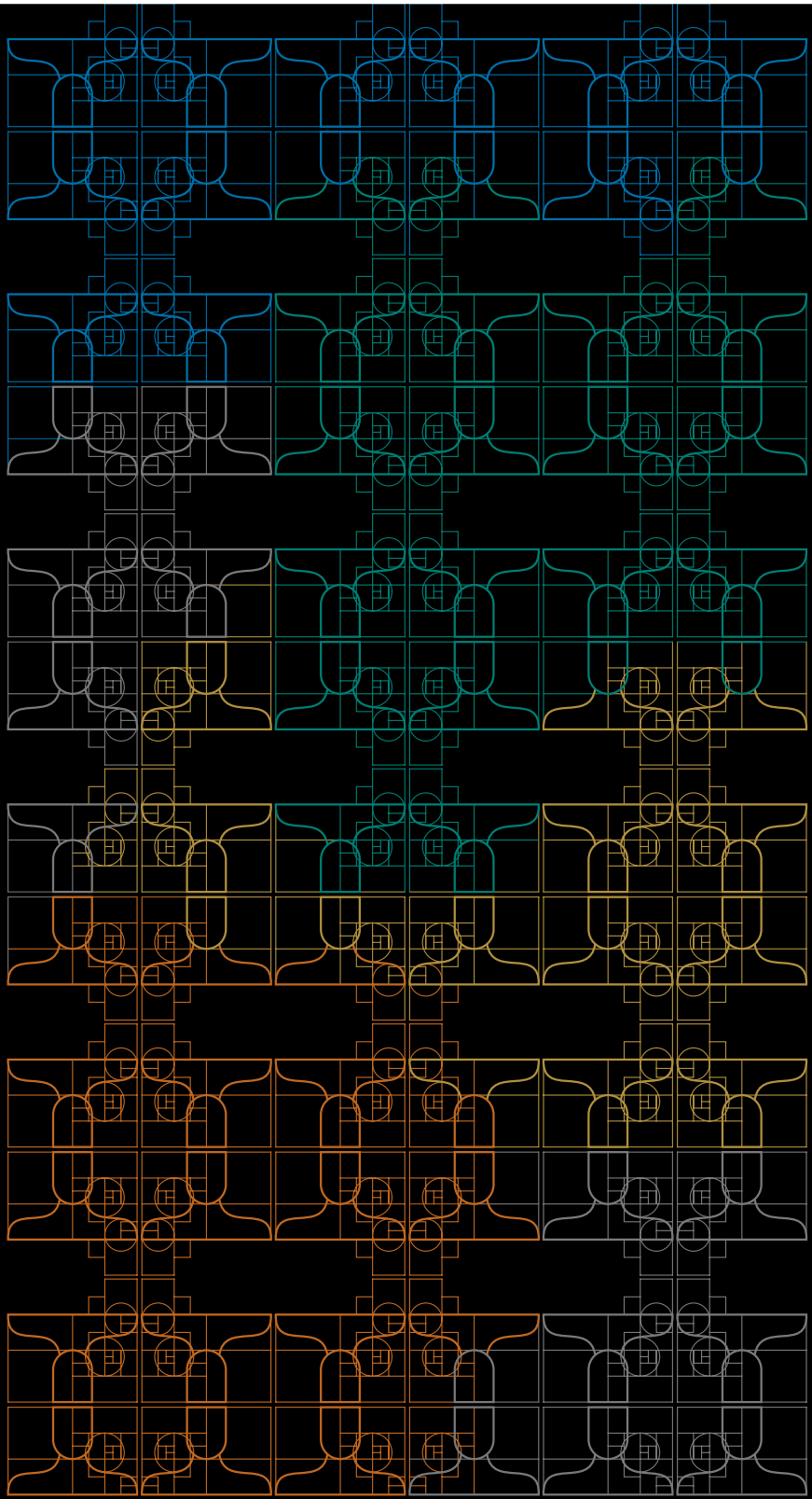

ISSN 1318 - 2099